Writing a Rosetta stone: insights into continental-margin sedimentary processes and strata

CHARLES A. NITTROUER*, JAMES A. AUSTIN JR†, MICHAEL E. FIELD‡, JOSEPH H. KRAVITZ§, JAMES P.M. SYVITSKI¶ *and* PATRICIA L. WIBERG**

**School of Oceanography and Department of Earth and Space Sciences, University of Washington, Seattle, WA 98195, USA (Email: nittroue@ocean.washington.edu)*
†Institute for Geophysics, John A. and Katherine G. Jackson School of Geosciences, University of Texas, Austin, TX 78759, USA
‡Pacific Science Centre, US Geological Survey, Santa Cruz, CA 95060, USA
§Department of Earth and Environmental Sciences, George Washington University, Washington, DC 20052, USA
¶Institute for Arctic and Alpine Research, University of Colorado, Boulder, CO 80309, USA
***Department of Environmental Sciences, University of Virginia, Charlottesville, VA 22904, USA*

ABSTRACT

Continental margins are valuable for many reasons, including the rich record of Earth history that they contain. A comprehensive understanding about the fate of fluvial sediment requires knowledge that transcends time-scales ranging from particle transport to deep burial. Insights are presented for margins in general, with a focus on a tectonically active margin (northern California) and a passive margin (New Jersey). Formation of continental-margin strata begins with sediment delivery to the seabed. Physical and biological reworking alters this sediment before it is preserved by burial, and has an impact upon its dispersal to more distal locations. The seabed develops strength as it consolidates, but failure can occur and lead to sediment redistribution through high-concentration gravity flows. Processes ranging from sediment delivery to gravity flows create morphological features that give shape to continental-margin surfaces. With burial, these surfaces may become seismic reflectors, which are observed in the subsurface as stratigraphy and are used to interpret the history of formative processes. Observations document sedimentary processes and strata on a particular margin, but numerical models and laboratory experimentation are necessary to provide a quantitative basis for extrapolation of these processes and strata in time and space.

Keywords Continental margin, continental shelf, continental slope, sedimentation, stratigraphy.

INTRODUCTION

The history of processes influencing the Earth is recorded in many ways. The sedimentary strata forming around the fringes of the ocean contain an especially rich record of Earth history, because they are impacted by a complex array of factors within the atmosphere (e.g. climate), the lithosphere (e.g. mountain building) and the biosphere (e.g. carbon fluxes).

Events that occur in coastal oceans and adjacent land surfaces have great impacts on humans, because most people live near the sea and depend on the bountiful resources formed or found there. Landslides, river floods, storm surges and tsunamis are examples of processes that can have sudden and catastrophic consequences for coastal regions. Other important processes have characteristic time-scales that are longer and the processes are somewhat more predictable; e.g. sea-level rise or fall, crustal uplift or subsidence, sediment accumulation or erosion. The confluence of terrestrial and marine processes occurs in the physiographical region known as the **continental margin**, extending

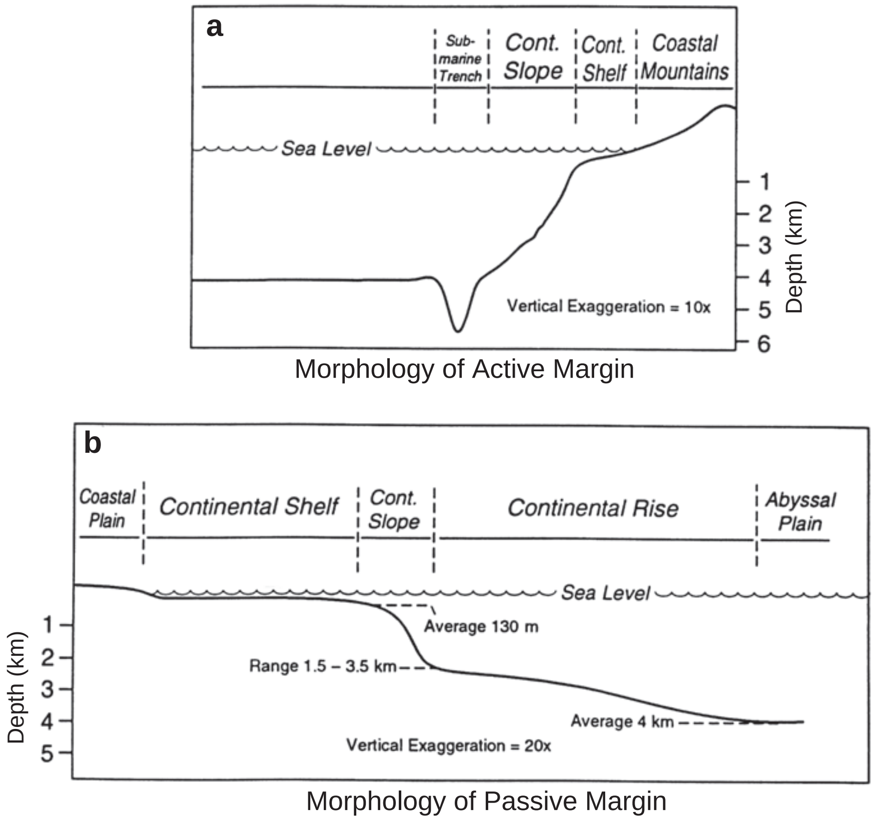

Fig. 1 Morphology of continental margins. (a) Typical morphology for a tectonically active continental margin, where oceanic and continental plates collide and subduction occurs. (b) A passive margin, where the continental and oceanic crust moves in concert. Significant distinctions include the presence of a coastal mountain range, narrow and steep continental shelf, and submarine trench (which can be filled with sediment) for the active margin. The passive margin is characterized by a coastal plain, broad continental shelf, and continental rise. (From Brink *et al.*, 1992.)

from coastal plains and coastal mountain ranges, across shorelines, to shallow continental shelves, and steeper and deeper continental slopes and rises (Fig. 1).

The interplay of terrestrial and marine processes on continental margins creates a complex mixture of stratigraphic signals in the sediments that accumulate there. This region of Earth, however, has the largest sediment accumulation rates, which create the potential for resolving diverse signals imparted over a range of time-scales (e.g. signals of river floods, and of sea-level change). Not only are the continental margins diverse and complex, but they are also very energetic. Waves, tides and currents are strong here, and provide the means to erase as well as form sedimentary records. Continental-margin stratigraphy represents a great archive of Earth history, but the challenges of reading it are also great, and require a fundamental understanding (a Rosetta stone) for translating stratigraphic character into a record of sedimentary processes.

The goal of this introductory paper is to distill the knowledge presented in the following papers of this volume, and integrate the recent insights that have been developed regarding sedimentary processes on continental margins, their impacts on strata formation, and how the preserved strata can be used to unravel Earth history. In contrast to the following papers that isolate topics, this paper highlights the linkages that come from a multi-dimensional perspective of margins. This is a summary of continental-margin sedimentation: from sediment transport to sequence stratigraphy.

THE BOUNDARY CONDITIONS

The full range of topics relevant to continental-margin sedimentation is extensive. In high latitudes, present or past glacial processes and sediments have a strong impact on sedimentation. In some low-latitude settings, biogenic carbonate sediments and their unique mechanisms of formation (e.g. coral reefs) dominate sedimentation. However, from polar to tropical environments, rivers can be the overwhelming sediment source for strata formation on continental margins. Margins affected by fluvial sediment, therefore, are the focus of this discussion.

Rivers add to the complexity of continental-margin processes through their discharge of freshwater and solutes. Rivers are also the dominant suppliers of particulate material from land to sea (globally ~85–95% is fluvial sediment; Milliman & Meade, 1983; Syvitski *et al.*, 2003). The largest rivers create extensive deposits near their mouths (e.g. Amazon, Ganges–Brahmaputra, Mississippi), but the combined discharges of moderate and small rivers (especially from coastal mountain ranges) dominate global sediment supply (Milliman & Meade, 1983; Milliman & Syvitski, 1992) and, therefore, are important to the creation of continental-margin stratigraphy.

Fluvial sedimentation on tectonically **active** and **passive** margins (Fig. 1) can now be examined over time-scales ranging from wave periods of seconds, to the stratigraphy formed and preserved over 10^7 years. Studies can span this broad range of time-scales with new rigour because numerous instruments (e.g. acoustic sensors for particle transport) and techniques (e.g. short-lived radioisotopes for seabed dynamics) have been developed recently to provide insights into important sedimentary processes. Similarly, significant advances have been made in seismic tools (e.g. CHIRP reflection profiling, multibeam swath mapping) that allow better resolution of stratigraphic surfaces. Recent advances in numerical modelling and laboratory simulations provide the opportunity quantitatively to span the temporal gap between processes operating over seconds and stratigraphy developed over millions of years.

The continental shelf and slope are the primary targets of this discussion because they are among the most dynamic environments on Earth, and record a wealth of information about environmental processes. At the boundary between land and ocean, they are impacted by energetic events characteristic of both regions (e.g. river floods, storm waves). On longer time-scales as sea level rises and falls, shelves are flooded and exposed, and slopes switch from sediment starvation to become recipients of all fluvial sediment. The boundaries between subaerial and submarine settings (i.e. the **shoreline**) and between shelf and slope (i.e. the **shelf break)** represent two dominant environmental and physiographical transitions on Earth. The transfers of sediment across these boundaries are also of special interest, because the particles on each side experience much different processes and therefore different fates. For example, on active margins, sediment crossing the shelf break can be subducted, but sediment remaining on the shelf cannot.

In this paper, fluvial sediment supply is taken as a source function on the landward side, without extensive discussion about the myriad processes occurring on land. On the seaward side, the evaluation of sedimentary processes and their effects on the formation and preservation of strata stops short of the continental rise, and the submarine fans formed there. The goal is a general understanding of sedimentary processes and stratigraphy on the continental shelf and slope, and the complex interrelationships are highlighted through two common study areas.

THE COMMON THREADS

The discussions within this paper cascade from short to long time-scales, from surficial layers of the seabed to those buried deeply within, and from shallow to deep water. Continuity in discussions is provided through examples from two diverse continental margins, which have been studied intensely throughout the STRATAFORM programme (STRATA FORmation on Margins; Nittrouer, 1999). The continental margin of northern California, near the Eel River (between Cape Mendocino and Trinidad Head; Fig. 2), is undergoing active tectonic motions and experiencing a range of associated sedimentary processes. In contrast, the margin of New Jersey (Fig. 3) is moving passively in concert with the adjacent continental and oceanic crust, and a distinctly different history of sedimentary processes is recorded.

Eel River (California) continental margin

The Eel basin is typical for rivers draining tectonically active continental margins. It is small (~9000 km^2), mountainous (reaching elevations > 2000 m), and composed of intensely deformed and easily erodible sedimentary rocks (Franciscan mélange and other marine deposits). These conditions lead to frequent subaerial landslides, especially because the high elevations cause orographic effects that intensify

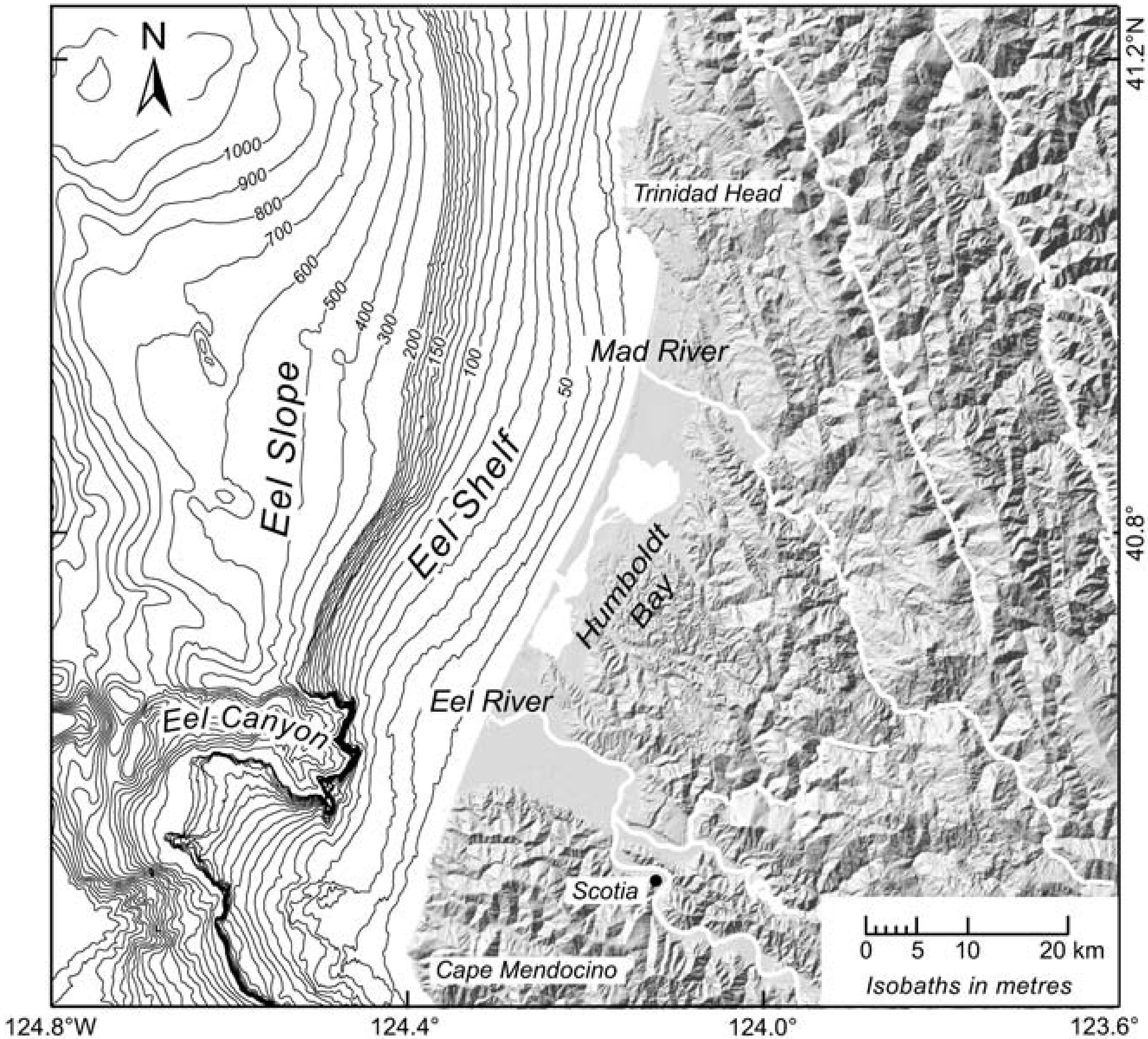

Fig. 2 The study area for the Eel margin, stretching from Cape Mendocino to Trinidad Head. The Eel River supplies an order of magnitude more sediment (~2×10^7 t yr^{-1}) than the Mad River. Below the town of Scotia (location of the lowermost river gauge), the river mouth has a small delta plain and most Eel River sediment escapes to the ocean. The shelf break is in a water depth of ~150 m, and is indented by Eel Canyon west of the river mouth. (Modified from Sommerfield *et al.*, this volume.)

rainfall from winter storm systems moving eastward off the Pacific. The annual **sediment yield** (mass discharge per basin area) is large (~2000 t km^{-2}), and although interannual discharge is highly variable, the mean value of sediment supplied to the ocean is estimated to be ~2×10^7 t yr^{-1} (Brown & Ritter, 1971; Wheatcroft *et al.*, 1997; Sommerfield & Nittrouer, 1999; Syvitski & Morehead, 1999). The grain size of the combined bedload and suspended load is relatively coarse (~25% sand; Brown & Ritter, 1971), due to the mountainous terrain and short length of the river (~200 km). Its size and orientation (generally parallel to the coastline) cause the entire basin to receive precipitation simultaneously during

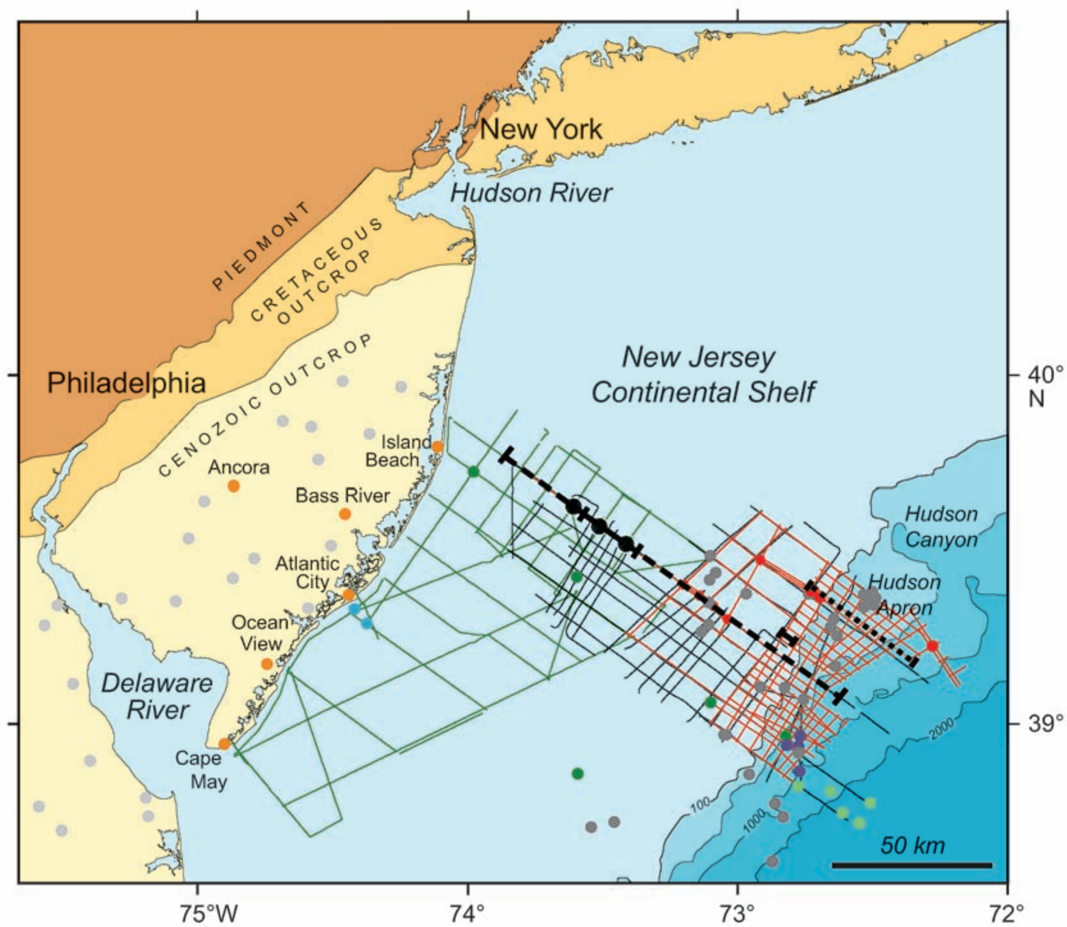

Fig. 3 The study area for the New Jersey margin, stretching between the mouths of the Delaware and Hudson Rivers. Most sediment is trapped in the estuaries at the river mouths and behind the New Jersey coastal barriers. The importance of the New Jersey margin is found in the underlying stratigraphy, which is a classic representation of passive-margin evolution. Some of the data used in this volume were collected at locations shown by the dots (drill sites) and lines (seismic profiles). Isobaths are metres. The shelf break is at ~100 m, and is indented by multiple submarine canyons including Hudson Canyon. (Modified from Mountain *et al.*, this volume.)

storms, and therefore the river discharge increases rapidly.

For the Eel River, major rainfall events commonly lead to episodic floods of the basin. Fluvial sediment discharge increases exponentially with water discharge (Syvitski *et al.*, 2000), and large floods dominate intra-annual and interannual variability of sediment transport. The mouth of the Eel River has no estuary and a very small delta plain (Fig. 2), so periods of sediment transport in the river become periods of sediment supply to the ocean. Most supply occurs during the winter (~90%; Brown & Ritter, 1971), and, for the past ~50 yr, decadal floods during the winter have had a significant impact on the river geomorphology and ocean sedimentation. The largest flood during this period was in 1964 and, more recently, a couplet of significant floods occurred in 1995 and 1997 (Wheatcroft & Borgeld, 2000).

Low-pressure cyclonic systems move eastward from the Pacific Ocean toward the west coast of North America. Commonly there is an asymmetry, such that the steepest pressure gradients are associated with the leading edges of the systems. Therefore, initial winds are strong, from the south or south-west, and Coriolis and frictional forces cause **Ekman transport** of surface water eastward toward the coast. Water elevations rise there, creating a seaward-sloping water surface that produces northward **barotropic** flow of shelf water. The eastward component of surface flows also causes **downwelling** and seaward bottom flows. The strong winds from the south and south-west create large waves approaching from those directions (as high as 10 m or more; Wiberg, 2000), and result in northward **alongshore transport** in the surf zone. This transport creates coastal landforms (e.g. spits) that direct the Eel River plume northward (Geyer *et al.*, 2000). As the low-pressure systems pass, the trailing portions of the cyclonic systems often cause winds to reverse and blow from the north.

An important aspect of sedimentation on the Eel margin is the rapid response of the Eel River to rainfall, and the occurrence of river floods during energetic ocean storms (see Hill *et al.*, this volume, pp. 49–99). These types of events can be described as **wet storms**, during which large fluvial discharges reach the ocean when sediment transport processes are strong. The river plume, coastal current, and wind waves during these periods are important dynamical processes for sediment dispersal on the Eel margin, but they are not the only processes. Energetic ocean conditions also occur without river floods (e.g. large swell waves), and these are described as **dry storms**. Tidal forcing is important on the Eel margin. A tidal range of ~2 m causes current speeds ~50 cm s^{-1} oriented primarily alongshelf. The tidal prism flowing in and out of Humboldt Bay (Fig. 2) influences shelf circulation near its mouth (Geyer *et al.*, 2000). In addition, tidal forcing in deeper water initiates internal waves that maintain suspended sediment near and below the shelf break (McPhee-Shaw *et al.*, 2004).

Sediment from the Eel River and the adjacent Mad River (~10% of the Eel discharge) is supplied to a relatively narrow continental shelf surface (~20 km wide) constrained by promontories: Cape Mendocino to the south and Trinidad Head to the north (Fig. 2). The shelf break is at ~150 m water depth and Eel Canyon incises the shelf surface just west of the river mouth. The morphological elements of the surface (e.g. narrow and steep shelf) and subsurface (e.g. structural folds and faults) are largely the result of tectonic activity. The present Eel margin is part of the larger Eel River Basin (Clarke, 1987, 1992; Orange, 1999), which became a forearc basin in the Miocene and accumulated > 3000 m of marine sediment by the middle Pleistocene (~1 Ma). At that time, the northward migration of the Mendocino Triple Junction and subduction associated with the Gorda Plate initiated modern tectonic conditions. The Gorda and North American plates are converging at ~3 cm yr^{-1} (DeMets *et al.*, 1990), and create localized uplift and subsidence with a WNW–ESE orientation. This is the tectonic framework on which Eel margin sedimentation has been imprinted for the past million years.

New Jersey continental margin

The modern Hudson and Delaware Rivers bracket the New Jersey continental margin (Fig. 3), but very little sediment escapes from the estuaries at the river mouths or from behind the New Jersey barrier coastline. New Jersey is a classic example of a passive margin, and its special value comes from the stratigraphic record buried beneath its surface. The margin began to form as the Atlantic Ocean opened with rifting in the Late Triassic and spreading in the Early Jurassic (Grow & Sheridan, 1988). A range of processes typical of passive margins caused subsidence of the margin, and created space that could be filled with sediment (i.e. **accommodation space**). Through the Cretaceous, it was fringed by a barrier reef, but it became a carbonate ramp in the early Tertiary (Jansa, 1981; Poag, 1985) due to continued subsidence and sediment starvation.

Sediment accumulation rates dramatically increased (to ~10–100 m Myr^{-1}) in the late Oligocene and early Miocene, due to tectonic activity in the source area that increased fluvial sediment supply to the margin (Poag, 1985; Poag & Sevon, 1989). The resulting stratigraphic record has been examined by many seismic and drilling investigations (Mountain *et al.*, this volume, pp. 381–458). Cycles of sea-level fluctuation are recorded by repetitive sequences of strata: a basal layer of **glauconite** sand (an authigenic mineral indicating negligible sedimentation) overlain by silt, which coarsens upward into quartz sand (Owens & Gohn, 1985; Sugarman & Miller, 1997). These sequences reflect sea-level rise, followed by seaward migration of shelf and nearshore sedimentary environments. During the Miocene, most of the sediment accumulation resulted from migration on the shelf of morphological structures known as **clinoforms** (Greenlee *et al.*, 1992). These have a shallow, gently dipping **topset** region of upward growth and, farther offshore, a steeper **foreset** region of seaward growth (see below). The extent of sea-level fluctuations during the Miocene is controversial, but probably was subdued (20–30 m;

Kominz *et al.*, 1998; Miller *et al.*, 1998) relative to fluctuations that followed (> 100 m) in the Pleistocene.

Glacial erosion in the source area was largely responsible for supplying sediment to the marine environment during the Pleistocene. Earlier sedimentation had built a wide shelf with a gentle gradient, but margin subsidence had slowed and was producing little new accommodation space on the inner shelf. During lowered sea level, glacial outwash streams incised the shelf and icebergs even scraped the surface (Duncan & Goff, 2001; Fulthorpe & Austin, 2004). Generally, sediment accumulation was displaced seaward to the outer shelf and upper slope, dramatically changing the sedimentation regime (Greenlee *et al.*, 1988, 1992; Mountain *et al.*, this volume, pp. 381–458). Clinoforms were active there, and the inflection in their bathymetric gradient became the shelf break. Sedimentation on the continental slope increased significantly, which caused seaward growth of the shelf break to its present position > 100 km from shore. The slope also grew seaward, but the influx of sediment initiated localized erosional processes. Miocene **submarine canyons** and smaller erosional features (**gullies**) were buried or reactivated by the substantial sediment supply to the relatively steep slope (Mountain, 1987; Pratson *et al.*, 1994). The long history of the New Jersey margin provides an opportunity to observe how a diverse range of sedimentary processes impacts the preserved strata on a passive margin.

SEDIMENT DELIVERY

Detailed aspects of sediment delivery on continental margins have been addressed in this volume by Hill *et al.* (pp. 49–99) and Syvitski *et al.* (pp. 459–529).

General considerations

The first step in the formation of continental-margin strata is sediment delivery. The timing and content of fluvial discharge depend on many factors, such as basin character, weather, glaciation and groundwater flow (Beschta, 1987), which can be observed and modelled. Commonly, a **rating curve** is developed to relate sediment flux to river discharge (Cohn, 1995; Syvitski *et al.*, 2000). The observations needed to generate a rating curve are confounded by difficulty in making measurements over a range of flow conditions – especially during large flood events, which are important periods because much sediment is transported (Wheatcroft *et al.*, 1997). Other difficulties are imposed by changes in the curve that occur when the river basin is altered naturally (e.g. landslides) or unnaturally (e.g. land use). Asymmetry in sediment discharge is commonly associated with rise and fall of river stage, and can cause a **hysteresis** whereby different sediment fluxes occur for the same discharge (Brown & Ritter, 1971; Meade *et al.*, 1990). Over longer time-scales of climatic and sea-level changes, adjustments to the snow pack and basin size have an impact upon the timing and amount of discharge (Mulder & Syvitski, 1996). Fluctuations in regional precipitation patterns also can modify the shape of the river hydrograph and the dominance of sustained flows or episodic floods, which are conditions that affect sediment transport substantially. For example, strengthening of the monsoonal regime in the early Holocene caused the Ganges–Brahmaputra system to have more than twice its present sediment load (Goodbred & Kuehl, 2000).

Rivers supply a range of grain sizes to the ocean. Sediment in suspension (mostly silt and clay, i.e. < 64 μm) generally represents ~90% of the discharge, and the remainder is bedload (almost entirely sand; Meade, 1996). Early recognition of patterns for modern sediment distribution on continental margins provided suggestions about delivery mechanisms to the seabed. Commonly, sand is concentrated on the inner shelf, and silt and clay are found farther seaward. Potential mechanisms for dispersal of the fine sediment are:

1 a land source with high concentrations of mud that diffuse seaward through wave and tidal reworking (Swift, 1970);
2 erosion of nearshore fluvial sediment by physical processes that intensify toward shore, and advection by currents to deeper, quiescent settings (McCave, 1972);
3 resuspension of sediment in concentrations turbid enough to flow seaward under the influence of gravity (Moore, 1969).

All three mechanisms (and others) are possible, with one or another dominating under particular conditions.

The first step in sediment delivery is for particles to leave the river plume. Sand settles rapidly and reaches the seabed near the river mouth. Silts and clays sink from surface plumes within a few kilometres of the river mouth (Drake, 1976). Individual silt and clay particles settle too slowly to explain this latter observation; they must form larger aggregates that sink rapidly. One possible mechanism is **biogenic aggregation** (Drake, 1976) into faecal pellets by filter-feeding organisms, but this cannot explain broad spatial distribution of particle settling, especially in turbid plumes. Most fine particles have surface charges which, in freshwater, cause the development of large, repulsive ion clouds. In brackish water with salinities of a few parts per thousand, the ion clouds compress and allow **van der Waals' forces** of attraction to dominate, forming larger aggregates that settle rapidly. When this process occurs inorganically (e.g. glacial meltwater), it is referred to as **coagulation**. If organic molecules help bridge the gap between particles, which is common in middle and low latitudes, the aggregation process is known as **flocculation**. In addition to the mechanism of aggregation, the length of time for aggregation, the suspended-sediment concentration and the turbulence of the environment are likely to control size and settling velocity (McCave, 1984; Hill, 1992; Milligan & Hill, 1998). Despite these complexities, aggregate settling velocities are generally ~1 mm s^{-1} (ten Brinke, 1994; Hill *et al.*, 1998).

The character of the river plume has a strong impact on the delivery of particles to the seabed. Most plumes are **hypopycnal** with densities less than the ambient seawater. They flow and spread at the surface (Fig. 4), controlled by local winds,

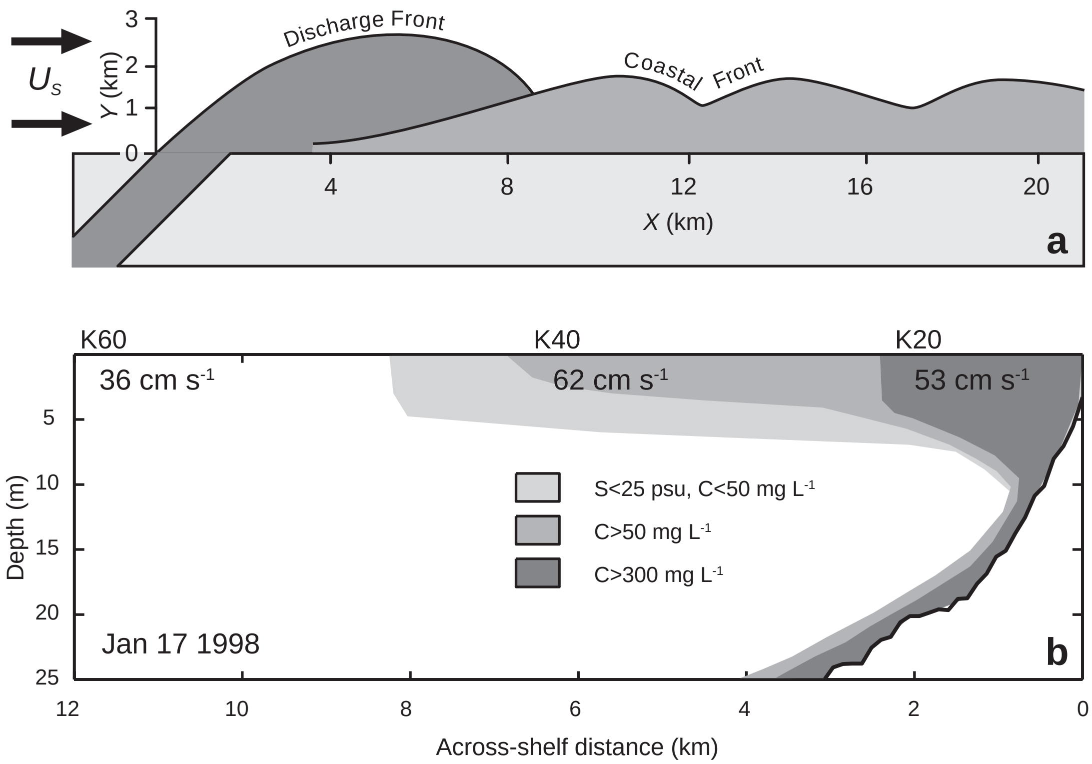

Fig. 4 Hypopycnal plumes. (a) A schematic map view for discharge of a general hypopycnal plume, with a river mouth at an angle to the shoreline. U_s is the velocity of an ambient current directed northward in the northern hemisphere. The combination of ambient current, Coriolis force, and mouth orientation causes the plume to flow to the right, creating a coastal current. (From Hill *et al.*, this volume; modified from Garvine, 1987.) (b) Cross-section (facing northward) of Eel plume on the continental shelf north of the river mouth during a period of northward winds (S = salinity; C = suspended-sediment concentration). The low-salinity and turbid river water extends offshore as a hypopycnal plume flowing northward; velocity measured 2 m below water surface shown in cm s^{-1}. Northward winds also produce downwelling against the coast and the seaward flow of bottom water with suspended sediment. (From Hill *et al.*, this volume; modified from Geyer *et al.*, 2000.)

currents, Coriolis force and the relative significance of inertial and buoyancy forces (Wright, 1977). The path of surface plumes (e.g. direction, speed) has an impact upon the trajectory of settling particles. Under special conditions, rivers can enter water bodies with similar densities, forming **homopycnal** plumes that spread throughout the water column as turbulent jets. If the density of the river plume is greater than the ambient seawater, it forms a **hyperpycnal** plume that sinks and moves near the bottom. Of special importance to this paper are conditions (e.g. floods) where freshwater has extremely high suspended-sediment concentrations (> 40 g L^{-1}) that cause the excess density. These plumes move as gravity-driven sediment flows deflected by Coriolis force and physical oceanographic conditions (e.g. currents), but primarily they follow the steepest bathymetric gradient. Although uncommon (Mulder & Syvitski, 1995), some rivers, especially those with mountainous drainage basins, can reach hyperpycnal conditions and transport massive amounts of sediment across continental margins.

During highstands of sea level, as at present, the processes of sediment delivery tend to be focused in shallow water. For fluvial systems where or when freshwater discharge is relatively weak, aggregation begins within **estuaries** at river mouths (or even within the rivers themselves) and sediment can be trapped there. This is particularly true for low-gradient rivers emptying onto passive margins, such as the Hudson and Delaware rivers. If river plumes with substantial sediment concentrations extend onto the shelves, sedimentation can occur there, and follow the mechanisms described previously in this section. Most active margins have coastal mountain ranges, steep river channels, small or no estuaries and narrow continental shelves (Fig. 1). Under these conditions, plumes can reach the continental slope. Hypopycnal plumes form surface **nepheloid layers** (diffuse clouds of turbid water), which are carried by the local currents and dissipate as suspended sediment settles onto the slope (known as **hemipelagic** sedimentation). Hyperpycnal plumes move down the steepest portions of the slope (commonly submarine canyons), and can accelerate to erode the seabed and refuel their excess density, thus becoming one of several means to create **turbidity currents**. Today, some submarine canyons extend into the mouths of rivers (e.g. Sepik River, Congo River) and gravity-driven sediment flows (e.g. hyperpycnal plumes, turbidity currents) usually dominate sediment transport (Kineke *et al.*, 2000; Khripounoff *et al.*, 2003). During lower stands of sea level, such situations were common.

Delivery of Eel margin sediment

Initial northward winds and currents, a northward-pointed river mouth and the Coriolis force cause the early stages of Eel River flood discharges (associated with winter storms) to be directed northward. The **radius of curvature** defines the turning distance of the plume at the river mouth. This radius is controlled by plume speed and the Coriolis force (Garvine, 1987), and is ~10 km near the Eel mouth. The plume turns into a northward-flowing coastal current (Fig. 4) that is restricted to regions < 40 m deep and is moving at ~50 cm s^{-1} (maximum 130 cm s^{-1}; Geyer *et al.*, 2000). Suspended silts and clays, which dominate the discharge, aggregate (mean floc size 230 μm; Curran *et al.*, 2002) and are largely removed from the surface plume within 10 km of the river mouth (Hill *et al.*, 2000). The correlation of discharge events and oceanic storm conditions guarantees turbulence within the coastal current. This turbulence results from wind-driven downwelling that destroys water-density stratification, and from a storm-wave surf zone that extends seaward to as far as 15-m water depth (Curran *et al.*, 2002). The intense turbulence within the surf zone keeps fine sediments suspended, providing a mechanism to resupply the coastal current. As the coastal current moves northward, it experiences some seaward transport due to **Ekman veering** in the bottom boundary layer (Smith & Long, 1976; Drake & Cacchione, 1985). When winds reverse, northward transport is slowed and the plume broadens seaward (Geyer *et al.*, 2000). For periods of low river discharge, correlation with meteorological events is not evident, and variable winds preclude a net direction of sediment transport. In some years, southward transport of shelf sediment can be significant (Ogston & Sternberg, 1999; Ogston *et al.*, 2004).

During coupled discharge and storm events, wave activity has a significant control on aggregate properties observed along the shelf, due to continual injection of particles from the surf zone into the coastal current (Curran *et al.*, 2002). Beyond the surf zone (> 15 m depth), a shelf frontal zone (Fig. 4) concentrates suspended sediment on the inner shelf (Ogston *et al.*, 2000); here, wave activity can stimulate across-shelf sediment transport. Although waves provide little net direction for sediment transport, they can create high-concentration (> 10 g L^{-1}) **fluid muds** in the wave boundary layer (< 10 cm thick) that produce gravity-driven sediment flows moving seaward at 10–30 cm s^{-1} (Traykovski *et al.*, 2000). The signature of these flows occurs within the current boundary layer (lowermost several metres of water column) where velocity normally decreases logarithmically toward the seabed. When concentrations of suspended sediment are very large, velocity increases near the bed within the wave boundary layer (5–10 cm above seabed).

These wave-supported sediment gravity flows transport much sediment mass as they move across shelf. As near-bed wave activity decreases seaward, the gradient of the shelf seabed is not sufficient to allow continued flow, and the sediment stops moving (Wright *et al.*, 2001). Within the resulting flood deposits are fine laminae (centimetre-scale **sedimentary structures**) that record pulses of sediment flux (Wheatcroft & Borgeld, 2000). The location of the gravity-flow deposits generally coincides with the convergence of sediment transport from shelf currents (Wright *et al.*, 1999; Ogston *et al.*, 2000), and together these processes create a locus of sediment deposition on the Eel shelf between 50-m and 70-m water depth and ~10–30 km north of the river mouth (Fig. 5).

Not all sediment discharged to the Eel continental shelf reaches the seabed; much (> 50%) continues to the continental slope. Turbid water in the bottom boundary layer of the shelf can detach near the shelf break and move seaward along an isopycnal surface within the water column as an **intermediate nepheloid layer** (INL). These layers are maintained, in part, by internal waves (McPhee-Shaw *et al.*, 2004). Eel sediment is broadcast across the slope, and rapid delivery is confirmed by the

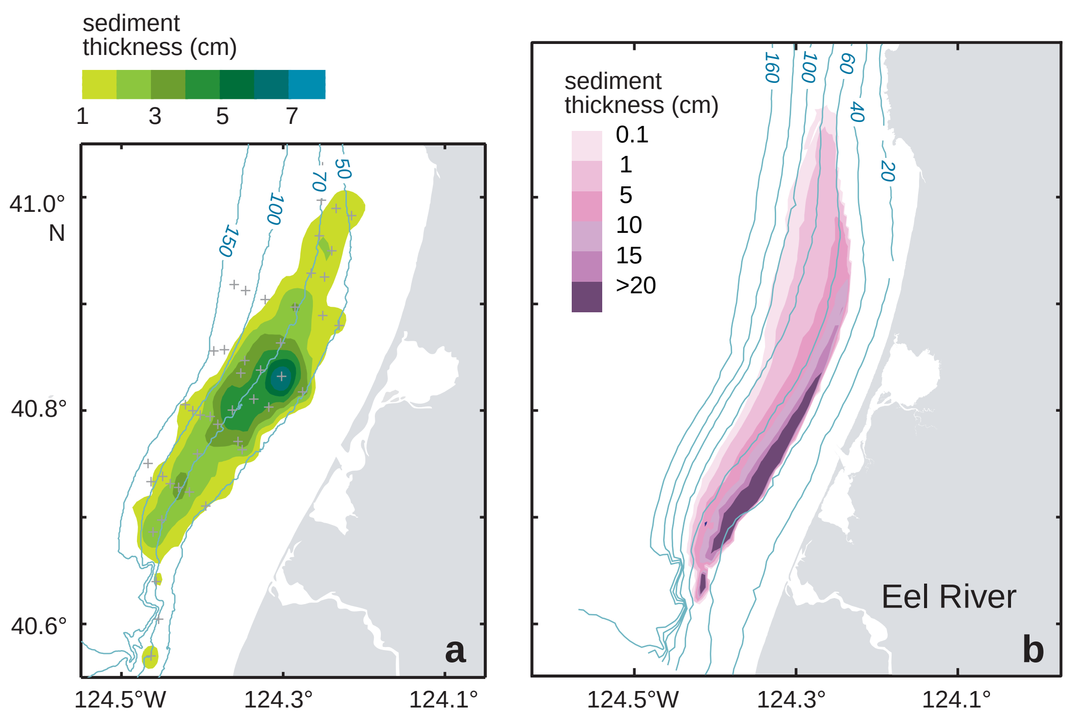

Fig. 5 Shelf sediments resulting from the 1997 flood of the Eel River. (a) Isopach map of the 1997 flood deposit. The thickest portion is found in ~70-m water depth and ~15–25 km north of the Eel River mouth. This compares well with the pattern of the 1995 flood deposit shown in Fig. 10. (From Hill *et al.*, this volume; based on Wheatcroft & Borgeld, 2000.) (b) Predicted thickness of a deposit resulting from wave-supported sediment gravity flows during the 1997 flood event (porosity assumed to be 0.75). Thicknesses are greater and extend farther north than those observed in (a), but the predicted pattern has many similarities to the flood deposit, including its shape and the location of the landward and seaward boundaries. (From Hill *et al.*, this volume; based on Scully *et al.*, 2003.)

presence of the short-lived radioisotope ^{7}Be (half-life 53 days) in sediment traps (Walsh & Nittrouer, 1999). This same isotope is found in the seabed of the open slope (Sommerfield *et al.*, 1999) and Eel Canyon (Mullenbach & Nittrouer, 2000), probably from input through intermediate nepheloid layers and other mechanisms. In the head of Eel Canyon, inverted velocity profiles (increasing near the seabed) similar to gravity-driven sediment flows on the shelf are observed (Puig *et al.*, 2003, 2004). Modelling studies indicate that substantial amounts of Eel sediment discharge are likely to be carried into the canyon by these flows (Scully *et al.*, 2003). During major flood periods (e.g. 1995, 1997), the river may become hyperpycnal, and bottom plumes may carry large fractions of the Eel discharge directly to the Canyon or the open slope north of the Canyon (Fig. 2; Imran & Syvitski, 2000). Therefore, a range of mechanisms associated with the Eel plume deliver sediment to the continental slope during the present highstand of sea level.

Modelling studies indicate that during the **Last Glacial Maximum** (LGM), the Eel basin was wetter and colder, and storm frequency was greater (Morehead *et al.*, 2001). These differences would have caused approximately a doubling of the water and sediment discharge (Syvitski & Morehead, 1999). Most discharge from the modern Eel River occurs with winter rains. For the LGM, increase in precipitation would have caused a more sustained discharge as snow pack melted during the spring and summer. Rains on low-elevation snow also would have caused more intense floods than today. These differences in water and sediment discharges and in the intra-annual variability of discharges distinguish modern and past conditions for sediment delivery to the Eel margin.

SEDIMENT ALTERATION

Processes affecting the preservation of the sediment record during deposition and the early stages of burial have been examined in this volume by Wheatcroft *et al.* (pp. 101–155).

General considerations

Sediment delivered to the seabed is altered in many ways before being preserved by burial. Especially important changes are those that alter the dynamical properties of the seabed thereby impacting lateral transfer of sediment across margins (e.g. alteration of particle-size distribution, bottom roughness, porosity), and those that cause vertical displacements of seabed particles thereby affecting stratigraphic signatures (e.g. alteration of sedimentary structures, acoustic properties). These alterations occur primarily over time-scales of days to years and over vertical length scales of millimetres to decimetres. Deposition of new particles applies a downward force (i.e. weight) to the underlying sediment. Physical processes erode and deposit particles, rearranging them based on hydrodynamic character. Macrobenthic organisms displace particles in the seabed through a wide assortment of activities, including ingestion and defaecation. Chemical processes also alter sediment after delivery to the seabed, but usually have less direct impact on transport and stratigraphy than the other processes (for summaries of chemical alteration see: Aller, 2004; McKee *et al.*, 2004).

Consolidation (also known as **compaction**) decreases **porosity**, as new overburden reduces pore space and displaces pore fluid. Initial changes occur near the surface of the seabed, such that a relatively uniform porosity is approached within a few centimetres (Fig. 6a), although consolidation continues much deeper in the seabed as overburden increases. Porosity profiles impact many properties in the seabed (e.g. bulk density, acoustic signature), and also influence sedimentary processes; high-porosity surface layers are easily eroded by weak shear stresses. Porosity profiles indicate whether the weight of overlying sediment is supported by a particle framework or by pore fluids, conditions that may ultimately determine the distribution of stresses and whether the seabed will fail. For all of these reasons, understanding the consolidation rate of natural sediment is important, as is understanding the factors affecting that rate (e.g. permeability, bioturbation). In general, sands consolidate quickly toward a minimum porosity of ~0.35 (fractional volume of pore space) and muds consolidate more slowly toward minimum values (Been & Sills, 1981; Wheatcroft, 2002). However, fluctuations in sedimentation complicate consolidation history of the seabed. Erosion of the seabed exposes sediment that is **overconsolidated** (Skempton, 1970) relative to

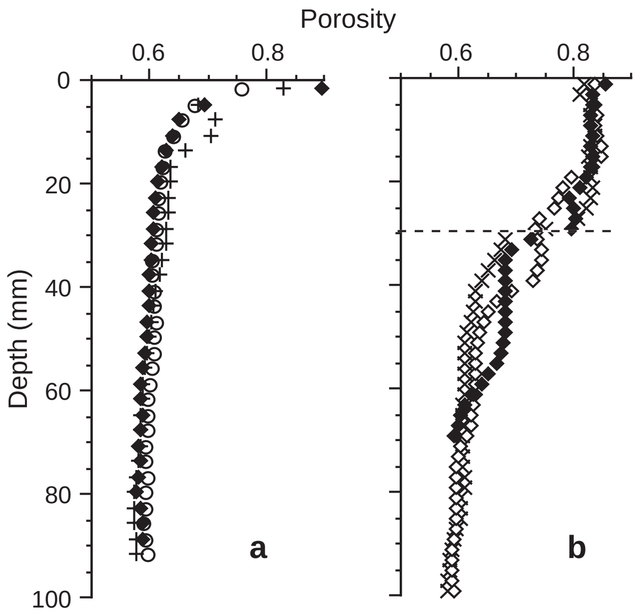

Fig. 6 Sediment porosity profiles on the Eel Shelf. (a) Replicate porosity profiles at a mid-shelf station (70-m water depth) six months before the 1997 flood of the Eel River. Relatively uniform porosity is reached within ~30 mm of seabed surface. (b) Replicate porosity profiles at the same station as (a), but 2 weeks after the 1997 flood. A uniform layer of higher porosity is observed within the upper ~30 mm, which is the thickness of the flood deposit at this location, as documented by X-radiography and radiochemistry. (From Wheatcroft *et al.*, this volume.)

what is expected at the surface. Rapid deposition of thick flood layers places sediment below the surface that is **underconsolidated** (Skempton, 1970) relative to what is expected at that depth in the seabed. Variable grain sizes and biological effects further complicate consolidation, and make modelling and prediction of porosity profiles more difficult.

Physical reworking adds and subtracts particles from locations on the seabed, often removing fine particles (i.e. **winnowing**) and coarsening (i.e. **armouring**) the surface. The fine particles (silts and clays) possess interparticle forces of attraction and, where these sediments deposit, the seabed develops **cohesion**. With consolidation, cohesive forces increase, and the fluid velocities needed for resuspension also increase. Armouring inhibits resuspension by developing a coarse surface layer, and cohesion causes an abrupt decrease in erodibility just below the surface of muddy deposits.

The extent of physical reworking depends on the strength of operative processes (e.g. surface waves, coastal currents) as well as seabed properties (e.g. grain size, porosity). Under special conditions (e.g. equatorial settings with sustained trade winds, shallow tide-dominated coastal areas), reworking can be relatively continuous (Nittrouer *et al.*, 1995). However, most continental margins are dominated by cyclonic storms, which cause episodic physical reworking that is largely the result of surface waves (Komar *et al.*, 1972; Drake & Cacchione, 1985). Waves impact the seabed in water depths less than about half their wavelength, and large waves can rework bottom sediments to depths of 100–200 m in extreme events (Komar *et al.*, 1972). The near-bed wave orbital velocities increase toward shore, and are additionally dependent on wave height and period (Komar & Miller, 1975; Madsen, 1994; Harris & Wiberg, 2001). A velocity of ~14 cm s^{-1} has been observed as the critical value needed for resuspension of muddy shelf deposits by waves (Wiberg *et al.*, 1994, 2002) but this value is influenced by many factors, including grain size and consolidation state.

In non-cohesive sandy sediment, the **active layer** of moving sediment can be a few centimetres thick but, where bedforms develop and migrate, it is comparable to their height (~5–10 cm). In cohesive muddy sediment, the active layer is dependent on the thickness of high-porosity surficial sediment. Erosion and redeposition of sediment create a **graded** deposit (i.e. fining upward) within the active layer (Reineck & Singh, 1972; Nittrouer & Sternberg, 1981). Subsequent to deposition, benthic organisms alter the seabed through a range of activities. Ingestion of particles and formation of faecal pellets change the effective grain size of sediment. Together with formation of mounds and burrows, these processes increase seabed roughness (Jumars & Nowell, 1984) and alter porosity, all of which influence sediment transport. The mucous that glues animal faecal pellets is similar to organic substances produced by microalgae on seabed surfaces, and adhesive coatings from both sources tend to bind the seabed and reduce physical reworking. Feeding, locomotion and dwelling construction

Fig. 7 Wave energy on the Eel margin. (a) Spatial variation of wave characteristics measured by buoys (NOAA National Buoy Center) along the northern California coast (north of San Francisco). Buoy 46022 is located near the Eel River, and has the most energetic wave climate, as shown by the return period for a given significant wave height. (b) The probability is shown of exceeding various near-bed orbital velocities (U_b) at different water depths across the Eel shelf. For the mid-shelf deposits (~50–70 m water depth), a velocity of ~15 cm s^{-1} is likely to erode the surface sediment. (From Wheatcroft *et al.*, this volume; modified from Wiberg, 2000.)

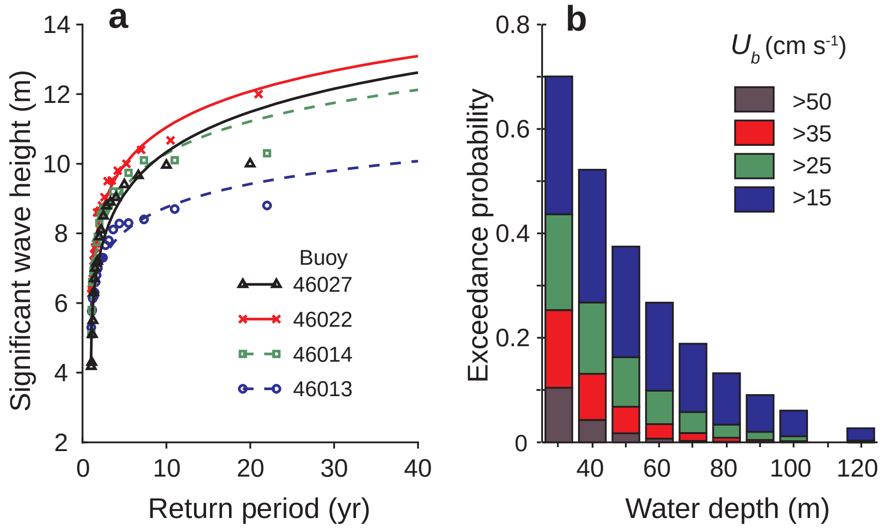

are processes by which benthic organisms stir sediment within the seabed (i.e. **bioturbation**), destroying physical sedimentary structures and creating biological structures. These processes occur within a region known as the **surface mixing layer**, which is ~5–20 cm thick.

Alteration of Eel margin sediment

The Eel margin is an instructive place to investigate seabed alteration, because the relevant processes operate intensely and cause the seabed to be dynamic. Floods of the river create thick layers of high-porosity sediment of variable grain size on the continental shelf. Energetic oceanic storms cause reworking of that sediment. An abundant and well-adapted benthic community rapidly mixes the seabed.

Beyond the inner-shelf sands (> 60 m depth), steady-state porosity profiles asymptotically approach values of 0.6–0.7 several centimetres below the seabed surface (Fig. 6a; Wheatcroft & Borgeld, 2000). The floods in 1995 and 1997 added significant perturbations, creating layers of uniform porosity many centimetres thick (up to ~8 cm) with values of 0.8–0.9 (Fig. 6b). The consolidation rate of this sediment had an important control on the erodibility of the seabed. The upper centimetre returned to steady-state porosities within months (< 4) and made the seabed resistant to erosion, even though a couple of years were needed for deeper flood sediments to reach the lower values (Wheatcroft *et al.*, this volume, pp. 101–155). Concurrent bioturbation imposed significant spatial variability on these general observations.

The Eel margin has the greatest wave energy along the northern California coast (north of San Francisco), with waves reaching heights > 10 m (Fig. 7a; Wiberg, 2000). The inner-shelf region (< 50 m depth) experiences relatively long durations when the near-bed wave orbital velocities exceed the critical value (totalling > 40% of the time; Fig. 7b). These events are sufficient to winnow most mud (silt and clay), and create a seabed dominated by sand. Farther seaward, mud becomes a substantial portion of the seabed (> 50%) and adds cohesion as a relevant property. Despite the energetic wave regime experienced by the Eel margin, the thickness of the active layer is surprisingly small. For a strong wave event estimated to have a 10-yr recurrence interval (December, 1995), erosion occurred to ~2 cm within the seabed at 50-m water depth (Wiberg, 2000). The estimated thickness increases to 5 cm for a 100-yr storm and to 10 cm for a 1000-yr storm. For most storms, however, the active layer is millimetres thick, especially in water depths > 50 m. In addition to redeposition of local sediment, some areas

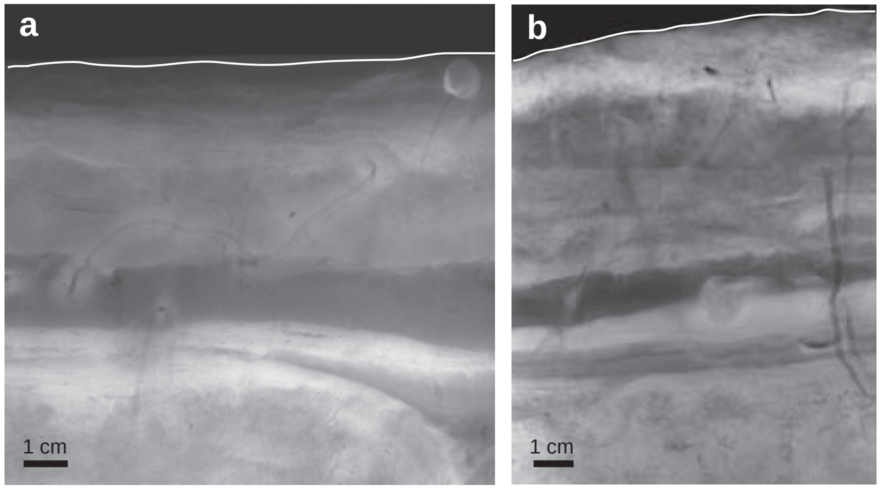

Fig. 8 X-radiograph negatives of sediment cores collected from the mid-shelf about (a) 15 km and (b) 25 km north of the Eel River mouth, illustrating various biogenic structures. (a) Collected from ~70-m water depth during February 1995, showing the January 1995 flood deposit. The burrow extending from middle left to upper right is most likely to be an escape structure of the bivalve mollusc at the sediment–water interface (upper right). (b) Collected from ~60-m water depth during July 1996. The physical sedimentary structures near the base of the radiograph are coarse silt and clay layers in the 1995 flood deposit. Bioturbation has partially destroyed the records of the flood and has imparted a general mottling to the sediment. In addition, animals have created discrete burrows that extend tens of centimetres into the seabed. In 18 months following the 1995 flood event, new sediment was added to the seabed above the flood deposit, a process that favoured preservation of the deposit. (X-radiographs are courtesy of R.W. Wheatcroft, Oregon State University; see also Wheatcroft *et al.*, this volume.)

can experience a convergence of sediment flux during dry storms (e.g. transfer from inner-shelf to mid-shelf depths) adding millimetres to 1 cm of sediment (Zhang *et al.*, 1999; Harris & Wiberg, 2002). The resulting storm deposits are graded, but bioturbation destroys them within weeks (Fig. 8; Harris & Wiberg, 1997; Bentley & Nittrouer, 2003; Wheatcroft & Drake, 2003).

Thicknesses of event deposits are greater during wet storms, due to the influx of new river sediment (Fig. 5). These deposits have relatively high clay contents (Drake, 1999), and can be easily identified by their physical sedimentary structures (Wheatcroft & Borgeld, 2000), radiochemical signatures (presence of ^{7}Be and low level of ^{210}Pb; Sommerfield *et al.*, 1999) and terrestrial carbon composition (Leithold & Hope, 1999). Subsequent to the formation of clay-rich flood deposits, the seabed coarsens by the addition of silts and fine sands from the inner shelf (Drake, 1999). In addition, animal bioturbation gradually destroys physical sedimentary structures and creates discrete biogenic structures (Fig. 8). Polychaete worms dominate macrofauna on the Eel margin, and most of the abundant species are subsurface-deposit feeders (Bentley & Nittrouer, 2003; Wheatcroft, 2006). They produce many small burrows (millimetres diameter) within the upper 3–5 cm and build a few larger burrows (1–10 cm diameter, some with reinforced lining) extending down as much as 15–20 cm (Fig. 8). On the Eel shelf, the dominance of subsurface-deposit versus surface-deposit feeders minimizes the importance of faecal pelletization at the seabed surface (Drake, 1999). Biogenic seabed roughness is important seaward of ~60 m depth (Cutter & Diaz, 2000), but monitoring observations in these deeper shelf locations (Ogston *et al.*, 2004) demonstrate significant temporal variability as storm events form ripples, even on substrates of silt and clay.

Subsurface bioturbation can be quantified from seabed profiles (upper 4–8 cm) of the short-lived radioisotope ^{234}Th (half-life 24 days; Aller & Cochran, 1976; Wheatcroft & Martin, 1996). The **biodiffusion coefficient** is moderately high (3 cm^{2} yr^{-1}

to > 100 $cm^2 yr^{-1}$, mean 20–30 $cm^2 yr^{-1}$; Bentley & Nittrouer, 2003; Wheatcroft, 2006) on the Eel margin. It reveals substantial small-scale variability over tens of metres, but also demonstrates a decrease between the shelf and the deeper continental slope (water depth > 500 m; Wheatcroft *et al.*, this volume, pp. 101–155). Most interesting is the temporal variability in bioturbation. Organism abundance shows an increase during summer and autumn, and a decrease in winter due to annual cycles of recruitment and growth (Wheatcroft, 2006). Although the extreme flood of January 1997 caused a subsequent drop in abundance, the mortality that year was comparable with other winters without major floods, and was consistent with weak seasonal changes in biodiffusive mixing intensity (slight increases in autumn). Winter is normally a period of low numbers of benthic organisms and low bioturbation activity in the seabed. Therefore, the Eel margin benthic community is well adapted to seasonal cycles in storm reworking and flood deposition.

The dominance of the subsurface-deposit feeders controls the preservation of sedimentary signals on the Eel margin. Important factors are thickness of event signals (storm reworking, flood deposits), thickness of the surface mixing layer, intensity of bioturbation (biodiffusion coefficient) and the sediment accumulation rate. Knowledge of these terms allows evaluation of the **transit time** for a signal to pass through the surface mixing layer, and the **dissipation time** for destruction of the signal (Wheatcroft, 1990). For the Eel shelf, the transit time is 9–65 yr and the dissipation time is ~2 yr; therefore, most signals are destroyed before they can be preserved (Wheatcroft & Drake, 2003). This is particularly true for physical sedimentary structures, which are lost due to particle mixing with overlying and underlying sediment. Event layers > 5 cm thick can be preserved, but those < 3 cm cannot. Other event signals (e.g. increased clay content, decreased ^{210}Pb activity, increased terrestrial carbon) are smeared vertically, but are still recognizable in preserved strata (Sommerfield & Nittrouer, 1999; Blair *et al.*, 2003; Wheatcroft & Drake, 2003). The timing of subsequent events can have an impact on preservation. For example, emplacement of the 1997 flood deposit effectively decreased the transit time for the 1995 flood deposit and allowed its partial preservation. Without such benefit, the 1997 flood deposit was destroyed in 2.5 yr (Wheatcroft & Drake, 2003).

SEDIMENT DISPERSAL SYSTEM

The dispersal of sediment on continental margins has been reviewed in this volume by Sommerfield *et al.* (pp. 157–212).

General considerations

Fluvial sediment is delivered to the seabed, where it undergoes alteration that influences its burial or transport to more distal locations. The integrated result over decades and centuries (i.e. longer than the transit time through the surface mixing layer) is a sedimentary deposit stretching along a succession of hydraulically contiguous sedimentary environments. This succession of environments is a **sediment dispersal system** (Sommerfield *et al.*, this volume, pp. 157–212) and the marine portion is just part of a longer system stretching from terrestrial sources. The expansion of time-scales brings new factors into the consideration of margin sedimentation. The slowing of **eustatic** (i.e. global) sea-level rise ~5000 yr ago (from ~5 mm yr^{-1} to ~2 mm yr^{-1}) has allowed some rivers to fill their estuaries, to extend sediment dispersal systems to the continental shelf and slope, and to form deposits with significant morphological expression (e.g. subaerial and subaqueous **deltas**). As such deposits build toward ambient sea level, they consume the space available for sediment accumulation (i.e. accommodation space). On active margins, vertical **tectonic motions** cause subsidence and uplift that adds or subtracts space for further sedimentation. Changes in accommodation space can put the seafloor into or out of energetic environments reworked by physical processes (e.g. surface waves), and can lead to displacement of sedimentation along a dispersal system.

The increased time-scale also brings climatic variability into consideration. Fluctuations in global precipitation patterns have caused periods, lasting from many decades to centuries during the late Holocene, when North America was wet and flood-prone (Ely *et al.*, 1993; Knox, 2000). On shorter time-scales, ENSO (El Niño–Southern Oscillation) and PDO (Pacific Decadal Oscillation) events have impacted fluvial discharge (Inman & Jenkins, 1999; Farnsworth & Milliman, 2003). Land use by humans has compounded the climatic impacts, both increasing sediment discharge (farming, logging) and decreasing discharge (damming, diverting). Global sediment budgets indicate there has been an anthropogenic increase in fluvial transport (from 14 to 16 Gt yr^{-1}). They also suggest ~30% trapping of this sediment landward of the coast, so that the net discharge to the ocean is ~10% less than natural levels (12.6 Gt yr^{-1}; Syvitski *et al.*, 2005). Global budgets mean nothing to individual rivers, where the scales of perturbations, the mechanisms associated with sediment routing and the storage capacity of the basin determine the impact of perturbations (Walling, 1999). Generally, these factors lead to anthropogenic impacts being greatest (and commonly most conspicuous) on rivers of small to moderate size.

The diversity and intensity of processes operating on continental margins creates the rich record of events preserved in the deposits of sediment dispersal systems. However, these same processes cause erosion and time gaps (i.e. **hiatuses**) in the record over a range of scales (e.g. storm erosion, sea-level change). In this regard, the metric for quantitatively evaluating sedimentation is the mass flux into the seabed, averaged over some time-scale. Ephemeral placement on the seabed is **deposition**, but the sediment is subsequently impacted by **erosion**. The integrated sum of deposition and erosion through time is **accumulation**. The relevant time-scales for deposition rate and accumulation rate can be set for any processes of interest (McKee *et al.*, 1983). As described for this discussion of sediment dispersal systems, deposition refers to sediment placement over days/months and accumulation is the net growth of the seabed over decades/centuries. The distinction is important, because mass flux into the seabed is inversely related to the time-scale of integration (e.g. Fig. 9; Sadler, 1981; Sommerfield, 2006), as the result of more and of more severe hiatuses impacting strata formation over progressively longer time-scales.

Fortunately, a range of natural and artificial **radioisotopes** is found in terrestrial and marine environments, and they can serve as chronometers tagged to sediment particles. The large surface area (per gram of sediment) and the surface charges of silt and clay particles allow them to adsorb large concentrations of particle-reactive chemical components, including radioisotopes. Analytical techniques typically limit sedimentological use of radioisotopes to a time-scale < 4–5 half-lives. Of

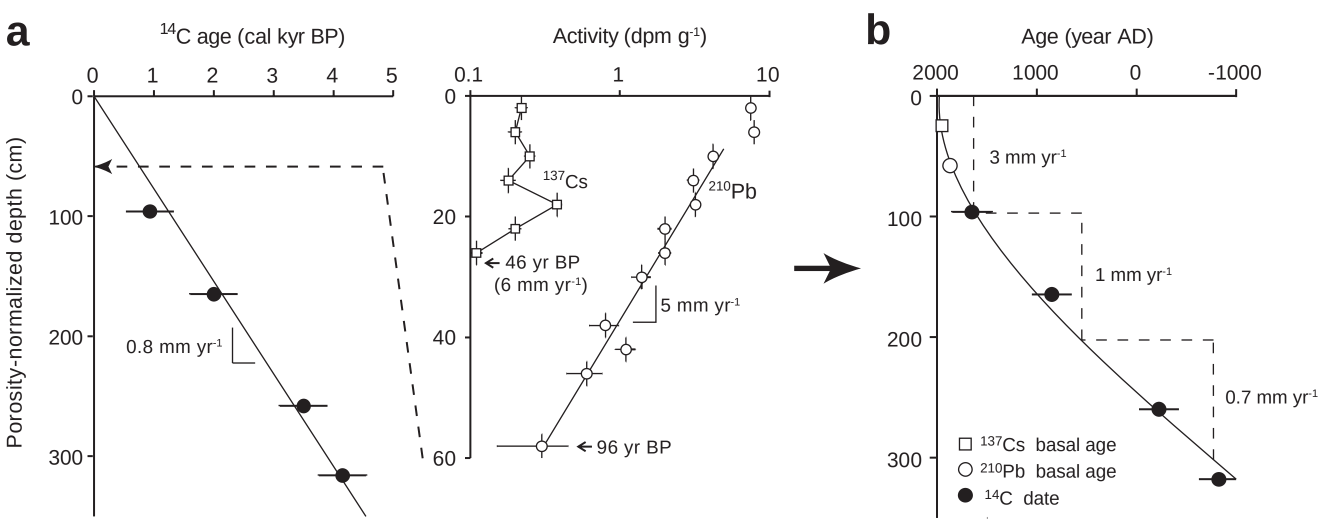

Fig. 9 Accumulation rates of Eel shelf sediments. (a) The two profiles show ^{14}C, ^{210}Pb and ^{137}Cs for the same site on the Eel shelf (95 m water-depth), and allow calculation of accumulation rates integrated over time-scales of ~3000 yr, ~100 yr and ~50 yr, respectively (data points have been adjusted vertically to a uniform bulk porosity). (b) Composite profile illustrating vertical changes in ages and accumulation rates within the seabed. The accumulation rates are greater for the uppermost sediment column, because it retains a record that is more complete than the underlying strata. (From Sommerfield *et al.*, this volume.)

special relevance here (Sommerfield *et al.*, this volume, pp. 157–212), ^{234}Th (half-life 24 days) and ^{7}Be (half-life 53 days) have primary sources, respectively, in ocean water (from decay of dissolved ^{238}U) and in terrestrial soils (from cosmogenic fallout). Lead-210 (half-life 22 yr) has several potential sources but, in ocean water, primarily comes from decay of ^{238}U-series radioisotopes. Lead-210 accumulation rates are commonly verified by profiles of ^{137}Cs (Fig. 9), a bomb-produced radioisotope. Caesium-137 was globally distributed by transport through the atmosphere and by subsequent fallout, and it first reached continental-margin sediments in ~1954. On the long end of these discussions, ^{14}C (half-life 5730 yr) ages are recorded in organic C (e.g. wood fragments) and inorganic $CaCO_3$ (e.g. shell fragments).

By using radiochemical tools with different half-lives, a composite understanding can be obtained for continental-margin sedimentation over a range of time-scales. For example, the dichotomy between deposition and accumulation rates can be related to processes and patterns of sediment dispersal. The Yangtze River undergoes flooding during the quiescent summer months, and rapidly deposits much sediment on the continental shelf near its mouth. However, longer-term accumulation rates indicate that winter storms remove and transport > 50% of this sediment to distal portions of the dispersal system (McKee *et al.*, 1983; DeMaster *et al.*, 1985). In contrast, the Amazon River has peak discharge during intervals of seasonally intense tradewinds and waves, and most of its sediment discharge (> 50%) is immediately displaced along the dispersal system > 200 km from the river mouth, to shelf areas where it deposits and near where it ultimately accumulates (Kuehl *et al.*, 1986, 1996).

Eel margin sediment dispersal system

The Eel basin has experienced multiple decades of sustained wet, dry and variable conditions during the past 100 yr (Sommerfield *et al.*, this volume, pp. 157–212). El Niño–Southern Oscillation events can bring unusual precipitation, but the location of the basin between latitudinal weather bands precludes a clear repetitive signal (e.g. El Niño brought the driest year in 1977, and the wettest year in 1983). The second half of the 1900s was a period with increased logging in the Eel basin, and, together with enhanced precipitation (Sommerfield *et al.*, 2002), this land use significantly increased sediment yield (by 23–45%). Other forms of human interaction (e.g. damming) were minimal, so the increased sediment flux was transferred to the ocean.

In addition to the storm-related physical oceanographic processes near the Eel mouth that have been described above, regional circulation influences distal portions of the dispersal system. Seaward of the shelf break, the **California Current** flows southward (Hickey, 1979, 1998) and, on the shelf, the **Davidson Current** flows northward during the autumn and winter (Strub *et al.*, 1987). The local promontories (Cape Mendocino, Trinidad Head) can deflect these currents (Pullen & Allen, 2000), leading to the seaward transport of water and suspended sediment and to the development of eddies (Washburn *et al.*, 1993; Walsh & Nittrouer, 1999). Other morphological features on the Eel margin influence the fate of water and sediment, especially Eel Canyon, which forms a chasm across the southern boundary. More subtle across-margin ridges (**anticlines**) and depressions (**synclines**) are moving up and down at rates of millimetres per year (averaged over millennia; Orange, 1999).

Sediment deposition on the Eel margin is clearly demonstrated by the distribution patterns associated with the 1995 and 1997 flood events, which discharged $\sim 24 \times 10^{6}$ t and $\sim 29 \times 10^{6}$ t of sediment, respectively (Wheatcroft & Borgeld, 2000). Both events formed elliptical deposits on the middle shelf north of the Eel mouth (Figs 5 & 10), representing 20–30% and 15–30% of the mass discharged, respectively. The similarity of the two deposits suggests that the mechanisms of emplacement operated in a repetitive manner. The remainder of the sediment could deposit landward, northward, southward or seaward of these deposits. The inner-shelf sands contain some intermixed mud, and Humboldt Bay might receive some sediment through tidal exchange and estuarine circulation. The Davidson and California Currents could move some surface plumes of sediment beyond the confines of the Eel margin (e.g. Mertes & Warrick, 2001). However, the bulk of sediment is thought to be transported seaward of the Eel shelf by a combination of hyperpycnal flows, storm-induced fluid muds and intermediate nepheloid layers.

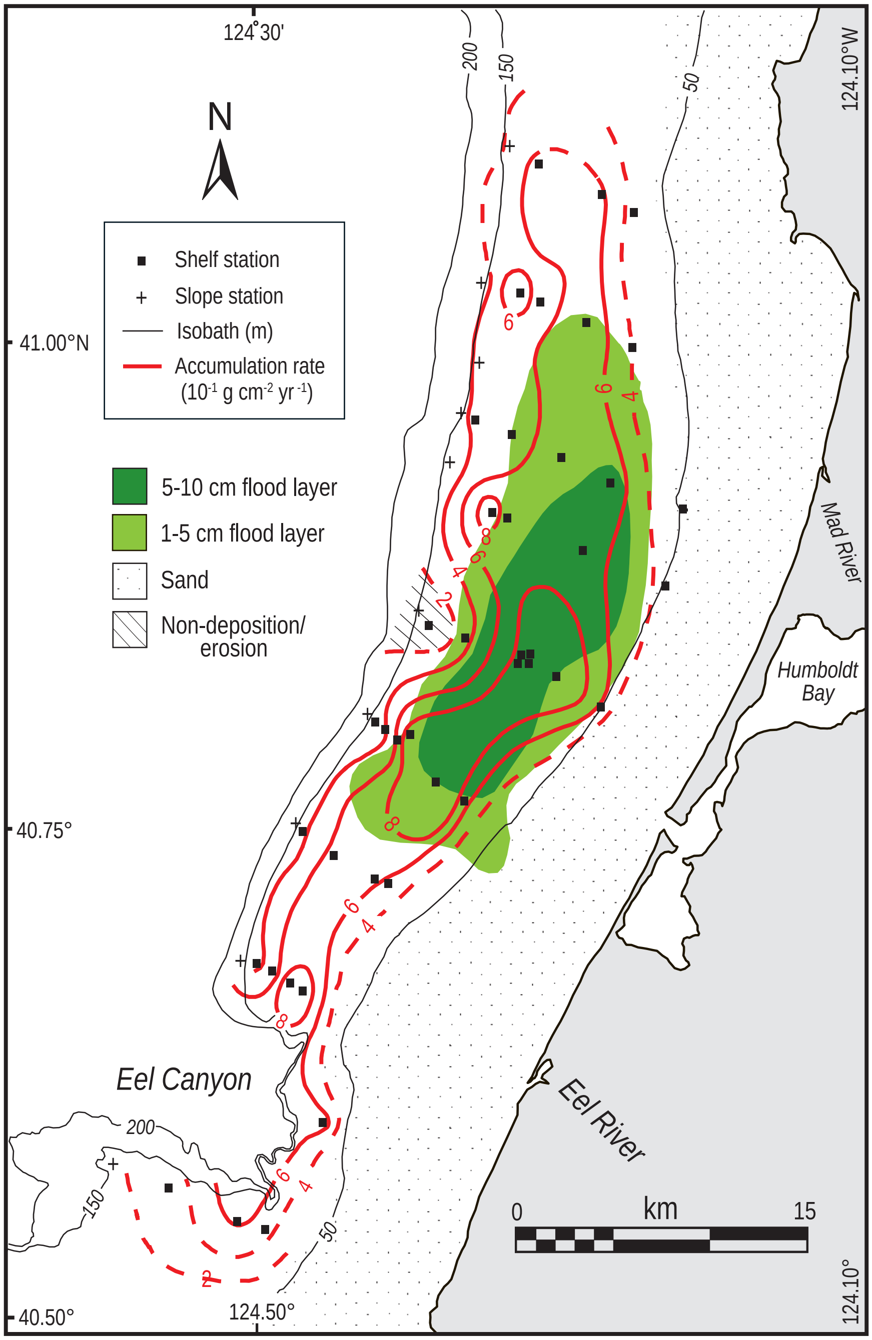

Fig. 10 Contour map of ^{210}Pb accumulation rates (red isopach lines) on the Eel shelf, superimposed on the thickness of the January 1995 flood deposit (green shaded areas). They coincide well, and indicate maximum values in ~50–70 m water depth and ~10–30 km north of the river mouth. Approximately 20–30% of sediment discharged by the 1995 flood remained on the shelf, and this fraction is similar to that retained over a 100-yr time-scale. (Modified from Sommerfield & Nittrouer, 1999.)

On time-scales of decades and centuries, the fate of silt and clay from the Eel River shows a similar pattern: ~10% is buried with inner-shelf sands (< 60-m water depth; Crockett & Nittrouer, 2004), ~20% accumulates on the middle and outer shelf (Fig. 10; Sommerfield & Nittrouer, 1999), and the remainder is exported to deeper water. Accumulation on the upper slope (150–800 m) accounts for ~20% of the Eel sediment discharge (Alexander & Simoneau, 1999) and Eel Canyon is the alternative pathway on the slope (Mullenbach & Nittrouer, 2000, 2006). These observations demonstrate that the Eel shelf traps less than a third of modern sediment discharge. They also highlight the importance of Eel Canyon for dispersing sediment seaward; as much as 50% of the river discharge could be moving into and through the canyon. Both the escape of sediment from the shelf and the large flux through Eel Canyon are occurring during the present highstand of sea level, and probably reflect sedimentation typical of narrow, tectonically active continental margins.

The accumulated strata reveal interesting sedimentary trends along the dispersal system. Grain size decreases progressively with distance from the Eel mouth, both northward and seaward. Fining continues across the slope, but includes an anomalously coarse zone below the shelf break (250–350 m water depth; Alexander & Simoneau, 1999), possibly due to winnowing by shoaling internal waves (Cacchione *et al.*, 2002). Organic carbon shows a progressive increase in the marine component relative to the terrestrial component with distance from the Eel River (Blair *et al.*, 2003). Temporal changes are also observed for the past ~4000 yr (Sommerfield *et al.*, this volume, pp. 157–212). The accumulating sediment has progressively become finer (less sand, more silt) as the dispersal system has evolved since sea-level rise slowed. For the past 200 yr the upward fining trend has been accelerated by human impacts on land use. The magnitude and frequency of flood events also have increased, imposing the sedimentary characteristics of those events: high sediment flux, increased clay content, much terrestrial carbon. The changes have been particularly acute during the past 50 yr (Sommerfield *et al.*, 2002), and reflect the combined effects of land use (clear cutting, road building) and climatic increases in precipitation intensity.

There is a distinct similarity of the shelf patterns in flood deposition and accumulation rates over decades/centuries (see Figs 5 & 10). This is due to the correlation of river discharge and energetic oceanic conditions. Most sediment is immediately transported to a stable location for accumulation (i.e. where it will not be eroded by strong boundary shear stresses), rather than being temporarily deposited and subsequently transported. In this regard, the Eel margin more closely approximates the conditions of shelf deposition/accumulation near the mouth of the Amazon River than those near the Yangtze River. However, the accumulation pattern over decades/centuries also matches well with thicknesses of late Holocene strata (see below), which are related to tectonic features on the shelf (Orange, 1999; Burger *et al.*, 2002; Spinelli & Field, 2003). Millenial accumulation rates are < 1 mm yr^{-1} over anticlines, and reach 6 mm yr^{-1} in synclines. The similarity of accumulation patterns suggests that tectonic activity on the margin impacts sedimentation on scales as short as decades (as detailed in Sommerfield *et al.*, this volume, pp. 157–212). Likely candidates for the operative mechanisms are gravity flows, which are common on the Eel margin and respond to subtle gradients of the seabed.

SEABED FAILURE

The processes and products of seabed failure on continental margins have been addressed in this volume by Lee *et al.* (pp. 213–274) and Syvitski *et al.* (pp. 459–529).

General considerations

The dispersal of sediment to sites of accumulation is a continuing process; new sediment buries old sediment, causing consolidation and development of strength to resist subsequent shear forces. However, in some cases, forces exerted on the seabed are stronger than the strength developed, and the seabed fails. The resulting **mass movement** is driven by body forces (i.e. gravity) rather than by fluid stresses exerted on the seabed surface. In this way, mass movement differs from sediment erosion and transport. Some famous failures have occurred in the past 100 yr, including the 1929 Grand Banks (Heezen & Ewing, 1952), 1964 Alaska (Coulter & Migliaccio, 1966; Lemke, 1967) and 1998 Papua New Guinea (Tappin *et al.*, 1999; Geist, 2000) landslides; all were triggered by earthquakes and all initiated tsunamis. Failures can be triggered by other processes, including large waves associated with storms, such as Hurricane Camille in 1969 (Sterling & Strohbeck, 1973; Bea *et al.*, 1983) and more recent hurricanes in the Gulf of Mexico. Large landslides have also occurred in the geological past leaving scars and deposits as evidence, such as the Storrega landslides (Bryn *et al.*, 2003) during the Pleistocene and Holocene (most recently ~8200 yr ago). These removed a large piece of the Norwegian continental margin (~3000 km^3) and displaced it over a region stretching ~800 km.

The largest landslides on Earth are found in the ocean.

Underwater **landslides** move sediment with a range of speed and internal deformation of the deposit (Varnes, 1958). Subclasses of movement include **creep,** when the movement is slow, and **slumps,** when sediment blocks rotate along a curved failure surface. **Liquefaction** occurs when loosely packed particles temporarily lose contact with each other, and the weight of the deposit becomes supported by pore fluids. All styles of failure can lead to disintegration of the sediment deposits, and development of gravity flows (e.g. debris flows, turbidity currents).

Failures and landslides are prevalent in environments of the continental margin where thick deposits of soft sediment accumulate. Fjords can receive large amounts of rock flour (with limited cohesion) that rapidly accumulate on steep gradients (some > 5°). Fjord sediments are commonly organic rich and produce methane gas. Subsequent earthquakes or even very low tides can initiate failure (Syvitski & Farrow, 1983; Prior *et al.*, 1986). Deltas are also loci of rapid accumulation, and despite gentle gradients (usually < 2°) can fail in response to earthquakes or storms (Coleman *et al.*, 1980; Field *et al.*, 1982). Continental slopes are extensive and steep (> 4°) regions with a propensity for failure, which is accentuated during lowstands of sea level when fluvial and glacial sediment discharge occurs directly at the top of the slope. Gas and gas hydrates, which commonly form on continental slopes, can be responsible for failures (Field & Barber, 1993), especially with sea-level fall that reduces hydrostatic pressure on the seabed and causes dissociation of hydrates (Kayen & Lee, 1991). Submarine canyons are regions of preferential sediment accumulation, and failures near their heads can lead to gravity flows that supply sediment to submarine fans at the bases of the canyons (Hampton, 1972; Booth *et al.*, 1993). Especially important are failures triggered by earthquakes on active margins that cause turbidity currents to transport much sediment long distances (e.g. Goldfinger *et al.*, 2003). During the present highstand of sea level, continental slopes are generally below the depth of surface-wave influence, but the heads of submarine canyons are in shallower water and can be impacted by energetic waves (Puig *et al.*, 2004). From observations in a range of sedimentary environments, the factors recognized to influence failures are sediment accumulation rates, bathymetric gradients, seismicity, storm waves and gas.

Failures and landslides occur when and where driving stresses exceed shear resistance. Bathymetry is important because it defines the gravity-induced stresses. Earthquakes cause cyclic accelerations in addition to gravity (Lee & Edwards, 1986). Similarly, large storm waves produce alternating pressures that create stresses superimposed on those from gravity (Henkel, 1970). In opposition to the applied stresses is the **shear strength** of the seabed, which is defined as the limit of stress before failure. The shear strength of sediment increases as it is buried by subsequent accumulation and as the seabed consolidates. The **factor of safety** for the seabed is the shear strength divided by the shear stress. In addition to large stresses, the factor of safety can be reduced by a loss of shear strength. A common mechanism is the development of excess pore pressures, due to (i) the inability to remove pore fluids during consolidation (e.g. under high accumulation rates; Coleman & Garrison, 1977), (ii) the development of gas bubbles (e.g. from the decay of organic matter or the dissociation of hydrates; Kayen & Lee, 1991) and (iii) the infusion of additional water (e.g. by groundwater seepage). Earthquakes and storm waves apply stresses cyclically, which destroys particle fabric (i.e. grain-to-grain contact), causes liquefaction (Seed, 1968), and increases pore pressures. Human activity can cause failure as well, commonly from construction at or near the shoreline that destabilizes the seabed. Sometimes, the resulting landslides even stimulate tsunamis, e.g. during 1979 in Nice, France (Seed *et al.*, 1988) and during 1994 in Skagway, Alaska (Rabinovich *et al.*, 1999).

Whether by increased stresses, reduced strength or both, marine sediments can fail. After failure, they create landslide deposits or disintegrate into fluid flows (Hampton *et al.*, 1996), depending on the bulk density (i.e. porosity) of the sediment (Poulos *et al.*, 1985; Lee *et al.*, 1991). A critical threshold separating these two fates (i.e. slide deposit from fluid flow) can be defined for each sediment type. If seabed conditions have densities below this threshold (**contractive sediment**), then excess pore pressures will develop after failure, and the sediment will flow. Densities above this threshold (**dilatant sediment**) will cause the sediment to strengthen after failure, and it will not flow. The transition to flow can be facilitated during failure by other factors, including large amounts of energy exerted and water added.

Eel margin failure

The Eel margin exhibits conditions conducive to seabed failure: rapid sediment accumulation; steep bathymetric gradients; intense seismicity; energetic storm waves; and plentiful gas. The largest feature on the Eel margin (~90 km^2) with the outward appearance of failure is known as the 'Humboldt Slide' (Field *et al.*, 1980), but its origin is controversial. It is found in an amphitheatre-like depression between 220-m and 650-m water depth (Fig. 11), just north of Eel Canyon. The upper portion of the amphitheatre (above 380-m water depth) is overconsolidated, consistent with removal of ~15 m of sediment (Lee *et al.*, 1981). Analysis of the sediment indicates that the density state would preclude transition to a flow, and that the failed sediment would create a deformed slide deposit at its base (Lee *et al.*, 1991). Recent multibeam surveys (Fig. 11; Goff *et al.*, 1999) and high-resolution seismic profiling (Fig. 12a; Gardner *et al.*, 1999) demonstrate that the lower portion of the deposit is a crenulated surface with ridges and swales, similar to subaerial landslide deposits. The profiles suggest that the greatest failure was in the middle of the 'slide', and that it underwent a small amount of downslope translation with shallow rotation, creating gentle compression folds at its base. Deeper profiles show older deposits of similar character and imply a long history of such events (Field *et al.*, 1980). The multibeam surveys also document many pockmarks, interpreted as evidence of gas escape from the seabed (Yun *et al.*, 1999), and many erosive gullies on the rim of the feature (above 380-m water depth, see Fig. 11).

These gullies possibly reflect processes related to an alternative origin: erosive gravity flows on the rim and depositional 'sediment waves' at the base (Fig. 11). Such processes and morphology have

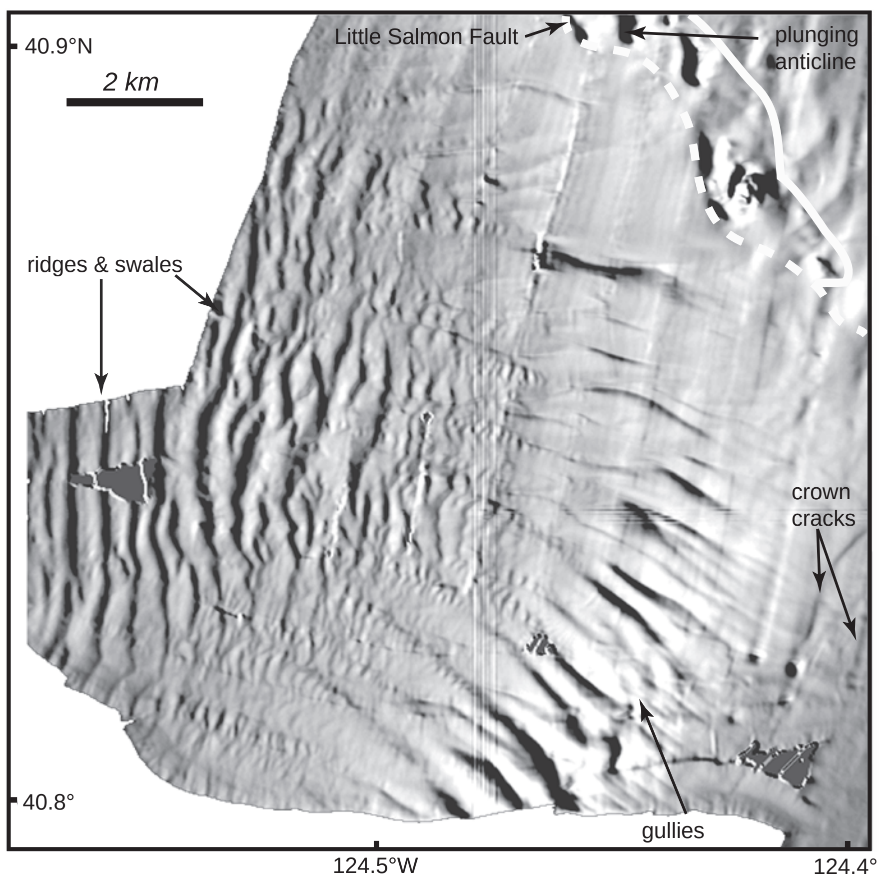

Fig. 11 Multibeam bathymetry of 'Humboldt Slide' on the Eel continental slope immediately north of Eel Canyon and south of the Little Salmon Anticline. Deep gullies are found on the upper rim, and ridges and swales are at the base. (Modified from Gardner *et al.*, 1999.)

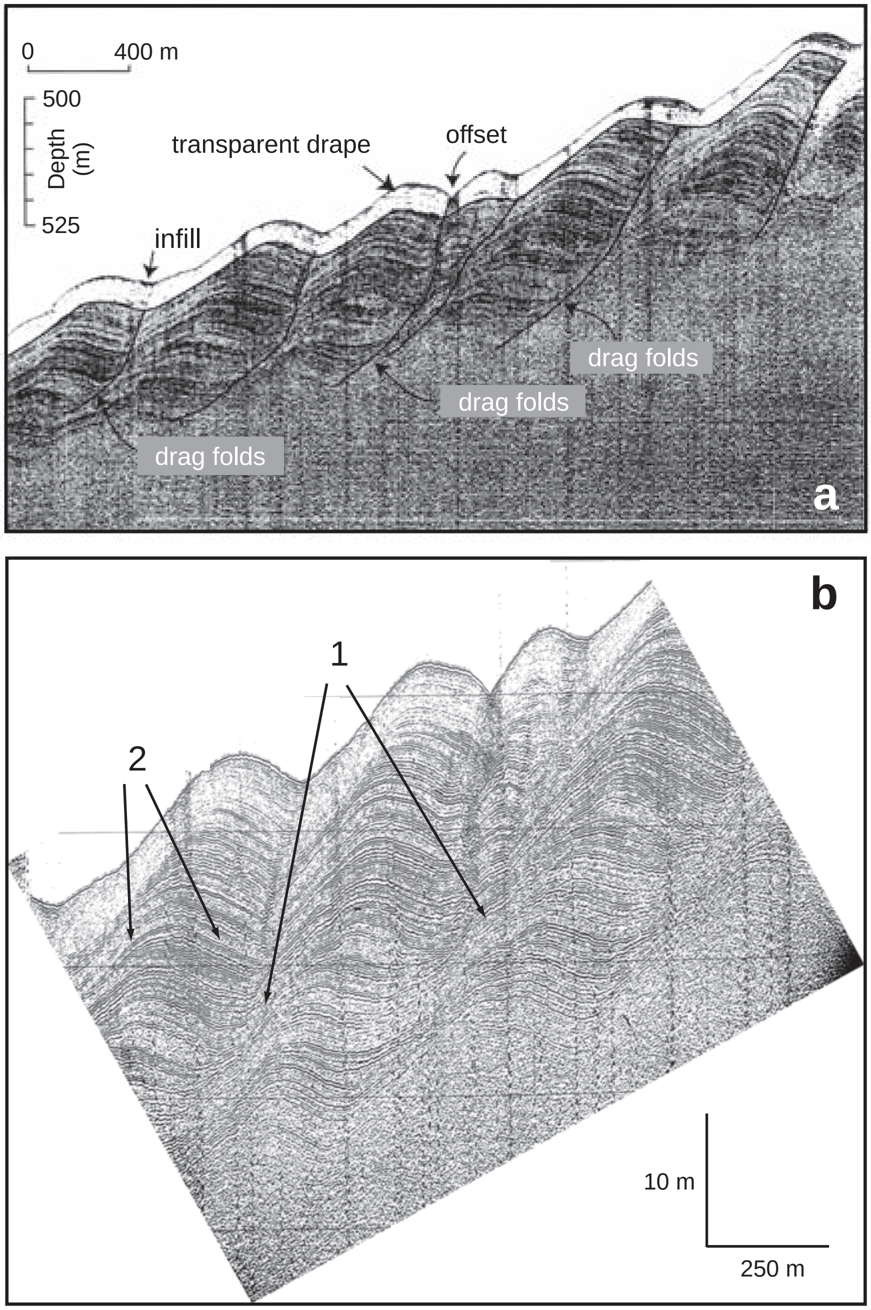

Fig. 12 Seismic profiles from the main body of the 'Humboldt Slide'. (a) Profile with an interpretation of folded and back-rotated slide blocks. Shear surfaces are shown by black lines, with drag folds near bases. (From Lee *et al.*, this volume; modified from Gardner *et al.*, 1999.) (b) Profile showing evidence of a 'sediment wave' origin: 1, internal reflectors can be followed between 'waves'; 2, beds on the upslope side are thicker than those on the downslope side. (From Lee *et al.*, this volume; modified from Lee *et al.*, 2002.)

been interpreted for similar features elsewhere in the world, and are extrapolated to the 'Humboldt Slide' (Lee *et al.*, 2002). Sediment transported as hyperpycnal flows directly from Eel River and sediment reconstituted with seawater to create fluid-mud flows move across the shelf break to the steeper slope. There, they undergo a transition into turbidity currents that erode the seabed. These currents create the gullies and expose overconsolidated sediment. Near the base, where the bathymetric gradient is more gentle, the turbidity currents deposit their load in the form of 'sediment waves', which explains the origin of the ridges and swales (Fig. 11). These contain internal reflectors that can be traced from one 'wave' to the next (Fig. 12b), which should not be the case for landslide deposits. The reflectors also show asymmetry, with greatest sediment thicknesses on the upslope side of the 'wave' (Fig. 12b) due to preferential sedimentation, a process observed for bedforms in other slope areas with active sediment waves.

Evidence remains on both sides of the argument whether 'Humboldt Slide' is truly the result of a slide or of sediment transport, but critical consideration of the controversy is important, because similar features abound on continental margins: off the west coast of Africa (Wynn *et al.*, 2000); off British Columbia (Bornhold & Prior, 1990); and in the Adriatic Sea (Correggiari *et al.*, 2001).

South of the 'Humboldt Slide', liquefaction has been invoked as an active mechanism for generating gravity flows of fluid mud in the head of Eel Canyon (Puig *et al.*, 2004), which is located at ~90-m water depth. These flows were observed soon after the beginning of dry storms with waves capable of reaching that depth. The speed of response, lack of river floods and measured wave impacts all suggest liquefaction due to wave-induced loading, a mechanism that was documented to occur many times during the winter (Puig *et al.*, 2004) and to provide seabed deposits widely observed through the canyon head (Mullenbach *et al.*, 2004; Drexler *et al.*, 2006).

Other than the controversial 'Humboldt Slide' and the liquefaction in the Eel Canyon head, the Eel margin is relatively devoid of evidence for failure, considering the environmental conditions that make it a prime candidate. Other factors have been invoked to explain the apparent stability of the seabed. Laboratory consolidation experiments suggest that the intense bioturbation on the Eel margin might be responsible for strengthening the seabed (Lee *et al.*, this volume, pp. 213–274). The sediment repackaging processes associated with faecal-pellet production can create sediment with greater bulk density than a rapidly deposited and unbioturbated seabed. This process is dependent on the ambient benthic community, because some other areas experience increased porosity from bioturbation (Bokuniewicz *et al.*, 1975; de Deckere *et al.*, 2001). Another possible explanation for the apparent stability of the Eel margin seabed is strengthening by seismic activity. Studies have shown that repeated seismic events below the threshold of failure can increase seabed density and strength (Boulanger, 2000). Laboratory experiments reveal the mechanism to be a development of excess pore pressures during earthquakes, which led to the subsequent drainage of pore fluids. The result is a seabed with properties of overconsolidation.

GRAVITY FLOWS

The properties and significance of sediment gravity flows on continental margins have been reviewed in this volume by Parsons *et al.* (pp. 275–337) and Syvitski *et al.* (pp. 459–529).

General considerations

Many seabed failures (contractive sediment) produce **gravity flows**, which continue down slope due to suspended-sediment concentrations sufficient to exceed the density of the surrounding fluid. In other cases, dense concentrations are injected from rivers or are formed in shallow water, generating hyperpycnal and fluid-mud flows, respectively. The fundamental importance of gravity flows is their ability to transport quickly large masses of sediment across isobaths: across sedimentary regimes (e.g. from inner-shelf sand to mid-shelf mud), across the shelf break, and across the continental slope to build submarine fans on the continental rise. Turbidity currents were studied relatively early in the history of marine sedimentology, because they were generated by the 1929 Grand Banks earthquake and failure. These turbidity currents left multiple records of their occurrence: deposits known as **turbidites**, and the sequential destruction of telegraph cables lying along the continental slope and rise. Turbidity currents are **autosuspending** (or **ignitive**), which means that they erode the seabed (replacing sediment left behind as turbidites), refuelling the currents and allowing them to travel long distances (Parker, 1982; Pantin, 2001). Distinctive strata deposited by turbidity currents have been recognized since the 1800s as the **flysch** deposits defined in Europe, but the formative mechanisms were not linked to them until much later (Kuenen & Migliorini, 1950). Subsequently, the repetitive signatures of turbidites were documented to be a series of distinctive sedimentary structures, which are formed by bedload and suspended load during successive phases of waning flow (Bouma, 1962).

Although turbidity currents occur in the modern ocean (e.g. Congo Canyon, Khripounoff *et al.*, 2003; Monterey Canyon, Xu *et al.*, 2004), their unpredictable and energetic nature makes them difficult to observe directly. As a consequence, most of our understanding about the mechanics of these flows comes from laboratory simulations and numerical modelling. The operation of turbidity currents is strongly influenced by turbulent mixing at several boundaries:

1 the bottom boundary, where frictional drag on the seabed causes erosion and constrains deposition;
2 the top boundary, where the current interacts with the overlying fluid and loses sediment due to mixing associated with shear;
3 the leading edge (**front**), which has the most intense mixing. This mixing slows the front, so it moves with a velocity less than the body. Three-dimensional instabilities occur at the front (Parsons, 1998), creating vortices that counter rotate in a plane perpendicular to the direction of current flow. The front develops an irregular shape with lobes and clefts (Hartel *et al.*, 2000).

The centre of a turbidity current is intensely erosional (García & Parker, 1993), but the periphery is depositional (Fig. 13a), creating constructional features on the sides that contain the flow (i.e. **levees**). The resulting channels have many morphological similarities with subaerial river channels (e.g. meanders, point bars, crevasse splays; Hagen *et al.*, 1994; Peakall *et al.*, 2000). However, the fluid surrounding the turbidity current is seawater of nearly equal density, not low-density air, and this distinction causes differences in operational processes and in details of the resulting morphological features. A good example is levee construction (Peakall

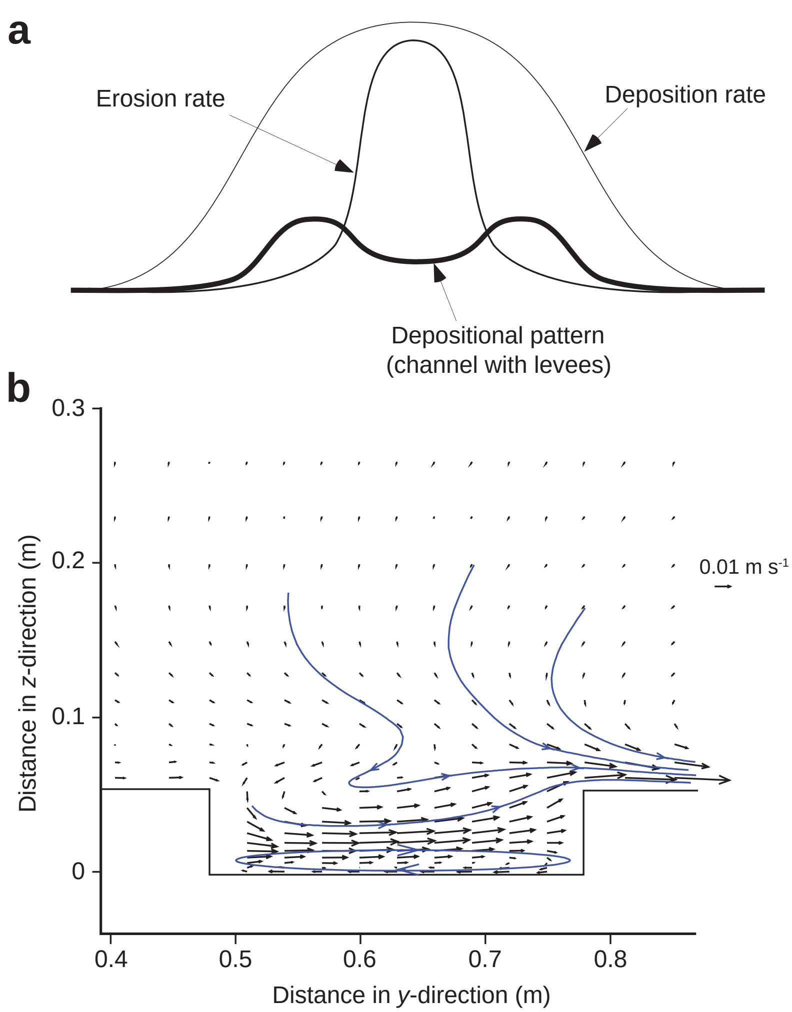

Fig. 13 (a) Diagram showing the relationships of deposition and erosion rates distributed across a turbidity current. The net result is a depositional pattern with levees and channel that confine the flow. (From Parsons *et al.*, this volume.) (b) From numerical modelling, secondary circulation (arrows) at a meander bend of a submarine channel experiencing a turbidity current. A suppressed circulation cell develops near the bed and substantial flow leaves the channel (known as flow stripping). (From Parsons *et al.*, this volume; modified from Kassem & Imran, 2004.)

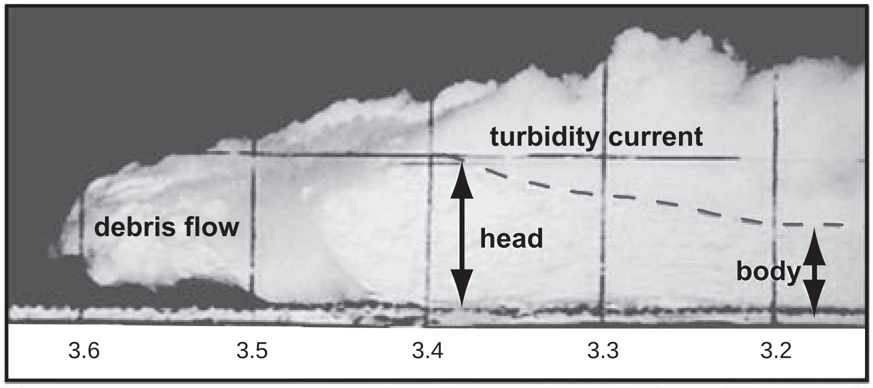

Fig. 14 A debris flow in flume experiment, with flow lifting above the bed as its head begins to hydroplane. A turbidity current can be seen developing on the upper surface of the debris flow. (From Parsons *et al.*, this volume; modified from Marr *et al.*, 2001.)

et al., 2000), which occurs due to **overspill** when turbidity-current water and suspended-sediment extend onto the flanks of the channel (Hiscott *et al.*, 1997). One cause of overspill is Coriolis force, which has a more significant impact in submarine channels than river channels (Klaucke *et al.*, 1998), and leads to dramatic asymmetry in levee heights (i.e. in direction of flow, the right levee is higher for channels in the northern hemisphere). **Superelevation** of the turbidity-current surface occurs due to centrifugal forces on the outside of meander bends. Although modest in rivers (few centimetres), superelevation in submarine channels (Hay, 1987; Imran *et al.*, 1999) is comparable to channel depth (i.e. flow thickness doubles). As levees build upward due to overspill from Coriolis and centrifugal forces, so does the channel bed, creating channel systems that are perched well above the surrounding seafloor (Flood *et al.*, 1991). Secondary circulation in these channels is much more complex (Fig. 13b) than in river channels (e.g. helical circulation), largely as a result of the ease with which turbidity currents can extend above the levees and flow independently (known as **flow stripping**; Piper & Normark, 1983).

Debris flows are gravity flows with greater sediment concentrations than turbidity currents, and in which turbulent motions are limited to the heads of the flows (Marr *et al.*, 2001). On land, debris flows have devastating impacts on communities in mountainous areas (Costa, 1984), and, in the ocean, they transport much sediment and create abundant strata (Elverhøi *et al.*, 1997). In contrast to turbidity currents, the dominant factors controlling the behaviour of debris flows come from pore pressures and grain-to-grain interactions. Some clay is necessary to reduce permeability and maintain excess pore pressures (Marr *et al.*, 2001). The mechanics of operation are similar on land and underwater, and are characterized by flow as non-Newtonian fluids. Differences between subaerial and submarine debris flows are again due to the density difference between air and seawater. Very strong pressures are created by a submarine debris flow as it accelerates down slope and displaces water. If the water is not displaced quickly enough, the debris flow will separate from the seafloor (Fig. 14) and begin to **hydroplane** on a thin layer of lubricating water (Mohrig *et al.*, 1998). Consequently, the head regions of submarine flows move faster than those of subaerial flows, and the submarine flows cover more distance (known as **runout**). The head also moves faster than the body of a submarine debris flow (in contrast to turbidity currents), commonly causing the head to separate and achieve much greater runout than the body of the flow (Prior *et al.*, 1984; Nissen *et al.*, 1999).

The generation and deposition of different types of gravity flows can be interrelated. Turbidity currents are commonly produced due to shear on the front and upper surface of a debris flow (Fig. 14). This process depends on how readily the debris-flow slurry breaks into pieces and becomes turbulent (Marr *et al.*, 2001), either by entrainment of fluid (most efficient) or by grain-by-grain erosion. After motion of a debris flow terminates, the associated turbidity current continues. Although only ~1% of the debris-flow sediment is needed to form a turbidity current, that current forms a flow about six times thicker (Mohrig *et al.*, 1998). When all motion has ended, the debris-flow deposit is surrounded by finer-grained turbidites on top and in front, reflecting another mechanism for creating turbidity currents.

8.2 Eel margin gravity flows

The modern Eel margin contains a broad range of gravity flows. Hyperpycnal plumes (> 40 g L^{-1} with freshwater) are thought to form during large, decadal flood events (Mulder & Syvitski, 1995), and possibly occurred during the 1995 and 1997 events (Imran & Syvitski, 2000). It is also possible that gravitational instability in turbid hypopycnal plumes (> 380 mg L^{-1}) from the Eel River (McCool & Parsons, 2004) caused a transfer of sediment to the bottom boundary layer by the process of **convective sedimentation** (Parsons *et al.*, 2001). This is one of several mechanisms that could create fluid-mud concentrations (> 10 g L^{-1} with salt water). Such concentrations are not reached by convergent estuarine flows on the Eel shelf (as described for the Amazon shelf by Kineke *et al.*, 1996), although a frontal zone might behave in a similar manner (Ogston *et al.*, 2000). The best-documented mechanism for reaching fluid-mud concentrations on the Eel shelf is by sediment resuspension within the wave boundary layer (< 10 cm thick; Ogston *et al.*, 2000; Traykovski *et al.*, 2000). Such thin layers are difficult to investigate, and require the use of downward-directed acoustic tools or the placement of optical sensors close to the seabed. Therefore, wave-supported fluid-mud flows are likely to be more common on other shelves than recognized in past studies.

Gravity flows generated by wave resuspension of seabed sediment differ from other types (e.g. turbidity currents, debris flows), because they commonly flow on very gentle seafloor gradients (continental shelves) and need continual infusion of energy from surface waves. The theory of sediment transport in the wave boundary layer (Grant & Madsen, 1979) has undergone some recent revision: e.g. with new information about the involvement of seabed permeability (Hsu & Hanes, 2004) and about the turbulence structure (Lamb *et al.*, 2004). However, a major factor affecting the mechanics of sediment transport remains the strong stratification at the top of the wave boundary layer. Below this, the large suspended-sediment concentrations are able to suppress further turbulence and limit seabed resuspension (Traykovski *et al.*, 2000; Wright *et al.*, 2001; as modified from Trowbridge & Kineke, 1994). A well-mixed boundary layer develops with a sharp turbidity (and density) gradient at its surface boundary (known as a **lutocline**). At 60-m water depth on the Eel shelf, the wave boundary layer can be 5–10 cm thick and have concentrations in the order of 100 g L^{-1}, which abruptly decrease to < 1 g L^{-1} above the lutocline (Traykovski *et al.*, 2000; Wright *et al.*, 2001). Sediment within the layer flows down slope at velocities > 10 cm s^{-1} (as much as ~60 cm s^{-1}) and continues seaward as long as sufficient energy is supplied from surface gravity waves. In Eel Canyon, liquefaction from cyclic wave action initiates failure that starts wave-supported gravity flows moving down canyon (~15 cm s^{-1}; Puig *et al.*, 2003, 2004).

The difference in the Eel River hydrograph between present and LGM conditions has had an impact on the operation of gravity flows (Parsons *et al.*, this volume, pp. 275–337). Today, sediment supply is reduced and characterized by episodic winter floods/storms, deposits of which can be partially preserved. During the LGM, more sediment was discharged and generally in a more sustained manner (due to spring/summer snow melt). However, when flood events occurred, they were typically more severe, due to the combination of rainfall and melting of low-elevation snow. Consequently, modelling studies (Morehead *et al.*, 2001) suggest that the net impact of higher accumulation rates and more severe floods during the LGM would be better preservation of gravity-flow deposits in the stratigraphic record. During the LGM, sea level was lower and these flows travelled down the continental slope, both through channels entering Eel Canyon and gullies to the north.

MARGIN MORPHOLOGY

The morphology of continental margins has been considered in this volume by Pratson *et al.* (pp. 339–380) and Syvitski *et al.* (pp. 459–529).

General considerations

Sedimentary processes from flocculation to debris flows create deposits that change bathymetry and give shape to continental margins: in other words, they produce a **seascape**. The seascape is a stratal surface that is buried and viewed later in the subsurface as a record of the formative processes. However, seascapes are not inert features that only respond to sedimentary processes, they also directly influence those processes. For example, topographic highs can put the seabed within the realm of wave reworking, and steep seabed gradients may initiate failures and gravity flows.

An understanding of the seascape for continental margins requires the inclusion of processes operating over longer time-scales (10^4–10^6 yr) than those discussed previously. When continents rift to form new ocean basins, the initial margins have a stair-step shape, due to the abrupt descent of several kilometres from the surfaces of thick, low-density continental crust down to the surfaces of thin, dense oceanic crust. The margin then moves passively as both continental and oceanic crust is carried away from the mid-ocean ridge, which is the situation with the New Jersey margin (Fig. 1b). Eventually, global forces within the Earth change and different plates, one with continental crust and another with oceanic crust, move in opposition. This creates a tectonically active margin, where the oceanic plate is **subducted** beneath the continental plate, as with the Eel margin. The operative processes and resulting morphologies (Fig. 1) are very different for passive and active margins, and depend primarily on the mechanisms forming and filling accommodation space (Van Wagoner *et al.*, 1988).

Sea-level fluctuation is another process relevant to margin seascapes, and for a particular location depends on global (**eustatic**) sea level and on vertical motions of the margin. These fluctuations have many impacts, including forced migration of the shoreline and other morphological features. Disequilibria result as erosive mechanisms associated with fluvial and marine processes begin to operate on new surfaces. The waxing and waning of coastal plains and continental shelves demonstrate the intimate relationship of seascapes and landscapes as sea level fluctuates, and as the important boundaries of shoreline and shelf break migrate and even merge. Sea-level rise causes landward migration (i.e. **transgression**) of the **shoreface**, which is the region from the low-tide shoreline to ~10-m water depth, where reworking by surface waves is most intense. This migration destroys shoreline landscapes (e.g. beaches, aeolian dunes, tidal flats, marshes) creating a **ravinement surface** on the continental shelf. During sea-level fall, the shoreline migrates seaward (i.e. **regression**) and these same landscapes are stranded on the newly formed coastal plain. The shelf seascape progressively dwindles as the shoreline approaches the shelf break. The new proximity of fluvial sediment supply dramatically impacts the seascape of the continental slope, causing both seaward growth and landward erosion (e.g. incisions by submarine canyons and gullies).

Glaciers and rivers are the primary suppliers of sediment to fill margin accommodation space. Temperate glaciers have especially large sediment yields (Milliman & Syvitski, 1992). During the LGM (and other glacial periods), the influence of glacial supply expanded toward lower latitudes, as demonstrated by sediment remnants on margins (e.g. moraines, jökulhlaup deposits; Shor & McClennen, 1988; Uchupi *et al.*, 2001). However, during all periods, fluvial sediment supply has dominated the global flux of terrestrial sediment to margins, supplying > 85% today (Milliman & Meade, 1983; Milliman & Syvitski, 1992). The pattern of fluvial discharge can be as a single, major river (e.g. Amazon, Ganges–Brahmaputra, Mississippi) within a large contiguous dispersal system, or as a collection of small rivers with coalescing dispersal systems (Jaeger & Nittrouer, 2000). The former are known as **point sources** and are usually limited to passive margins; the latter are **line sources** and are common on active margins. Substantial discharge of sediment associated with both geometries of sediment supply can create significant morphological features on continental shelves, including subaerial and subaqueous deltas.

Subaerial deltas (e.g. Mississippi and Nile Deltas) are well known because many people live on or near them, and the dynamic processes affecting morphology are easily recognized. One of the most dramatic processes results from consolidation of deltaic deposits, which leads to abrupt changes in the locus of deltaic sedimentation (i.e. **lobe switching**) associated with the formation and filling of accommodation space (Penland *et al.*, 1988). Subaqueous deltas are not as easily observed, but can represent the dominant sink for fluvial sediment (e.g. Amazon River; Nittrouer *et al.*, 1986). They are the result of energetic processes (waves, tides, currents) inhibiting sediment accumulation in shallow water (Walsh *et al.*, 2004), and of shelf width/depth providing sufficient accommodation space for accumulation in deeper water. Surface waves are especially important physical processes reworking the inner shelf. Their influence is greatest on the shoreface and continues to dominate seaward to a depth (known as **wave base**) dependent on wave properties (e.g. wavelength of storm waves) and seabed character (e.g. grain size). Fine-grained sediments are delivered farther seaward (e.g. by wave- or tide-driven diffusion, Ekman veering, downwelling bottom currents, or fluid-mud flows) and accumulate there. Silts and clays represent the bulk of fluvial supply, so accumulation rates can be great and subaqueous deltas can form. Shelf stratigraphy largely results from the interplay and relative motion of three important morphological features (Fig. 15a): the shoreline and possible subaerial delta; the subaqueous delta; and the shelf break (Swenson *et al.*, 2005).

The continental slope receives sediment shed from land and from landward portions of the continental margin, creating the ocean's largest repository for sediment mass (> 40% of marine sediment; Kennett, 1982). A complex mixture of sediment deposition, failure and mass movement impacts the morphology of the open slope (Adams & Schlager, 2000). This would predict a bathymetric gradient similar to the angles of repose for saturated sand, silt or clay, which are all > 10° (Allen, 1985). However, the observed gradient is ~4° and, therefore, other mechanisms must also be operating. Earthquakes and rapid sediment accumulation cause excess pore pressures, and could lead to reduced gradients (Pratson & Haxby, 1996; O'Grady *et al.*, 2000). Groundwater flowing out of continental slopes due to tectonic squeezing or differential loading can destabilize the seabed and reduce gradients (Iverson & Major, 1986; Orange & Breen, 1992). Internal waves triggered by tides or storms create a bore that propagates up slope, inhibiting deposition and creating nepheloid layers (Cacchione *et al.*, 2002; Cacchione & Pratson, 2004). This mechanism

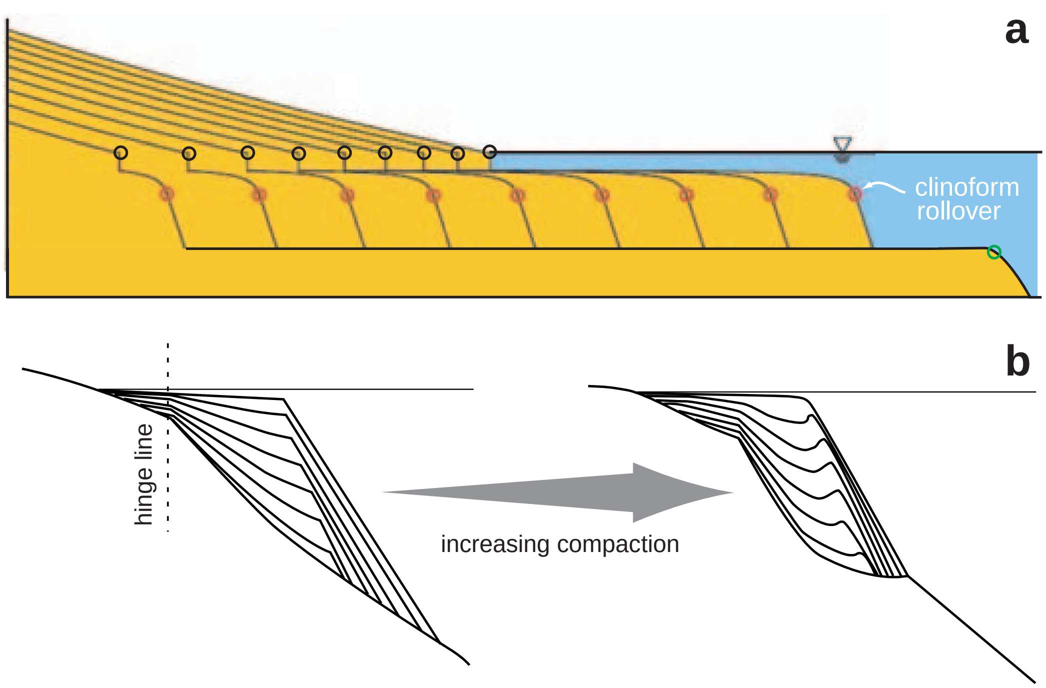

Fig. 15 Stratal geometries on continental margins. (a) Model representation of the shoreline (black circles), clinoform rollover (red circles) and shelf break (green circle), which are critical boundaries on continental margins. The stratigraphy produced by shelf sedimentation (especially on passive margins) is largely the result of the interplay and relative motions among these three important morphological features. (From Pratson *et al.*, this volume; modified from Swenson *et al.*, 2005.) (b) Model representation of shelf and slope strata impacted by isostatic subsidence (left) and sediment compaction (right) on a passive margin. Both of these processes operate where sediment accumulates, causing a feedback that creates the thickest sediment deposits, commonly near the shelf break. (From Pratson *et al.*, this volume; modified from Reynolds *et al.*, 1991.)

might constrain the gradient of the slope to the angle of internal-wave propagation (~4°), and is attractive because it provides a global process for explaining the bathymetric gradient of continental slopes. Turbidity currents are another possible mechanism, because they become erosional (ignitive) for seabeds steeper than ~4°, and become depositional for more gentle seabeds (Kostic *et al.*, 2002). A range of mechanisms is available, therefore, for controlling the bathymetric gradient of continental slopes, and it is not surprising that global observations converge to a relatively uniform value (e.g. Pratson & Haxby, 1996).

Although continental slopes undergo significant sediment accumulation, the Earth's most dramatic erosional features also occur there. These are submarine canyons, some of which dwarf the largest subaerial canyons (Normark & Carlson, 2003). However, a spectrum of sizes and shapes is found on continental slopes, probably related to their age and formative processes. Some smaller canyons (short, narrow, little vertical incision) have U-shaped cross-sections, with heads that do not reach the shelf break (Twichell & Roberts, 1982). Failures and subsequent landslides, with or without gravity flows, are probable mechanisms of formation (Farre *et al.*, 1983). In some cases, the regular spacing of these canyons suggests that groundwater seepage may play a role in their formation (Orange *et al.*, 1994). The largest canyons are V-shaped and incise the shelf break. Regardless of the mechanisms initially forming them, gravity flows (and associated scour) are the mechanisms ultimately causing the large magnitude of these canyons. Sedimentary deposits within the submarine fans at their termini indicate that turbidity currents are a more dominant transport process than debris flows (Ericson *et al.*, 1961). Excavation of the large canyons is tied to lowstands of sea level, when rivers delivered sediment directly to their heads (Emery & Uchupi, 1972). In addition to being dependent on river discharge, these canyons have morphologies similar to rivers (Shepard, 1977; Pratson, 1993): multiple tributaries at their heads; V-shaped cross-sections; concave-up longitudinal profiles; and division into distributaries at their bases (on submarine fans). The history of submarine-canyon development is made complex by periods of variable activity, and by multiple processes impacting their evolution (Shepard, 1981; Goodwin & Prior, 1989).

New Jersey margin morphology

On passive margins, **thermal subsidence** is an important process controlling accommodation space and sedimentation, as the plates cool with time and with spreading distance from the mid-ocean ridge (Parsons & Sclater, 1977). The rate of subsidence decreases landward to a negligible level at the **hinge line**, which is near the landward edge of the initial rift. Where subsidence is rapid, sediment accumulation leads to upward **aggradation** of the shelf and, where slow, seaward **progradation** of the slope is dominant (Reynolds *et al.*, 1991). Although thermal subsidence accounts for ~40% of accommodation space generated on the New Jersey margin (Steckler *et al.*, 1988), other processes are also operating. As sediment accumulates, the additional weight causes **isostatic subsidence** and the margin sinks into the plastic portions of the Earth's upper mantle (Watts & Ryan, 1976). Sediment consolidation is another important process, as thick deposits of sand and mud have their porosities reduced from high values at the seabed surface to 0.3 and 0.2, respectively, by burial to depths of many kilometres (Sclater & Christie, 1980; Bahr *et al.*, 2001). Isostatic subsidence and sediment consolidation operate where sediment accumulates (Fig. 15b), causing a feedback that creates the thickest sediment deposits, commonly beneath the shelf break (Reynolds *et al.*, 1991). Other processes can cause localized impacts on accommodation space. Extensional forces associated with rifting create **normal faults** that allow the underlying structure of the margin to break into segments that move downward and seaward. Similarly, in areas of rapid sediment accumulation (Suppe, 1985), **growth faults** form as thickening sedimentary deposits slowly rotate downward and seaward (Emery & Uchupi, 1984). However, New Jersey strata discussed in this paper of Cretaceous age and younger show relatively little evidence of such faulting (Poag, 1985).

The passive origin of the New Jersey margin has created the breadth and depth needed for substantial accumulation on its continental shelf. Major components of the stratigraphy underlying the New Jersey margin are those of deltaic sequences, with the typical morphology of **clinoforms**. Gently dipping topset strata change gradient across the **rollover point** to steeper-dipping foreset

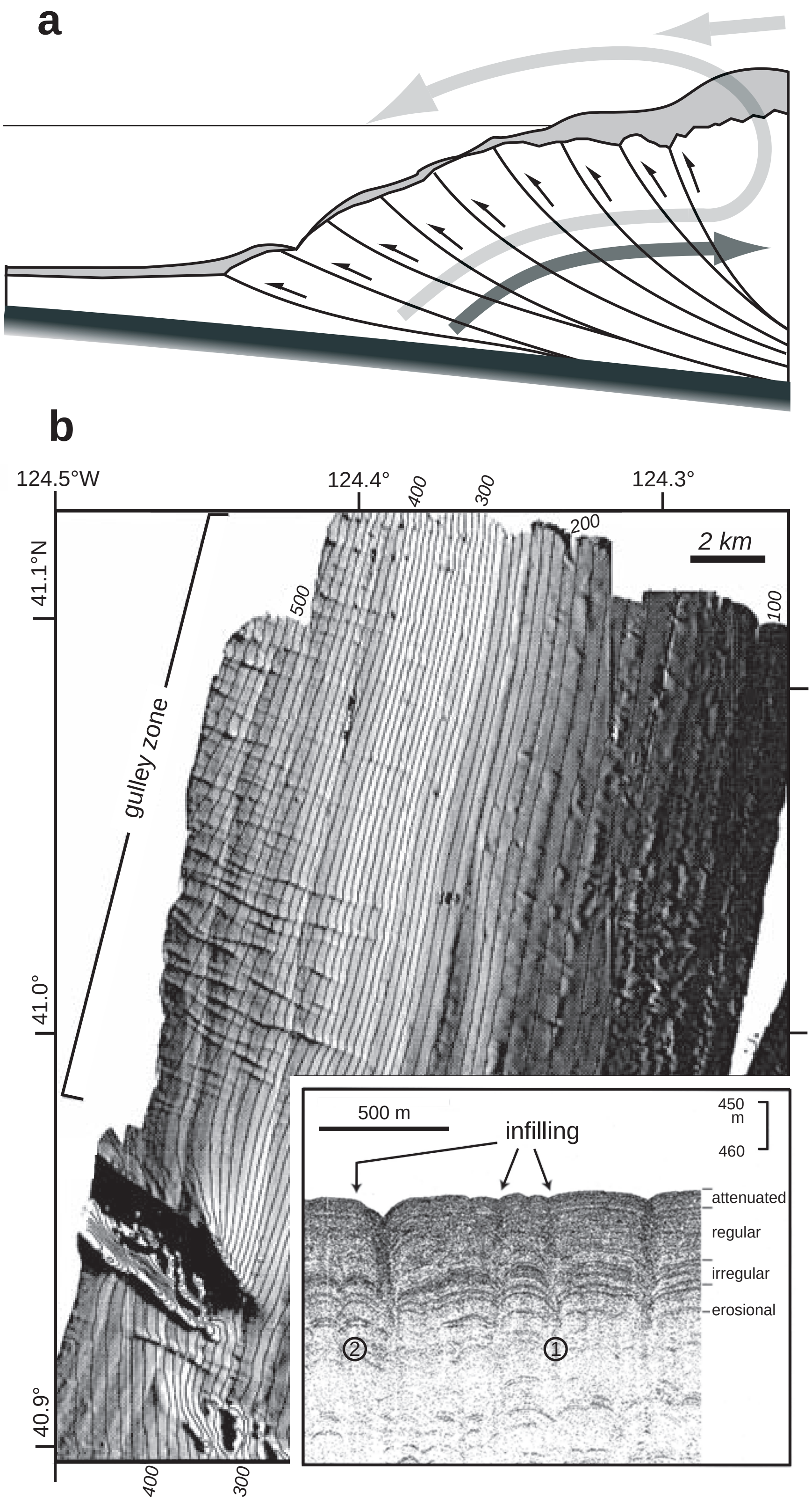

Fig. 16 (a) On an active margin, sediments scraped off the subducting oceanic plate create an accretionary prism, causing shelf and slope deposits to be uplifted and recycled by erosion. Uplift also reduces shelf accommodation space and displaces sedimentation to the continental slope. (From Pratson *et al.*, this volume; modified from Kulm & Fowler, 1974.) (b) Multibeam survey showing one mode of Eel slope sedimentation: aggradational gullies north of the Little Salmon Anticline. They are ~100 m wide and only 1–2 m deep in this figure, but extend long distances (> 10 km) and become larger farther down slope. The inset is a seismic profile proving (1) the vertical continuity of some gullies and (2) the termination of others. (From Pratson *et al.*, this volume; modified from Field *et al.*, 1999 and from Spinelli & Field, 2001.)

strata, and at the base become nearly flat **bottomset** strata. The foreset region is comparable to the **delta front** of a subaerial delta, and the bottomset is similar to the **prodelta** region. A fundamental difference is that the rollover point is the shoreline for a subaerial delta, and is below sea level (usually 20–50 m) for a subaqueous delta. The latter is probably the dominant origin for the clinoforms found within the New Jersey margin. When energy expenditure inhibited sediment accumulation on the topset, it was displaced seaward, creating relatively steep foreset strata and an **oblique** clinoform shape (Mitchum *et al.*, 1977a; Pirmez *et al.*, 1998). When transport processes caused sediment accumulation to be distributed more broadly, the resulting clinoform had a gentler morphology and a **sigmoidal** shape. These clinoform features were created during periods of plentiful sediment supply, and were responsible for aggrading and prograding the New Jersey margin.

Eel margin morphology

On active margins, tectonic uplift associated with plate motions controls accommodation space and sedimentation. Sediments that have accumulated on the subducting oceanic plate are scraped off, folded and amalgamated into margin deposits known as **accretionary prisms**. Shelf and slope strata are rotated upward (Fig. 16a), ultimately providing mountainous source rock that can be eroded and returned to the margin (Kulm & Fowler, 1974; Kulm *et al.*, 1975), thus recycling sediment (like the Eel margin). Uplift also reduces shelf accommodation space, and the recycled sediment predominantly accumulates on the continental slope (also like the Eel margin).

Eel Canyon is an important conduit for sediment transfer from shelf to slope, but much sediment also crosses the shelf break to the open slope farther north. Regardless of the origin for the 'Humboldt Slide', the gullies found on its upper rim (Fig. 11) clearly indicate the paths for some sediment transfer. Similar features are found farther north (Fig. 16b), where the gullies start small near the shelf break and enlarge with distance down slope (Field *et al.*, 1999). Several different geometries of these features can be identified on continental slopes. **Rills** are ~5–300 m wide and ~1–40 m deep, extending downslope many kilometres (commonly > 10 km) and converging with each other at low angles (Pratson *et al.*, 1994). **Dendritic gullies** are relatively short (< 5 km) and intersect submarine canyons at high angles, creating dendritic erosion patterns (Farre *et al.*, 1983). Although many rills and gullies are erosional, those on the northern Eel slope (Fig. 16b) are building upward (i.e. they are **aggradational gullies**), and grow by differential sediment accumulation associated with turbidity currents (Spinelli & Field, 2001). Sediment accumulation on the banks of adjacent gullies overlaps and grows upward together with the gully channels (similar to mechanisms shown in Fig. 13a). In contrast to a submarine canyon, gullies represent a line source of sediment to a continental slope and rise.

MARGIN STRATIGRAPHY

The startigraphy of continental margins has been reviewed in this volume by Mountain *et al.* (pp. 381–458) and Syvitski *et al.* (pp. 459–529).

General considerations

Sedimentary laminae (millimetres to centimetres thick) are stacked to create beds (metres to tens of metres thick), and beds are stacked to create sequences of strata (tens to hundreds of metres thick) that become the continental-margin sediment record. The sequences record repetitive cycles of sedimentation driven by processes that operate over large spatial scales (e.g. eustatic sea-level fluctuations, tectonic motions, sediment dispersal mechanisms). The time-scales of sequences that build margins vary with the inherent scales of the controlling processes, but are all $> 10^4$ yr. Examination of long-term stratigraphy is important for a number of reasons:

1 documenting the history of the Earth;
2 evaluating the operation of natural processes that fluctuate on long time-scales (parts of which may not be operative today);
3 validating predictive and diagnostic models relating sedimentary processes and strata.

The sedimentary record of continental margins is divided by abrupt breaks (**unconformities**) caused by large-scale erosion or non-deposition associated both with migration of the shoreline and reduction of sediment supply. Eustatic sea-level change has been suggested as a cause of stratal breaks that are globally synchronous over 10^6 yr (Vail *et al.*, 1977; Posamentier *et al.*, 1988) and even shorter time-scales (Haq *et al.*, 1987). This is the foundation of **sequence stratigraphy**. However, other processes (e.g. glacial rebound, tectonic motions, even deltaic lobe switching) cause similar transgressions and regressions on a local basis (Christie-Blick, 1991; Miall, 1991) and can complicate interpretation of the sedimentary record. Regardless of cause, margin stratigraphy is segmented on many time-scales and genetically related sediment deposits (e.g. from shelf clinoforms) are bounded by unconformities (Mitchum *et al.*, 1977a).

Recognition of stratigraphic relationships on continental margins is enabled by seismic tools (Payton, 1977; Hamilton, 1980), which detect the physical contrasts in sediments (e.g. changes in bulk density and sound velocity) that cause acoustic reflections. For adequate identification of seismic reflectors, the sedimentary contrasts must be vertically abrupt (scale of metres) and laterally persistent (scale of hundreds of metres). Direct sampling of strata (e.g. rotary drilling) gives access to sediment for age estimation (e.g. by biostratigraphy, magnetogeochronology and isotopic dating; Berggren *et al.*, 1995; Lowrie & Kent, 2004) and allows evaluation of a wide range of physical and chemical properties (by downhole measurements using electrical, nuclear and acoustic tools; Goldberg, 1997). Together, seismic profiling and seabed drilling provide the data necessary to document the geometric and temporal relationships of strata, which also can be adjusted (known as **backstripping**) for post-depositional changes that affect spatial relationships (e.g. isostatic subsidence, sediment consolidation; Steckler *et al.*, 1988, 1999). The angular terminations of strata and unconformities allow for development of insights about the processes creating sequences (e.g. sea-level fluctuations, tectonic motions, sediment supply, ocean currents; Karner & Driscoll, 1997). Among the common geometric relationships are (Fig. 17; Mitchum *et al.*, 1977b):

1 an unconformity defining the top of a sequence (**toplap**);
2 strata building landward against a basal unconformity (**onlap**);
3 strata building seaward across an underlying unconformity (**downlap**).

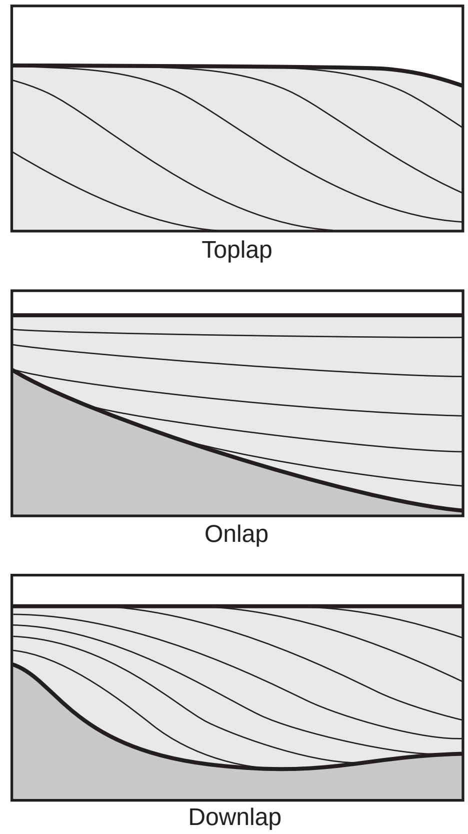

Fig. 17 Common geometric relationships between seismic reflectors (thin lines) and bounding unconformities (bold lines). Toplap, an unconformity defining the top of sequence; onlap, strata building landward against a basal unconformity; downlap, strata building seaward across an underlying unconformity. (From Mountain *et al.*, this volume pp. 381–458; modified from Mitchum *et al.*, 1977b.)

Dating provides information that can be used in many ways (e.g. calculation of accumulation rates), and can determine whether the age of a seismic reflector varies spatially (i.e. time transgressive). With rare exceptions, all strata above a sequence boundary are younger than all strata below it (Vail *et al.*, 1977).

A common mechanism for creation of a sequence boundary is subaerial exposure (Van Wagoner *et al.*, 1988), which causes erosion into the underlying sequence. Another potential stratigraphic break is associated with sea-level rise and the resulting transgression, which creates the

maximum flooding surface onto which subsequent sedimentation builds (e.g. prograding clinoforms). Intrasequence stratigraphic geometry commonly reveals mud sitting abruptly above sand, followed upward by gradual coarsening back to sand (representing seaward migration of the shoreline). The coarsening-upward strata are known as **parasequences** (Van Waggoner *et al.*, 1988), and are stacked to create larger-scale sequences. During the various stages of sea level (high, falling, low, rising), different types of parasequences are distributed across a continental margin to create unique patterns known as **systems tracts** (Posamentier *et al.*, 1988).

New Jersey margin stratigraphy

During the Miocene and Pleistocene, sediment accumulation reached rates of ~10–100 m Myr^{-1}. The Miocene phase of sedimentation contained drainage systems from the ancestral Delaware/Susquehanna and Hudson Rivers that flowed southeastward (Poag & Sevon, 1989; Poag & Ward, 1993). They created at least eight sequences of well-preserved clinoforms (Fig. 18; Greenlee *et al.*, 1992), which compare favourably with eustatic sea-level fluctuations (Sugarman *et al.*, 1997). Sequences along the northern coastal plain and shelf of New Jersey are thicker than those along southern New

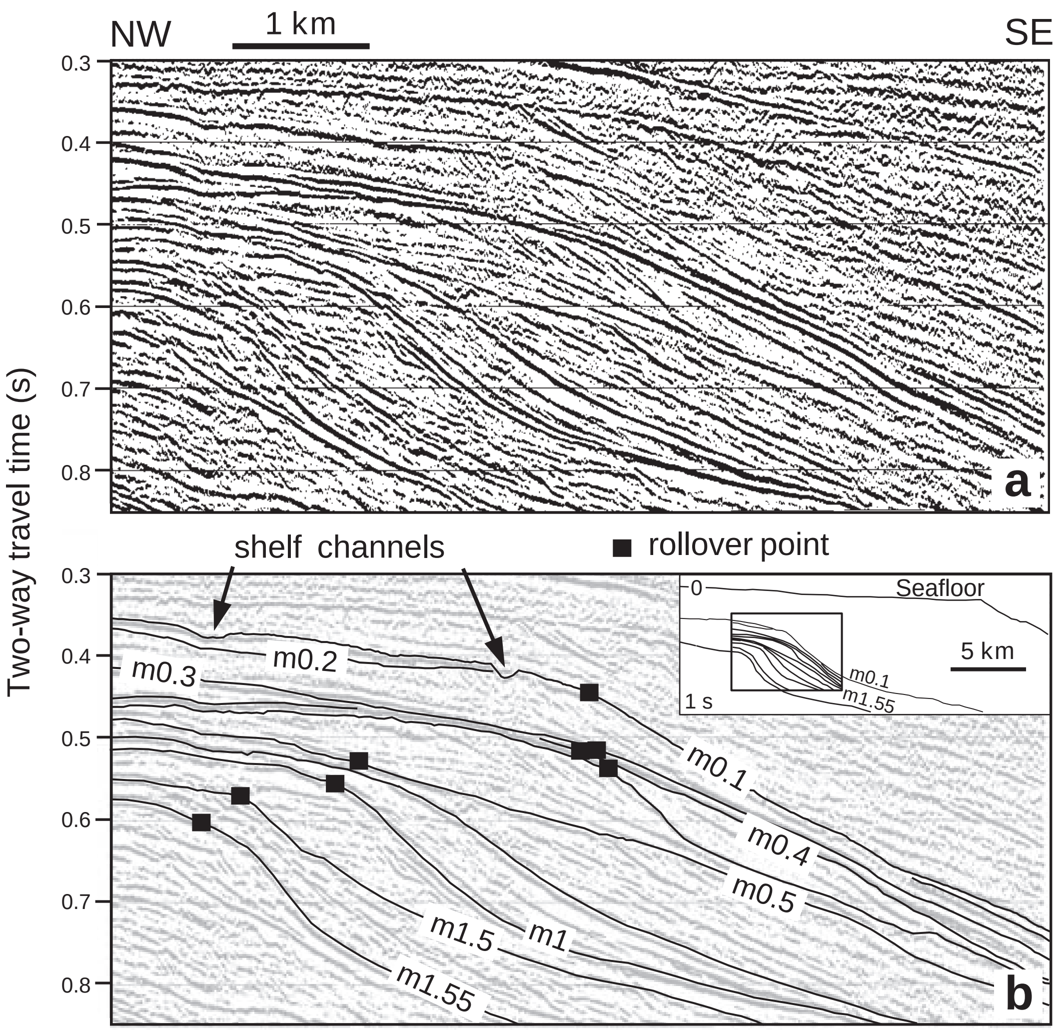

Fig. 18 Across-shelf seismic profile for Miocene sequences underlying the New Jersey margin. (a) Original profile. (b) Interpreted profile. These are prograding clinoforms, and rollover points are shown by black squares. Several channels can be seen incising topset surfaces. (From Mountain *et al.*, this volume; after Fulthorpe *et al.*, 1999.)

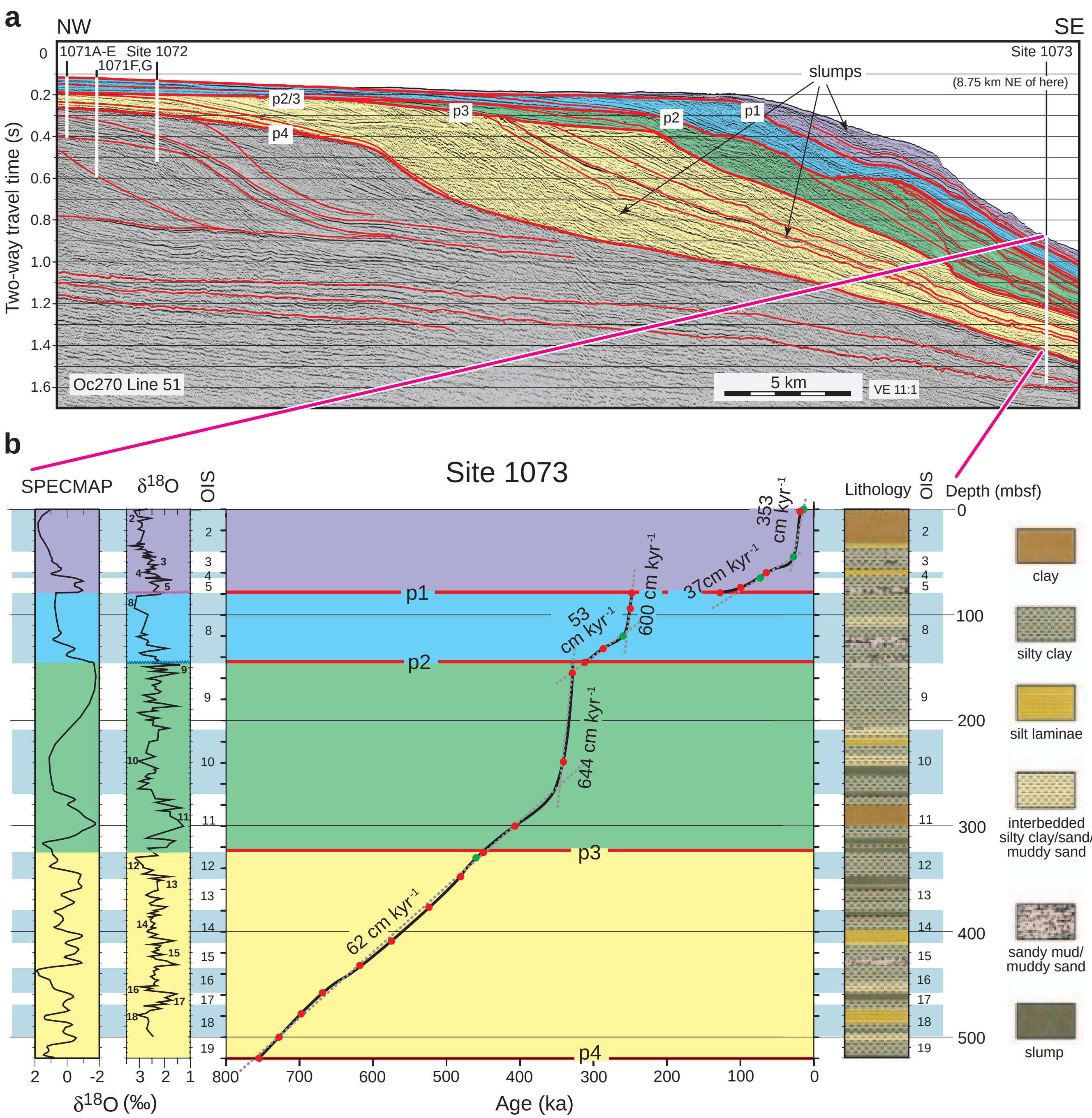

Fig. 19 Sediment profiles on the New Jersey margin. (a) Interpreted seismic profile crossing several Ocean Drilling Program (ODP) drill sites, including site 1073. Four Pleistocene sequences are identified by different colours, each representing clinoforms that have prograded across the outer shelf and upper slope. (From Mountain *et al.*, this volume.) (b) Age profiles for Site 1073, with defining isotopic data (on left; see Mountain *et al.*, this volume, for description of SPECMAP chronology), and lithological information and oxygen isotope stage (OIS; right). The top three Pleistocene sequences show an upward increase in accumulation rate. (From Mountain *et al.*, this volume; modified from McHugh & Olson, 2002.)

Jersey, presumably due to differences in accommodation space and fluvial sediment supply. A few clinoforms have foresets with small incisions but the surfaces are generally unscarred (Fulthorpe *et al.*, 2000), suggesting that sediment was delivered to the foresets as non-channelized flows. In contrast, there are well-developed valleys on the topsets, whose origins are linked to incisions during lowstand of sea level (Fulthorpe *et al.*, 1999). The contrast between topset and foreset incisions indicates that the rollover depth was about the same as the lower extent of sea-level fluctuations, ~20–30 m (Kominz *et al.*, 1998; Miller *et al.*, 1998). This magnitude of fluctuation compares well with numerical modelling based on backstripping of stratal surfaces (Steckler *et al.*, 1999).

During the Pleistocene, sedimentation extended the shelf width by tens of kilometres (Mountain *et al.*, this volume, pp. 381–458). The Hudson Apron is located on the upper slope south-west of Hudson Canyon and reveals four well-developed sedimentary sequences (Fig. 19a), whose bounding surfaces extend conformably across the shelf break and demonstrate the relationships of shelf and slope strata. The bathymetric gradient for the base of each sequence becomes progressively steeper (from ~1:60 to ~1:20) as they move seaward through time. A number of chaotic reflectors are observed within the sequences, suggesting failure and mass movement (i.e. slumps). Three of the four sequences have accumulation rates increasing upward by an order of magnitude (Fig. 19b). Eustatic sea level does not seem to be the only cause for clinoform evolution during this time, but, rather, it also involves processes associated with glacial advance/retreat, isostatic response and glacial sediment discharge. In areas where continental margins are impacted by glaciation, sequence stratigraphy is particularly complicated.

The uppermost strata on the New Jersey shelf reveal bathymetric features related to the most recent transgression. The seafloor was eroded (3–10 m) and modified into sand ridges as the shoreface moved landward, and subsequently waves and currents on the shelf have continued to rework the ridges (Goff *et al.*, 2005). Beneath these surface strata (0–20 m thick) lies evidence for multiple fluvial drainage systems, which were cut by glacial meltwater pulses flowing across the pre-existing coastal plain (Nordfjord *et al.*, 2005). Some of these pulses were probably associated with catastrophic breaks of glacial-lake dams (~12–19 ka; Uchupi *et al.*, 2001), which disrupted stratigraphy by creating erosional blocks of old, layered deposits and stranding them within buried channels now containing acoustically transparent sediments (Fulthorpe & Austin, 2004). A diverse assortment of incision geometries provides evidence for across-shelf flows and sediment supply to the New Jersey continental slope during sea-level lowstands in both the Miocene and the Pleistocene.

The New Jersey slope reveals Miocene gullies and canyons, many of which have been partially or completely filled (Miller *et al.*, 1987; Mountain, 1987), especially on the upper slope. Pleistocene processes excavated some of the old canyons, and many remained open and unfilled on the lower slope (Pratson *et al.*, 1994). The sedimentary deposits filling the canyons reveal a consistent pattern of coarse basal material, followed upward by fine-grained turbidites, and finally hemipelagic deposits (May *et al.*, 1983; Mountain *et al.*, 1996). The general expectation is for canyon filling to occur during sea-level rise (Posamentier *et al.*, 1988) and that may be the case for the burial of Miocene canyons. However, many canyons active during the LGM on the New Jersey slope are still exposed today (and elsewhere in the world; Fig. 3), so the process of filling during transgression is not guaranteed to be complete.

Eel margin stratigraphy

The modern tectonic conditions that started in the middle Pleistocene on the Eel margin created a widespread unconformity, and since then 13 more have formed (Fig. 20; Burger *et al.*, 2002). During that time, ~1 km of sediment has accumulated (Clarke, 1987), although tectonic structures cause significant local variability in thickness. The sequences bounded by the unconformities are not characterized by prograding clinoforms (as observed on the New Jersey margin), but are dominated by fill of relatively small, segmented basins. Early sources of sediment (> 500 ka) were from a northern river and the depocentre was located west of Trinidad Head. The locus of greatest sediment preservation shifted southward, and accumulation rates have generally decreased for the past 500 kyr (Burger *et al.*, 2002). During that

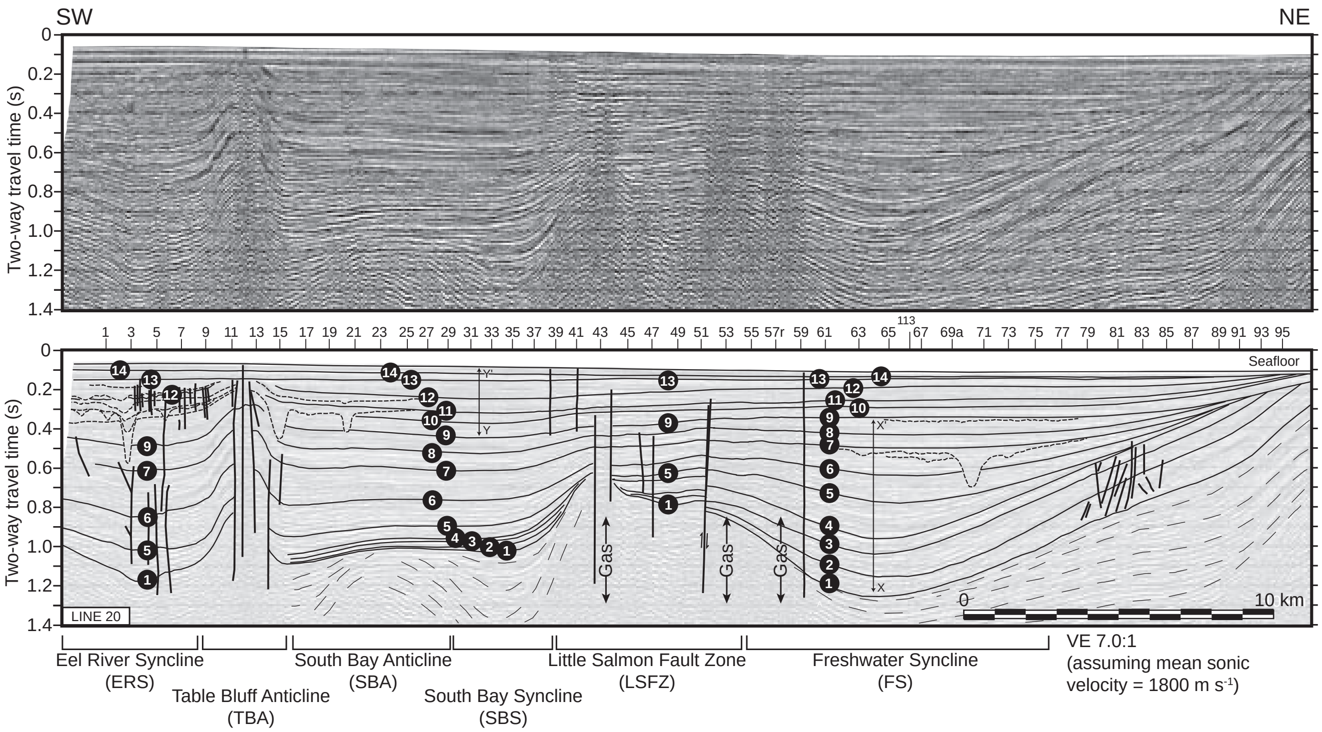

Fig. 20 Along-shelf seismic profile for Pleistocene sequences (past ~500 kyr) underlying the Eel margin. (a) Original profile. (b) Interpreted profile. The strata are segmented into basins by anticlines (labelled) and faults (near-vertical bold lines). Regional unconformities are shown by near-horizontal lines (14 total). Gas disturbs the seismic record in several areas. (From Mountain *et al.*, this volume; after Burger *et al.*, 2002.)

period, ancestral versions of both the Eel and Mad Rivers became significant sediment sources with recognizable basins of accumulation. For the past 360 kyr, Eel Canyon has been active and has provided a conduit for substantial sediment transport beyond the shelf break. Modern sediment dispersal processes (i.e. dominant input from Eel River, minor input from Mad River; Sommerfield *et al.*, this volume, pp. 157–212) have shaped the margin for the past ~43 kyr (Burger *et al.*, 2002).

Table Bluff Anticline is one of the dominant structural highs (Fig. 20) oriented across the shelf (Clarke, 1987), and has separated Eel and Mad River sedimentation at times in the past. Shelf channels on the surface of the anticline had a south-westward gradient, heading toward Eel Canyon (Burger *et al.*, 2002). The overall dendritic pattern of the channels is similar to channels on the New Jersey shelf (Duncan *et al.*, 2000), which have been interpreted as fluvial systems operating during lower stands of sea level (Austin *et al.*, 1996). Ten stratigraphic surfaces stacked vertically are identified by incised channels, and represent the past ~500 kyr (Burger *et al.*, 2001). There are too many surfaces to be the result of only eustatic sea-level lowering, so tectonic uplift must be responsible for some of the erosional surfaces.

On the Eel slope, the Little Salmon Anticline (which is breached at its crest) is another cross-margin structural high that separates sedimentation regimes (Figs 11 and 16b). Eel Canyon and the large gullies on the rim of ‘Humboldt Slide’ occur to the south, and smaller, aggradational gullies are observed to the north. During lowstands of sea level, the Little Salmon Anticline separated the discharges of the Eel and Mad rivers, and the Mad probably had a major impact on the northern gullies at these times (Burger *et al.*, 2001). Biogenic and thermogenic gas are common on this portion of the Eel slope (Kvenvolden & Field, 1981; Lorenson *et al.*, 1998). Gas commonly impacts seismic observations (e.g. Figure 20) and is probably responsible for pockmarks observed by multibeam data (Yun *et al.*, 1999). Some of the pockmarks are found in linear orientations near the gullies on the slope, but no formative relationship has been established (Field *et al.*, 1999).

Modelling studies of the Eel margin (Mountain *et al.*, this volume, pp. 381–458) indicate a number of fundamental differences in strata formation relative to the New Jersey margin. Tectonic subsidence on the Eel margin (~2 mm yr^{-1}; Orange, 1999) has a significant impact on the observed sequences, because it leads to seaward divergence of shelf reflectors, not prograding clinoforms, as with New Jersey. Accommodation space on the Eel margin has been sufficient to balance sediment supply, and this results in a stationary shelf break, not seaward progradation, as with New Jersey. Other differences include the dominance of segmented depocentres on the Eel margin and the potential for erosional unconformities due to periods of uplift. The relative importance of operational processes leads to distinct differences in the stratigraphic imprints of these passive and active margins.

CONCLUSIONS

This paper integrates recent knowledge about continental-margin sedimentation across several domains, as highlighted in Table 1. The challenges and benefits are briefly summarized here.

1 *Shelves and slopes*. As with the topset and foreset on a clinoform, the linkage between the upward aggrading and seaward prograding segments of a margin (shelf and slope, respectively) depends on the operative processes. At the crossroads of land and ocean, continental margins exhibit a wealth of potential processes, and there is a nearly infinite range of combinations and magnitudes for those processes. However, the dual representation of stratigraphy in response to both shelf and slope processes provides twice the perspective for interpreting Earth history.

2 *Processes and stratigraphy*. The goal is to use a fundamental understanding of short-term processes transporting and accumulating sediment to interpret preserved stratigraphic signatures better. In return, stratigraphy documents the relative importance of sedimentary processes, not necessarily according to their spatial and temporal dominance in modern environments, but according to their impact on preserved signatures. This allows investigations to focus on understanding the stratigraphically important processes, which differ with the time-scales of interest.

3 *Observations and modelling*. Observations are important for describing a particular continental margin but, by themselves, provide limited means to extrapolate

Table 1 Examples of the multidimensional evaluation of continental-margin sedimentation, as presented by this paper and described in detail in this volume

Location	Focus	Method	Topic
Shelf	Process	Observation	Wave-supported sediment gravity flows (Hill *et al.*, this volume; Parsons *et al.*, this volume)
Shelf	Process	Modelling	Sediment delivery during the Last Glacial Maximum (Syvitski *et al.*, this volume)
Shelf	Stratigraphy	Observation	Flood-deposit signature, preservation and distribution (Wheatcroft *et al.*, this volume; Sommerfield *et al.*, this volume)
Shelf	Stratigraphy	Modelling	Backstripping of New Jersey shelf (Mountain *et al.*, this volume; Syvitski *et al.*, this volume)
Slope	Process	Observation	Gullies formed by turbidity currents (Pratson *et al.*, this volume; Mountain *et al.*, this volume)
Slope	Process	Modelling	Hydroplaning debris flows (Parsons *et al.*, this volume)
Slope	Stratigraphy	Observation	'Humboldt Slide' (Lee *et al.*, this volume)
Slope	Stratigraphy	Modelling	Submarine-canyon evolution (Pratson *et al.*, this volume; Syvitski *et al.*, this volume)

in time and space. That is the potential of numerical modelling and laboratory experimentation. Predictive models are valuable for developing a fundamental understanding of complex systems, but inverse models (that are diagnostic) provide special benefits for reading the stratigraphic record. Observational studies then give validation to the models. Knowledge is best attained by using observation and modelling in tandem.

The benefits of integrated studies of continental margins are limited by boundary conditions, such as those introduced at the beginning of this paper. Not all details of Earth history are recorded in fluvial deposits on shelves and slopes. Future integrated studies should expand to high-latitude settings, investigating systems dominated by both temperate glaciation and by the full range of polar processes. Similarly, low-latitude carbonate sedimentation has some unique attributes, and requires focused attention. The time-scales of the present paper have stopped short of the deep stratigraphy on margins and of rock records on land. Integration of margin studies is valuable for the time-scales of this paper, and should be even more important when extended to the full spectrum of margin stratigraphy. Terrestrial and coastal environments are largely untouched in this paper, and the same is true for submarine fans, continental rises and abyssal plains, all of which are intimately related to continental-margin sedimentation. Source-to-sink programmes examining sediment dispersal systems from mountain tops to deep ocean floors have been initiated in several places around the world, and this trend should be continued and encouraged.

ACKNOWLEDGEMENTS

The authors express great thanks to the participants in STRATAFORM and the authors of papers in this volume for contributing the material summarized here. We especially thank Paul Hill, Rob Wheatcroft, Chris Sommerfield, Homa Lee, Lincoln Pratson and Greg Mountain, who provided valuable comments that helped improve the paper. Tina Drexler kindly prepared the figures. The Office of Naval Research is responsible for supporting the research efforts that produced this paper, and we appreciate their commitment over many years. Other agencies also sponsored parts of the work summarized, and all deserve credit for support of investigations into continental-margin sedimentation.

REFERENCES

Adams, E.W. and Schlager, W. (2000) Basic types of submarine slope curvature. *J. Sediment. Res.*, **70**, 814–828.

Alexander, C.R. and Simoneau, A.M. (1999) Spatial variability in sedimentary processes on the Eel continental slope. *Mar. Geol.*, **154**, 243–254.

Allen, J.R.L. (1985) *Principles of Physical Sedimentology*. Allen & Unwin, Boston, 272 pp.

Aller, R.C. (2004) Conceptual models of early diagenetic processes: the muddy seafloor as an unsteady, batch reactor. *J. Mar. Res.*, **62**, 815–835.

Aller, R.C. and Cochran, J.K. (1976) ^{234}Th/^{238}U disequilibrium in near-shore sediment, particle reworking and diagenetic time scales. *Earth Planet. Sci. Lett.*, **29**, 37–50.

Austin, J.A., Fulthorpe, C.S., Mountain, G.S., Orange, D.L. and Field, M.E. (1996) Continental-margin seismic stratigraphy: Assessing the preservation potential of heterogeneous geological processes operating on continental shelves and slopes. *Oceanography*, **9**, 173–177.

Bahr, D.B., Hutton, E.W.H., Syvitski, J.P.M. and Pratson, L.F. (2001) Exponential approximations to compacted sediment porosity profiles. *Comput. Geosci.*, **27**, 691–700.

Bea, R.G., Wright, S.G., Sircar, P. and Niedoroda, A.W. (1983) Wave-induced slides in South Pass Block 70, Mississippi Delta. *J. Geotech. Eng.*, **109**, 619–644.

Been, K. and Sills, G.C. (1981) Self-weight consolidation of soft soils: an experimental and theoretical study. *Géotechnique*, **31**, 519–535.

Bentley, S.J. and Nittrouer, C.A. (2003) Emplacement, modification and preservation of event strata on a flood-dominated continental shelf, Eel shelf, northern California. *Cont. Shelf Res.*, **23**, 1465–1493.

Berggren, W.A., Kent, D.V., Swisher, C.C. and Aubry, M.-P. (1995) A revised Cenozoic geochronology and chronostratigraphy. In: *Geochronology, Time Scales and Global Stratigraphic Correlation* (Ed. W.A. Berggren), pp. 129–212. Special Publication 54, Society of Economic Paleontologists and Mineralogists, Tulsa, OK.

Beschta, R.L. (1987) Conceptual models of sediment transport in streams. In: *Sediment Transport in Gravel-bed Rivers* (Eds C.R. Thorne, J.C. Bathurst, J.C. and R.D. Hey), pp. 387–419. John Wiley & Sons, Chichester.

Blair, N.E., Leithold, E.L., Ford, S.T., *et al.* (2003) The persistence of memory: the fate of ancient sedimentary organic carbon in a modern sedimentary system. *Geochim. Cosmochim. Acta*, **67**, 63–73.

Bokuniewicz, H.J., Gordon, R. and Rhoads, D.C. (1975) Mechanical properties of the sediment–water interface. *Mar. Geol.*, **18**, 263–278.

Booth, J.S., O'Leary, D.W., Popenoe, P. and Danforth, W.W. (1993) U.S. Atlantic contintental slope landslides: their distribution, general attributes and implications. In: *Submarine Landslides: Selected Studies in the U.S. EEZ* (Eds W.C. Schwab, H.J. Lee and D.C. Twichell). *U.S. Geol. Surv. Bull.*, **2002**, 14–39.

Bornhold, B.D and Prior, D.B. (1990) Morphology and sedimentary processes on the subaqueous Noeick River delta, British Columbia, Canada. In: *Coarse-grained Deltas* (Eds A. Colella and D.B. Prior), pp. 169–184. Special Publication 10, International Association of Sedimentologists. Blackwell Scientific Publications, Oxford.

Boulanger, E. (2000) *Comportement cyclique des sédiments de la marge continentale de la rivière Eel: une explication possible pour le peu de glissements sous-marins superficiels dans cette region*. MSc thesis, Department Geology and Geological Engineering, Laval University, Quebec.

Bouma, A.H. (1962) *Sedimentology of Some Flysch Deposits: a Graphic Approach to Facies Interpretation*. Elsevier, Amsterdam.

Brink, K.H., Bane, J.M., Church, T.M., *et al.* (1992) *Coastal Ocean Processes: a Science Prospectus*. Technical Report WHOI–92–18, Woods Hole Oceanographic Institute, 88 pp.

Brown, W.M. and Ritter, J.R. (1971) Sediment transport and turbidity in the Eel River basin, California. *U.S. Geol. Surv. Wat. Supply Pap.*, **1986**, 70 pp.

Bryn, P., Solheim, A., Berg, K., *et al.* (2003) The Storegga slide complex: repeated large scale sliding in response to climatic cyclicity. In: *Submarine Mass Movements and their Consequences* (Eds J. Locat and J. Mienert), pp. 215–222. Kluwer, Amsterdam.

Burger, R.L., Fulthorpe, C.S. and Austin, J.A., Jr. (2001) Late Pleistocene channel incisions in the southern Eel River Basin, northern California: implications for tectonic vs. eustatic influences on shelf sedimentation patterns. *Mar. Geol.*, **177**, 317–330.

Burger, R.L., Fulthorpe, C.S., Austin Jr, J.A. and Gulick, S.P.S. (2002) Lower Pleistocene to present structural deformation and sequence stratigraphy of the continental shelf, offshore Eel River Basin, northern California. *Mar. Geol.*, **185**, 249–281.

Cacchione, D.A. and Pratson, L.F. (2004). Internal tides and the continental slope. *Am. Sci.*, **92**, 130–137.

Cacchione, D.A., Pratson, L.F. and Ogston, A.S. (2002) The shaping of continental slopes by internal tides. *Science*, **296**, 724–727.

Christie-Blick, N. (1991) Onlap, offlap and the origin of unconformity-bounded depositional sequences. *Mar. Geol.*, **97**, 35–56.

Clarke, S.H. (1987) Late Cenozoic geology and structure of the onshore-offshore Eel River Basin, northern California. In: *Tectonics, Sedimentation and Evolution of the Eel River and Other Coastal Basins of Northern California* (Eds H. Schymiczek and R. Suchland), pp. 31–40. Miscellaneous Publication 37, San Joaquin Geological Society.

Clarke, S.H. (1992) Geology of the Eel River Basin and adjacent region: implications for Late Cenozoic tectonics of the southern Cascadia subduction zone and Mendocino Triple Junction. *Bull. Am. Assoc. Petrol. Geol.*, **76**, 199–224.

Cohn, T.A. (1995) Recent advances in statistical methods for the estimation of sediment and nutrient transport in rivers. *Rev. Geophys.*, **33** (IUGG Suppl.), 1117–1123.

Coleman, J.M. and Garrison, L.E. (1977) Geological aspects of marine slope stability, northwestern Gulf of Mexico. *Mar. Geol.*, 2, 9–44.

Coleman, J.M., Prior, D.B. and Garrison, L.E. (1980) Subaqueous sediment instabilities in the offshore Mississippi River delta. *U.S. Bur. Land Man. Open-file Rep.*, **80–01**, 60 pp.

Correggiari, A., Trincardi, F., Langone, L. and Roveri, M. (2001) Styles of failure in late Holocene highstand prodelta wedges on the Adriatic shelf. *J. Sediment. Res.*, **71**, 218–236.

Costa, J.E. (1984) Physical geomorphology of debris flows. In: *Developments and Applications of Geomorphology* (Eds J.E. Costa and P.J. Fleisher), pp. 269–317. Springer-Verlag, Berlin.

Coulter, H.W. and Migliaccio, R.R. (1966) Effects of the earthquake of March 27, 1964 at Valdez, Alaska. *U.S. Geol. Surv. Prof. Pap.*, **542-C**.

Crockett, J.S. and Nittrouer, C.A. (2004) The sandy inner shelf as a repository for muddy sediment: an example from northern California. *Cont. Shelf Res.*, **24**, 55–73.

Curran, K.J., Hill, P.S. and Milligan, T.G. (2002) Fine-grained suspended sediment dynamics in the Eel River flood plume. *Cont. Shelf Res.*, **22**, 2537–2550.

Cutter, G.R. and Diaz, R.J. (2000) Biological alteration of physically structured flood deposits on the Eel margin, northern California. *Cont. Shelf Res.*, **20**, 235–253.

De Deckere, E.M., Tolhurst, T.J. and de Brouwer, J.F.C. (2001) Destabilization of cohesive intertidal sediments by infauna. *Estuarine Coastal Shelf Sci.*, **53**, 665–669.

DeMaster, D.J., McKee, B.A., Nittrouer, C.A., Qian, J. and Cheng, G. (1985) Rates of sediment accumulation and particle reworking based on radiochemical measurements from continental shelf deposits in the East China Sea. *Cont. Shelf Res.*, **4**, 143–158.

DeMets, C., Gordon, R.G., Argus, D.F. and Stein, S. (1990) Current plate motions. *Geophys. J. Int.*, **101**, 425–478.

Drake, D.E. (1976) Suspended sediment transport and mud deposition on continental shelves. In: *Marine Sediment Transport and Environmental Management* (Eds D.J. Stanley and D.J.P. Swift), pp. 127–158. John Wiley & Sons, New York.

Drake, D.E. (1999) Temporal and spatial variability of the sediment grain-size distribution on the Eel shelf: the flood layer of 1995. *Mar. Geol.*, **154**, 169–182.

Drake, D.E. and Cacchione, D.A. (1985) Seasonal variation in sediment transport on the Russian River shelf, California. *Cont. Shelf Res.*, **4**, 495–514.

Drexler, T.M., Nittrouer, C.A. and Mullenbach, B.L. (2006) Impact of local morphology on sedimentation in a submarine canyon, ROV studies in Eel Canyon, northern California, U.S.A. *J. Sediment. Res.*, **76**, 839–853.

Duncan, C.S. and Goff, J.A. (2001) Relict iceberg keel marks on the New Jersey outer shelf, southern Hudson Apron. *Geology*, **29**(5), 411–414.

Duncan, C.S., Goff, J.A., Austin, J.A., Jr. and Fulthorpe, C.S. (2000) Tracking the last sea-level cycle: seafloor morphology and shallow stratigraphy of the latest Quaternary New Jersey middle continental shelf. *Mar. Geol.*, **170**, 395–421.

Elverhøi, A., Norem, H., Andersen, E.S., *et al.* (1997) On the origin and flow behavior of submarine slides on deep-sea fans along the Norwegian Barents Sea continental margin. *Geo-Mar. Lett.*, **17**, 119–125.

Ely, L.L., Enzel, Y., Baker, V.R. and Cayan, D.R. (1993) A 5000-year record of extreme floods and climate change in the southwestern United States. *Science*, **262**, 410–412.

Emery, K.O. and Uchupi, E. (1972) *Western North Atlantic Ocean; Topography, Rocks, Structure, Water, Life and Sediments*. Memoir 17, American Association of Petroleum Geologists, Tulsa, OK, 532 pp.

Emery, K.O. and Uchupi, E. (1984). *The Geology of the Atlantic Ocean*. Springer-Verlag, New York, 1050 pp.

Ericson, D.B., Ewing, M., Wollin, G. and Heezen, B.C. (1961) Atlantic deep-sea sediment cores. *Geol. Soc. Am. Bull.*, **72**, 193–285.

Farnsworth, K.L. and Milliman, J.D. (2003) Effects of climatic and anthropogenic change on small mountainous rivers: the Salinas River example. *Global Planet. Change*, **39**, 53–64.

Farre, J.A., McGregor, B.A., Ryan, W.B.F. and Robb, J.M. (1983). Breaching the shelf break; passage from youthful to mature phase in submarine canyon evolution. In: *The Shelf Break; Critical Interface on Continental Margins* (Eds D.J. Stanley and G.T. Moore), pp. 25–39. Special Publication 33, Society of Economic Paleontologists and Mineralogists, Tulsa, OK.

Field, M.E. and Barber, J.H., Jr. (1993) A submarine landslide associated with shallow sea-floor gas and gas hydrates off northern California. In: *Submarine Landslides: Selected Studies in the U.S. EEZ* (Eds W.C. Schwab, H.J. Lee and D.C. Twichell). *U.S. Geol. Surv. Bull.*, **2002**, 151–157.

Field, M.E., Clarke, S.H., Jr. and White, M.E. (1980) Geology and geologic hazards of offshore Eel River Basin, northern California continental margin. *U.S. Geol. Surv. Open-File Rep.*, **80–1080**.

Field, M.E., Gardner, J.V., Jennings, A.E. and Edwards, B.D. (1982) Earthquake-induced sediment failures on a 0.250 slope, Klamath River delta, California. *Geology*, **10**, 542–546.

Field, M.E., Gardner, J.V. and Prior, D.B. (1999) Geometry and significance of stacked gullies on the northern California slope. *Mar. Geol.*, **154**, 271–286.

Flood, R.D., Manley, P.L., Kowsmann, R.O., Appi, C.J. and Pirmez, C. (1991) Seismic facies and late Quaternary growth of Amazon submarine fan. In: *Seismic Facies and Sedimentary Processes of Modern and Ancient Submarine Fans* (Eds P. Weimer and M.H. Link), pp. 415–433. Spring-Verlag, New York.

Fulthorpe, C.S. and Austin, J.A., Jr. (2004) Shallowly buried, enigmatic seismic stratigraphy on the New Jersey outer shelf: evidence for latest Pleistocene catastrophic erosion? *Geology*, **32**, 1013–1016.

Fulthorpe, C.S., Austin, J.A., Jr. and Mountain, G.S. (1999) Buried fluvial channels off New Jersey: did sea-level lowstands expose the entire shelf during the Miocene? *Geology*, **27**, 203–206.

Fulthorpe, C.S., Austin, J.A., Jr. and Mountain, G.S. (2000) Morphology and distribution of Miocene slope incisions off New Jersey: are they diagnostic of sequence boundaries? *Geol. Soc. Am. Bull.*, **112**, 817–828.

García, M. and Parker, G. (1993) Experiments on the entrainment of sediment into suspension by a dense bottom current. *J. Geophys. Res.*, 98, 4793–4807.

Gardner, J.V., Prior, D.B. and Field, M.E. (1999) Humboldt slide – a large shear-dominated retrogressive slope failure. *Mar. Geol.*, 154, 323–338.

Garvine, R.W. (1987) Estuary plumes and fronts in shelf waters: a layer model. J. *Phys. Ocean.*, **17**, 1877–1896.

Geist, E.L. (2000) Origin of the 17 July 1998 Papua New Guinea tsunami; earthquake or landslide. *Seism. Res. Lett.*, **71**, 344–351.

Geyer, W.R., Hill, P.S., Milligan, T.G. and Traykovski, P. (2000) The structure of the Eel River plume during floods. *Cont. Shelf Res.*, **20**, 2067–2093.

Goff, J.A., Orange, D.L., Mayer, L.A. and Hughes Clarke, J.E. (1999) Detailed investigation of continental shelf morphology using a high-resolution swath sonar survey: the Eel margin, northern California. *Mar. Geol.*, **154**, 255–270.

Goff, J.A., Austin, J.A., Jr., Gulick, S., *et al.* (2005) Recent and modern erosion on the New Jersey outer shelf. *Mar. Geol.*, **216**, 275–296.

Goldberg, D. (1997) The role of downhole measurements in marine geology and geophysics. *Rev. Geophys.*, **35**, 315–342.

Goldfinger, C., Nelson, C.H. and Johnson, J.E. (2003) Holocene earthquake records from the Cascadia subduction zone and northern San Andreas fault based on precise dating of offshore turbidites. *Ann. Rev. Earth Planet. Sci.*, **31**, 555–577.

Goodbred, S.L. and Kuehl, S.A. (2000) Enormous Ganges–Brahmaputra sediment discharge during strengthened early Holocene monsoon. *Geology,* **28**, 1083–1086.

Goodwin, R.H. and Prior, D.B. (1989) Geometry and depositional sequences of the Mississippi Canyon, Gulf of Mexico. *J. Sediment. Petrol.*, **59**, 318–329.

Grant, W.D. and Madsen, O.S. (1979) Combined wave and current interaction with a rough bottom. *J. Geophys. Res.*, **84**, 1797–1808.

Greenlee, S.M., Schroeder, F.W. and Vail, P.R. (1988) Seismic stratigraphic and geohistory analysis of Tertiary strata from the continental shelf off New Jersey – calculation of eustatic fluctuations from stratigraphic data. In: *Atlantic Continental Margin: U.S.* (Eds R.E. Sheridan and J.A. Grow), pp. 437–444. DNAG Series, Geological Society of America, Boulder, CO.

Greenlee, S.M., Devlin, W.J., Miller, K.G., Mountain, G.S. and Flemings, P.B. (1992) Integrated sequence stratigraphy of Neogene deposits, New Jersey continental shelf and slope: comparison with the Exxon model. *Geol. Soc. Am. Bull.*, **104**, 1403–1411.

Grow, J.A. and Sheridan, R.E. (1988) U.S. Atlantic continental margin; a typical Atlantic-type or passive continental margin. In: *Atlantic Continental Margin: U.S.* (Eds R.E. Sheridan and J.A. Grow), pp. 1–8. DNAG Series, Geological Society of America, Boulder, CO.

Hagen, R.A., Bergersen, D., Moberly, R. and Coulbourn, W.T. (1994) Morphology of a large meandering submarine canyon system the Peru–Chile forearc. *Mar. Geol.*, **119**, 7–38.

Hamilton, E.L. (1980) Geoacoustic modeling of the seafloor. *J. Acoust. Soc. Am.*, **68**, 1313–1340.

Hampton, M. (1972) The role of subaqueous debris flow in generating turbidity currents. *J. Sediment. Petrol.*, **42**, 775–993.

Hampton, M.A., Lee, H.J. and Locat, J. (1996) Submarine landslides. *Rev. Geophys.*, **34**, 33–59.

Haq, B.U., Hardenbol, J. and Vail, P.R. (1987) Chronology of fluctuating sea levels since the Triassic (250 million years ago to Present). *Science,* **235**, 1156–1167.

Harris, C.K. and Wiberg, P.L. (1997) Approaches to quantifying long-term continental shelf sediment transport with an example from the northern California STRESS mid-shelf site. *Cont. Shelf Res.*, **17**, 1389–1418.

Harris, C.K. and Wiberg, P.L. (2001) A two-dimensional, time-dependent model of suspended sediment transport and bed reworking for continental shelves. *Comput. Geosci.*, **27**, 675–690.

Harris, C.K. and Wiberg, P.L. (2002) Across-shelf sediment transport, interactions between suspended sediment and bed sediment. *J. Geophys. Res.*, **107**(C1), doi: 10.1029/2000JC000634.

Hartel, C., Carlsson, F. and Thunblom, M. (2000) Analysis and direct numerical simulation of the flow at a gravity-current head, Part 2. The lobe-and-cleft instability. *J. Fluid Mech.*, **418**, 213–229.

Hay, A.E. (1987) Turbidity currents and submarine channel formation in Rupert Inlet, British Columbia, Part 2: The roles of continuous and surge type flow. *J. Geophys. Res.*, **92**, 2883–2900.

Heezen, B.C. and Ewing, M. (1952) Turbidity currents and submarine slumps and the 1929 Grand Banks Earthquake. *Am. J. Sci.*, **250**, 849–873.

Henkel, D.J. (1970) The role of waves causing submarine landslides. *Géotechnique*, **20**, 75–80.

Hickey, B.M. (1979) The California Current system-hypotheses and facts. *Progr. Ocean.*, **8**, 191–279.

Hickey, B.M. (1998) Coastal oceanography of western North America from the tip of Baja California to Vancouver Island. In: *The Sea*, Vol. 11, *The Global Coastal Ocean: Regional Studies and Syntheses* (Eds A.R. Robinson and K.H. Brink), pp. 345–393. John Wiley & Sons, New York.

Hill, P.S. (1992) Reconciling aggregation theory with observed vertical fluxes following phytoplankton blooms. *J. Geophys. Res.*, **97**, 2295–2308.

Hill, P.S., Syvitski, J.P., Cowan, E.A. and Powell, R.D. (1998) *In situ* observations of floc settling velocities in Glacier Bay, Alaska. *Mar. Geol.*, **145**, 85–94.

Hill, P.S., Milligan, T.G. and Geyer, W.R. (2000) Controls on effective settling velocity in the Eel River flood plume. *Cont. Shelf Res.*, **20**, 2095–2111.

Hiscott, R.N., Hall, F.R. and Pirmez, C. (1997) Turbidity-current overspill from the Amazon channel: Texture of the silt/sand load, pale flow from anisotropy of magnetic susceptibility and implications for flow processes. *Proc. ODP Sci. Res.*, **155**, 53–78.

Hsu, T.J. and Hanes, D.M. (2004) Effects of wave shape on sheet flow sediment transport. *J. Geophys. Res.*, **109**, Art. C05025.

Imran, J. and Syvitski, J.P.M. (2000) Impact of extreme river events on coastal oceans. *Oceanography,* **13**, 85–92.

Imran, J., Parker, G. and Pirmez, C. (1999) A nonlinear model of flow in meandering submarine and subaerial channels. *J. Fluid Mech.*, **400**, 295–331.

Inman, D.L. and Jenkins, S.A. (1999) Climate change and the episodicity of sediment flux of small California rivers. *J. Geol.*, **107**, 251–270.

Iverson, R.M. and Major, J.J. (1986) Groundwater seepage vectors and the potential for hillslope failure and debris flow mobilization. *Water Resour. Res.*, **22**, 1543–1548.

Jaeger, J.M. and Nittrouer, C.A. (2000). The formation of point- and multiple-source deposits on continental shelves. In: *Coastal Ocean Processes (CoOP): Transport and Transformation Processes over Continental Shelves with Substantial Freshwater Inflows* (Eds S. Henrichs, N. Bond, R. Garvine, G. Kineke and S. Lohrenz) pp. 78–89. Technical Report TS-237-00, Center for Environmental Science, University of Maryland, Cambridge, MD.

Jansa, L.F. (1981) Mesozoic carbonate platforms and banks of the eastern North American margin. *Mar. Geol.*, **44**, 97–117.

Jumars, P.A. and Nowell, A.R.M. (1984) Effects of benthos on sediment transport, difficulties with functional grouping. *Cont. Shelf Res.*, **3**, 115–130.

Karner, G.D. and Driscoll, N.W. (1997) Three-dimensional interplay of advective and diffusive processes in the generation of sequence boundaries. *J. Geol. Soc. London*, **154**, 443–449.

Kassem, A. and Imran, J. (2004) Three-dimensional modeling of density current. II. Flow in sinuous confined and unconfined channels. J. *Hydraul. Res.*, **42**, 591–602.

Kayen, R.E. and Lee, H.J. (1991) Pleistocene slope instability of gas hydrate-laden sediment on the Beaufort Sea margin. *Mar. Geotech.*, **10**, 125–141.

Kennett, J.P. (1982) *Marine Geology*. Prentice-Hall, Englewood Cliffs, NJ, 813 pp.

Khripounoff, A., Vangriesheim, A., Babonneau, N., *et al.* (2003) Direct observation of intense turbidity current activity in the Zaire submarine valley at 4000 m water depth. *Mar. Geol.*, **194**, 151–158.

Kineke, G.C., Sternberg, R.W., Trowbridge, J.H. and Geyer, W.R. (1996) Fluid-mud processes on the Amazon continental shelf. *Cont. Shelf Res.*, **16**, 667–696.

Kineke, G.C., Woolfe, K.J., Kuehl, S.A., *et al.* (2000) Sediment export from the Sepik River, Papua New Guinea: evidence for a divergent sediment plume. *Cont. Shelf Res.*, **20**, 2239–2266.

Klaucke, I., Hesse, R. and Ryan, W.B.F. (1998) Morphology and structure of a distal submarine trunk channel: The north-west Atlantic Mid-Ocean Channel between lat 53°N and 44°30′N. *Geol. Soc. Am. Bull.*, **110**, 22–34.

Knox, J.C. (2000) Sensitivity of modern and Holocene floods to climate change. *Quat. Sci. Rev.*, **19**, 439–457.

Komar, P.D. and Miller, M.C. (1975) On the comparison between the threshold of sediment motion under waves and unidirectional currents with a discussion of the practical evaluation of the threshold. *J. Sediment. Petrol.*, **45**, 362–367.

Komar, P.D., Neudeck, R.H. and Kulm, L.D. (1972) Observations and significance of deep-water oscillatory ripple marks on the Oregon continental shelf. In: *Shelf Sediment Transport: Process and Pattern* (Eds D.J.P. Swift, D.B. Duane and O.H. Pilkey), pp. 601–624. Dowden, Hutchinson and Ross, Stroudsburg, PA.

Kominz, M.A., Miller, K.G. and Browning, J.V. (1998) Long-term and short-term global Cenozoic sea-level estimates. *Geology*, **26**, 311–314.

Kostic, S., Parker, G. and Marr, J.G. (2002) Role of turbidity currents in setting the foreset slope of clinoforms prograding into standing fresh water. *J. Sediment. Res.*, **72**, 353–362.

Kuehl, S.A., DeMaster, D.J. and Nittrouer, C.A. (1986) Nature of sediment accumulation on the Amazon continental shelf, *Cont. Shelf Res.*, **6**, 209–225.

Kuehl, S.A., Nittrouer, C.A., Allison, M.A., *et al.* (1996) Sediment deposition, accumulation and seabed dynamics in an energetic, fine-grained coastal environment. *Cont. Shelf Res.*, **16**, 787–816.

Kuenen, Ph.H. and Migliorini, C.I. (1950) Turbidity currents as a cause of graded bedding. *J. Geol.*, **58**, 91–127.

Kulm, L.D. and Fowler, G.A. (1974) Oregon continental margin structure and stratigraphy; a test of the imbricate thrust model. In: *The Geology of Continental Margins* (Eds C.A. Burk and C.L. Drake), pp. 261–233. Springer-Verlag, New York.

Kulm, L.D., Roush, R.C., Harlett, J.C., Neudeck, R.H., Chambers, D.M. and Runge, E.J. (1975) Oregon continental shelf sedimentation; interrelationships of facies distribution and sedimentary processes. *J. Geol.*, **83**, 145–175.

Kvenvolden, K.A. and Field, M.E. (1981) Thermogenic hydrocarbons in unconsolidated sediments of the Eel River Basin, offshore northern California. *Bull. Am. Assoc. Petrol. Geol.*, **65**, 1642–1646.

Lamb, M.P., D'Asaro, E. and Parsons, J.D. (2004) Turbulent structure of high-density suspensions formed under waves. *J. Geophys. Res.*, **109**, Art. C12026.

Lee, H.J. and Edwards, B.D. (1986) Regional method to assess offshore slope stability. *ASCE J. Geotech. Eng.*, **112**, 489–509.

Lee, H.J., Edwards, B.D. and Field, M.E. (1981) Geotechnical analysis of a submarine slump, Eureka, California. *Proceedings of the Offshore Technology Conference, Houston*, pp. 53–59.

Lee, H.J., Schwab, W.C., Edwards, B.D. and Kayen, R.E. (1991) Quantitative controls on submarine slope failure morphology. *Mar. Geotech.*, **10**, 143–158.

Lee, H.J., Syvitski, J.P.M., Parker, G., *et al.* (2002) Distinguishing sediment waves from slope failure deposits: field examples, including the 'Humboldt Slide' and modeling results. *Mar. Geol.*, **192**, 79–104.

Leithold, E.L. and Hope, R.S. (1999) Deposition and modification of a flood layer on the northern California shelf: lessons from and about the fate of terrestrial particulate organic carbon. *Mar. Geol.*, **154**, 183–195.

Lemke, R.W. (1967) Effects of the earthquake of March 27, 1964, at Seward, Alaska. *U.S. Geol. Surv. Prof. Pap.*, **542-E**.

Lorenson, T.D., McLaughlin, R.J., Kvenvolden, K.A., *et al.* (1998) Comparison of offshore and onshore gas occurrences, Eel River basin, Northern California. *U.S. Geol. Surv. Open-File Rep.*, **98–781**.

Lowrie, W. and Kent, D.V. (2004) Geomagnetic polarity timescale and reversal frequency regimes. In: *Timescales of the Internal Geomagnetic Field* (Eds J.E.T. Channell, D.V. Kent, W. Lowrie and J. Meert), pp. 287–298. Geophysical Monograph 145, American Geophysical Union, Washington, DC.

Madsen, O.S. (1994) Spectral wave-current bottom boundary layer flows. In: *Coastal Engineering 1994, Proceedings, 24th International Conference,* pp. 384–397. Coastal Engineering Research Council/American Society of Civil Engineers, Kobe, Japan.

Marr, J.G., Harff, P.A., Shanmugam, G. and Parker, G. (2001) Experiments on subaqueous sandy gravity flows: the role of clay and water content in flow dynamics and depositional structures. *Geol. Soc. Am. Bull.*, **113**, 1377–1386.

May, J.A., Warme, J.E. and Slater, R.A. (1983) Role of submarine canyons on shelfbreak erosion and sedimentation: modern and ancient examples. In: *The Shelfbreak; Critical Interface on Continental Margins* (Eds D.J. Stanley and G.T. Moore), pp. 315–332. Special Publication 33, Society of Economic Paleontologists and Mineralogists, Tulsa, OK.

McCave, I.N. (1972) Transport and escape of fine-grained sediment from shelf areas. In: *Shelf Sediment Transport: Process and Pattern* (Eds D.J.P. Swift, D.B. Duane and O.H. Pilkey), pp. 225–248. Dowden, Hutchinson and Ross, Stroudsburg, PA.

McCave, I.N. (1984) Size spectra and aggregation of suspended particles in the deep ocean. *Deep-sea Res.*, **31**, 329–352.

McCool, W.W. and Parsons, J.D. (2004) Sedimentation from buoyant fine-grained suspensions. *Cont. Shelf Res.*, **24**, 1129–1142.

McHugh, C.M.G. and Olson, H.C. (2002) Pleistocene chronology of continental margin sedimentation: New insights into traditional models, New Jersey. *Mar. Geol.*, **186**, 389–411.

McKee, B.A., Nittrouer, C.A. and DeMaster, D.J. (1983) The concepts of sediment deposition and accumulation applied to the continental shelf near the mouth of the Yangtze River. *Geology*, **11**, 631–633.

McKee, B.A., Aller, R.C., Allison, M.A., Bianchi, T.A. and Kineke, G.C. (2004) Transport and transformation of dissolved and particulate materials on continental margins influenced by major rivers: benthic boundary layer and seabed processes. *Cont. Shelf Res.*, **24**, 899–926.

McPhee-Shaw, E.E., Sternberg, R.W., Mullenbach, B. and Ogston, A.S. (2004) Observations of intermediate nepheloid layers on the northern California continental margin. *Cont. Shelf Res.*, **24**, 693–720.

Meade, R.H. (1996) River-sediment inputs to major deltas. In: *Sea-level Rise and Coastal Subsidence* (Eds J.D. Milliman and B.U. Haq), pp. 63–85. Kluwer Academic Publishers, Dordrecht.

Meade, R.H., Yuzyk, T.R. and Day, T.J. (1990) Movement and storage of sediment in rivers of the United States and Canada. In: *Geology of North America: Surface Water Hydrology* (Eds M.G. Wolman and H.C. Riggs), pp. 255–280. Geological Society of America, Boulder, CO.

Mertes, L.A.K. and Warrick, J.A. (2001) Measuring flood output from 110 coastal watersheds in California with field measurements and SeaWiFS. *Geology,* **29**, 659–662.

Miall, A.D. (1991) Stratigraphic sequences and their chronostratigraphic correlation. *J. Sediment. Petrol.*, **61**, 497–505.

Miller, K.G., Melillo, A.J., Mountain, G.S., Farre, J.A. and Poag, C.W. (1987) Middle to late Miocene canyon cutting on the New Jersey continental slope: biostratigraphic and seismic stratigraphic evidence. *Geology,* **15**, 509–512.

Miller, K.G., Mountain, G.S., Browning, J.S., *et al.* (1998) Cenozoic global sea level, sequences and the New Jersey transect: results from coastal plain and continental slope drilling. *Rev. Geophys.*, **36**, 569–601.

Milligan, T.G. and Hill, P.S. (1998) A laboratory assessment of the relative importance of turbulence, particle composition and concentration in limiting maximal floc size. *J. Sea Res.*, **39**, 227–241.

Milliman, J.D. and Meade, R.H. (1983) World-wide delivery of river sediment to the oceans. *J. Geol.*, **91**, 1–21.

Milliman, J.D. and Syvitski, J.P.M. (1992) Geomorphic/tectonic control of sediment discharge to the ocean:

the importance of small mountainous rivers. *J. Geol.*, **100**, 525–544.

Mitchum, R.M., Vail, P.R. and Thompson, S. (1977a) Seismic stratigraphy and global changes of sea level; Part 2, The depositional sequence as a basic unit for stratigraphic analysis. In: *Seismic Stratigraphy; Applications to Hydrocarbon Exploration* (Ed. C.E. Payton), pp. 53–62. Memoir 26, American Association of Petroleum Geologists, Tulsa, OK.

Mitchum, R.M., Vail, P.R. and Sangree, J.B. (1977b) Seismic stratigraphy and global changes of sea level; Part 6, Stratigraphic interpretation of seismic reflection patterns in depositional sequences. In: *Seismic Stratigraphy; Applications to Hydrocarbon Exploration* (Ed. C.E. Payton), pp. 117–133. Memoir 26, American Association of Petroleum Geologists, Tulsa, OK.

Mohrig, D., Whipple, K.X., Hondzo, M., Ellis, C. and Parker, G. (1998) Hydroplaning of subaqueous debris flows. *Geol. Soc. Am. Bull.*, **110**, 387–394.

Moore, D.G. (1969) *Reflection Profiling Studies of the California Continental Borderland: Structure and Quaternary Turbidite Basins*. Special Paper 107, Geological Society of America, Boulder, CO, 142 pp.

Morehead, M.D., Syvitski, J.P.M. and Hutton, E.W.H. (2001) The link between abrupt climate change and basin stratigraphy: A numerical approach. *Global Planet. Change*, **28**, 115–135.

Mountain, G.S. (1987) Cenozoic margin construction and destruction offshore New Jersey. In: *Timing and Depositional History of Eustatic Sequences: Constraints on Seismic Stratigraphy* (Eds C. Ross and D. Haman), pp. 57–83. Special Publication 24, Cushman Foundation for Foraminiferal Research.

Mountain, G.S., Damuth, J.E., McHugh, C.M.G., Lorenzo, J.M. and Fulthorpe, C.S. (1996) Origin, reburial and significance of a middle Miocene canyon, New Jersey continental slope. *Proc. ODP Sci. Results*, **150,** 283–292.

Mulder, T. and Syvitski, J.P.M. (1995) Turbidity currents generated at river mouths during exceptional discharges to the world oceans. *J. Geol.*, **103**, 285–299.

Mulder, T. and Syvitski J.P.M. (1996) Climatic and morphologic relationships of rivers: Implications of sea level fluctuations on river loads. *J. Geol.*, **104**, 509–523.

Mullenbach, B.L. and Nittrouer, C.A. (2000) Rapid deposition of fluvial sediment in the Eel Canyon, northern California. *Cont. Shelf Res.*, **20**, 2191–2212.

Mullenbach, B.L. and Nittrouer, C.A. (2006) Decadal record of sediment export to the deep sea via Eel Canyon. *Cont. Shelf Res.*, **26**, 2157–2177.

Mullenbach, B.L., Nittrouer, C.A., Puig, P. and Orange, D.L. (2004) Sediment deposition in a modern submarine canyon: Eel Canyon, northern California. *Mar. Geol.*, **211**, 101–119.

Nissen, S.E., Haskell, N.L, Steiner, C.T. and Coterill, K.L. (1999) Debris flow outrunner blocks, glide tracks and pressure ridges identified on the Nigerian continental slope using 3-D seismic coherency. *Leading Edge*, **18**, 595–599.

Nittrouer, C.A. (1999) STRATAFORM: overview of its design and synthesis of its results. *Mar. Geol.*, **154**, 3–12.

Nittrouer, C. and Sternberg, R.W. (1981) The formation of sedimentary strata in an allochthonous shelf environment: application to the Washington continental shelf. *Mar. Geol.*, **42**, 201–232.

Nittrouer, C.A., Kuehl, S.A., DeMaster, D.J. and Kowsmann, R.O. (1986) The deltaic nature of Amazon shelf sedimentation. *Geol. Soc. Am. Bull.*, **97**, 444–458.

Nittrouer, C.A., Kuehl, S.A., Sternberg, R.W., Figueiredo, A.G. and Faria, L.E.C. (1995) An introduction to the geological significance of sediment transport and accumulation on the Amazon continental shelf. *Mar. Geol.*, **125**, 177–192.

Nordfjord, S., Goff, J.A., Austin, J.A., Jr. and Sommerfield, C.K. (2005) Seismic geomorphology of buried channel systems on the New Jersey outer shelf: assessing past environmental conditions. *Mar. Geol.*, **214**, 339–364.

Normark, W.R. and Carlson, P.R. (2003) Giant submarine canyons: is size any clue to their importance in the rock record? In: *Extreme Depositional Environments: Mega End Members in Geologic Time* (Eds M.A. Chan and A.W. Archer), pp. 1–15. Special Paper 370, Geological Society of America, Boulder, CO.

O'Grady, D.B., Syvitski, J.P.M., Pratson, L.F. and Sarg, J.F. (2000) Categorizing the morphologic variability of siliciclastic passive continental margins. *Geology*, **28**, 207–210.

Ogston, A.S. and Sternberg, R.W. (1999) Sediment-transport events on the northern California continental shelf. *Mar. Geol.*, **154**, 69–82.

Ogston, A.S., Cacchione, D.A., Sternberg, R.W. and Kineke, G.C. (2000) Observations of storm and river flood-driven sediment transport on the northern California continental shelf. *Cont. Shelf Res.*, **20**, 2141–2162.

Ogston, A.S., Guerra, J.V. and Sternberg, R.W. (2004) Interannual variability of nearbed sediment flux on the Eel River shelf, northern California. *Cont. Shelf Res.*, **24**, 117–136.

Orange, D.L. (1999) Tectonics, sedimentation and erosion in northern California: submarine geomorphology and sediment preservation potential as a result of three competing forces. *Mar. Geol.*, **154**, 369–382.

Orange, D.L. and Breen, N.A. (1992). The effects of fluid escape on accretionary wedges; 2, Seepage force, slope failure, headless submarine canyons and vents. *J. Geophys. Res.*, **97**, 9277–9295.

Orange, D.L., Anderson, R.S. and Breen, N.A. (1994) Regular canyon spacing in the submarine environment; the link between hydrology and geomorphology. *GSA Today*, **4**, 29, 36–39.

Owens, J.P. and Gohn, G.S. (1985) Depositional history of the Cretaceous series in the U.S. coastal plain: stratigraphy, paleoenvironments and tectonic controls of sedimentation. In: *Geologic Evolution of the United States Atlantic Margin* (Ed. C.W. Poag), pp. 25–86. Van Nostrand Reinhold, New York.

Pantin, H.M. (2001) Experimental evidence for autosuspension. In: *Particulate Gravity Currents* (Eds W.D. McCaffrey, B.C. Kneller and J. Peakall), pp. 189–205, Special Publication 31, International Association of Sedimentologists. Blackwell Science, Oxford.

Parker, G. (1982) Conditions for the ignition of catastrophically erosive turbidity currents. *Mar. Geol.*, **46**, 307–327.

Parsons, B. and Sclater, J.G. (1977) An analysis of the variation of ocean floor bathymetry and heat flow with age. *J. Geophys. Res.*, **82**, 803–827.

Parsons, J.D. (1998) *Mixing mechanisms in density intrusions*. Unpublished PhD thesis, University of Illinois, Urbana-Champaign.

Parsons, J.D., Bush, J.W.M. and Syvitski, J.P.M. (2001) Hyperpycnal plumes with small sediment concentrations. *Sedimentology*, **48**, 465–478.

Payton, C.E. (Ed.) (1977) *Seismic Stratigraphy – Applications to Hydrocarbon Exploration*. Memoir 26, American Association of Petroleum Geologists, Tulsa, OK, 516 pp.

Peakall, J., McCaffrey, B. and Kneller, B. (2000) A process model for the evolution and architecture of sinuous submarine channels. *J. Sediment. Res.*, **70**, 434–448.

Penland, S., Boyd, R. and Suter, J.R. (1988) Transgressive depositional systems of the Mississippi delta plain: a model for barrier shoreline and shelf sand development. *J. Sediment. Petrol.*, **58**, 932–949.

Piper, D.J.W. and Normark, W.R. (1983) Turbidite depositional patterns and flow characteristics, Navy submarine fan, California Borderland. *Sedimentology*, **30**, 681–694.

Pirmez, C., Pratson, L.F. and Steckler, M.S. (1998) Clinoform development by advection-diffusion of suspended sediment; modeling and comparison to natural systems. *J. Geophys. Res.*, **103**, 24,141–24,157.

Poag, C.W. (1985) Depositional history and stratigraphic reference section for central Baltimore Canyon trough. In: *Geologic Evolution of the United States Atlantic Margin* (Ed. C.W. Poag), pp. 217–263. Van Nostrand Reinhold, New York.

Poag, C.W. and Sevon, W.D. (1989) A record of Appalachian denudation in postrift Mesozoic and Cenozoic sedimentary deposits of the U.S. middle Atlantic continental margin. *Geomorphology*, **2**, 119–157.

Poag, C.W. and Ward, L.W. (1993) Allostratigraphy of the U.S. middle Atlantic continental margin – characteristics, distribution and depositional history of principal unconformity-bounded Upper Cretaceous and Cenozoic sedimentary units. *U.S. Geol. Surv. Prof. Pap.*, **1542**.

Posamentier, H.W., Jervey, M.T. and Vail, P.R. (1988) Eustatic controls on clastic deposition I: conceptual framework. In: *Sea Level Changes: an Integrated Approach* (Eds C.K. Wilgus, B.S. Hastings, C.G. St.C. Kendall, *et al.*), pp. 125–154. Special Publication 42, Society of Economic Paleontologists and Mineralogists, Tulsa, OK.

Poulos, S.G., Castro, G. and France, J.W. (1985) Liquefaction evaluation procedure. *J. Geotech. Eng.*, **111**, 772–791.

Pratson, L.F. (1993) *Morphologic studies of submarine sediment drainage*. PhD dissertation, Columbia University, New York.

Pratson, L.F. and Haxby, W.F. (1996) What is the slope of the U.S. continental slope? *Geology*, **24**, 3–6.

Pratson, L.F., Ryan, W.B.F., Mountain, G.S. and Twichell, D.C. (1994) Submarine canyon initiation by downslope-eroding sediment flows; evidence in late Cenozoic strata on the New Jersey continental slope. *Geol. Soc. Am. Bull.*, **106**, 395–412.

Prior, D.B., Bornhold, B.D. and Johns, M.W. (1984) Depositional characteristics of a submarine debris flow. *J. Geol.*, **92**, 707–727.

Prior, D.B., Bornhold, B.D. and Johns, M.W. (1986) Active sand transport along a fjord-bottom channel, Bute Inlet, British Columbia. *Geology*, **14**, 581–584.

Puig, P., Ogston, A.S., Mullenbach, B.L., Nittrouer, C.A. and Sternberg, R.W. (2003) Shelf-to-canyon sediment-transport processes on the Eel continental margin (northern California). *Mar. Geol.*, **193**, 129–149.

Puig, P., Ogston, A.S., Mullenbach, B.L., *et al.* (2004) Storm-induced sediment-gravity flows at the head of the Eel submarine canyon. *J. Geophys. Res.*, **109**, C03019, doi:10.1029/2003JC001918.

Pullen, J.D. and Allen, J.S. (2000) Modeling studies of the coastal circulation off Northern California: shelf response to a major Eel River flood event. *Cont. Shelf Res.*, **20**, 2213–2238.

Rabinovich, A.B., Thomson, R.E., Kulikov, E.A., *et al.* (1999) The landslide-generated tsunami November 3, 1994, in Skagway. *Geophys. Res. Lett.*, **26**, 3009–3012.

Reineck, H.-E. and Singh, I.B. (1972) Genesis of laminated sand and graded rhythmites in storm-sand layers of shelf mud. *Sedimentology*, **18**, 123–128.

Reynolds, D.J., Steckler, M.S. and Coakley, B.J. (1991) The role of the sediment load in sequence stratigraphy; the influence of flexural isostasy and compaction. *J. Geophys. Res.*, **96**, 6931–6949.

Sadler, P.M. (1981) Sediment accumulation rates and the completeness of stratigraphic sections. *J. Geol.*, **89**, 569–584.

Sclater, J.G. and Christie, P.A.F. (1980) Continental stretching; an explanation of the post-Mid-Cretaceous subsidence of the central North Sea basin. *J. Geophys. Res.*, **85**, 3711–3739.

Scully, M.E., Friedrichs, C.T. and Wright, L.D. (2003) Numerical modeling of gravity-driven sediment transport and deposition on an energetic continental shelf: Eel River, northern California. *J. Geophys. Res.*, **108** (C4), paper 17, 1–14.

Seed, H.B. (1968) Landslides during earthquakes due to soil liquefaction. *ASCE J. Soil Mech. Found. Div.*, **94**, 1055–1122.

Seed, H.B., Seed, R.B., Schlosser, F., Blondeau, F. and Juran, I. (1988) *The Landslide at the Port of Nice on October 16, 1979*. Report UCB/EERC–88/10, Earthquake Engineering Research Center, University of California, Berkeley, 68 pp.

Shepard, F.P. (1977) *Geological Oceanography: Evolution of Coasts, Continental Margins and the Deep-Sea Floor*. Crane, Russak and Co., New York, 214 pp.

Shepard, F.P. (1981) Submarine canyons: multiple causes and long-time persistence. *Bull. Am. Assoc. Petrol. Geol.*, **65**, 1062–1077.

Shor, A.N. and McClennen, C.E. (1988) Marine physiography of the U.S. Atlantic margin. In: *The Atlantic Continental Margin; U.S.* (Eds R.E. Sheridan and J.A. Grow), pp. 9–18. The Geology of North America, I–2. Geological Society of America, Boulder, CO.

Skempton, A.W. (1970) The consolidation of clays by gravitational compaction. *Q. J. Geol. Soc. London*, **125**, 373–411.

Smith, J.D. and Long, C.E. (1976) The effects of turning in the bottom boundary layer on continental shelf sediment transport. *Soc. Roy. Sci. Liege Mem.*, **10**, 369–396.

Sommerfield, C.K. (2006) On sediment accumulation rates and stratigraphic completeness: Lessons from Holocene ocean margins. *Cont. Shelf Res.*, **26**, 2225–2240.

Sommerfield, C.K. and Nittrouer, C.A. (1999) Modern accumulation rates and a sediment budget for the Eel shelf: a flood-dominated depositional environment. *Mar. Geol.*, **154**, 227–241.

Sommerfield, C.K., Nittrouer, C.A. and Alexander, C.R. (1999) ^{7}Be as a tracer of flood sedimentation on the northern California continental margin. *Cont. Shelf Res.*, **19**, 335–361.

Sommerfield, C.K., Drake, D.E. and Wheatcroft, R.A. (2002) Shelf record of climatic changes in flood magnitude and frequency, north-coastal California. *Geology*, **30**, 395–398.

Spinelli, G.A. and Field, M.E. (2001). Evolution of continental slope gullies on the Northern California margin. *J. Sediment. Res.*, **71**, 237–245.

Spinelli, G.A. and Field, M.E. (2003) Controls of tectonics and sediment source locations on along-strike variations in transgressive deposits on the northern California margin. *Mar. Geol.*, **197**, 35–47.

Steckler, M.S., Watts, A.B. and Thorne, J.A. (1988) Subsidence and basin modeling at the U.S. Atlantic passive margin. In: *The Atlantic Continental Margin; U.S.* (Eds R.E. Sheridan and J.A. Grow), pp. 399–416. The Geology of North America, I–2. Geological Society of America, Boulder, CO.

Steckler, M.S., Mountain, G.S., Miller, K.G. and Christie-Blick, N. (1999) Reconstruction of Tertiary progradation and clinoform development on the New Jersey passive margin by 2-D backstripping. *Mar. Geol.*, **154**, 399–420.

Sterling, G.H. and Strohbeck, G.E. (1973) The failure of South Pass 70B Platform in Hurricane Camille. *Proceedings of the Offshore Technology Conference*, Vol. 1, 123–150.

Strub, P.T., Allen, J.S., Huyer, A. and Smith, R.L. (1987) Seasonal cycles of currents, temperatures, winds and sea level over the Pacific continental shelf: 35N to 48N. *J. Geophys. Res.*, **92**, 1507–1526.

Sugarman, P.J. and Miller, K.G. (1997) Correlation of Miocene sequences and hydrogeologic units, New Jersey Coastal Plain. *Sediment. Geol.*, **108**, 3–18.

Sugarman, P., McCartan, L., Miller, K., *et al.* (1997) Strontium-isotopic correlation of Oligocene to Miocene sequences, New Jersey and Florida. *Proc. ODP Sci. Results*, **150X**.

Suppe, J. (1985) *Principles of Structural Geology*. Prentice-Hall, Englewood Cliffs, NJ, 537 pp.

Swenson, J.B., Paola, C., Pratson, L., Voller, V.R. and Murray, A.B. (2005) Fluvial and marine controls on combined subaerial and subaqueous delta progradation: morphodynamic modeling of compound clinoform development. *J. Geophys. Res.*, **110**, 2013–2029.

Swift, D.J.P. (1970) Quaternary shelves and the return to grade. *Mar. Geol.*, **8**, 5–30.

Syvitski, J.P.M. and Farrow, G.E. (1983) Structures and processes in bayhead deltas: Knight and Bute Inlet, British Columbia. *Sediment. Geol.*, **36**, 217–244.

Syvitski, J.P.M. and Morehead, M.D. (1999) Estimating river-sediment discharge to the ocean: application to the Eel Margin, northern California. *Mar. Geol.*, **154**, 13–28.

Syvitski, J.P.M., Morehead, M.D., Bahr, D. and Mulder, T. (2000) Estimating fluvial sediment transport: the rating parameters. *Water Resour. Res.*, **366**, 2747–2760.

Syvitski, J.P.M., Peckham, S.D., Hilberman, R.D. and Mulder, T. (2003) Predicting the terrestrial flux of sediment to the global ocean: a planetary perspective. *Sediment. Geol.*, **162**, 5–24.

Syvitski, J.P.M., Vörösmarty, C.J., Kettner, A.J. and Green, P. (2005) Impact of humans on the flux of terrestrial sediment to the global coastal ocean. *Science*, **308**, 376–380.

Tappin, D.R., Matsumoto, T. and Shipboard Scientists (1999) Offshore surveys identify sediment slump as likely cause of devastating Papua New Guinea Tsunami 1998. *Trans. Am. Geophys. Union*, **80**, 329, 334, 340.

Ten Brinke, W.B.M. (1994) Settling velocities of mud aggregates in the Oosterchelde tidal basin (the Netherlands), determined by a submersible video system. *Estuarine Coastal Shelf Sci.*, **39**, 549–564.

Traykovski, P., Geyer, W.R., Irish, J.D. and Lynch, J.F. (2000) The role of wave-induced density-driven fluid mud flows for cross-shelf transport on the Eel River continental shelf. *Cont. Shelf Res.*, **20**, 2113–2140.

Trowbridge, J.H. and Kineke, G.C. (1994) Structure and dynamics of fluid muds on the Amazon continental-shelf. *J. Geophys. Res.*, **99**, 865–874.

Twichell, D.C. and Roberts, D.G. (1982) Morphology, distribution and development of submarine canyons on the United States Atlantic continental slope between Hudson and Baltimore canyons. *Geology*, **10**, 408–412.

Uchupi, E., Driscoll, N., Ballard, R.D. and Bolmer, S.T. (2001) Drainage of late Wisconsin glacial lakes and the morphology and late Quaternary stratigraphy of the New Jersey–southern New England continental shelf and slope. *Mar. Geol.*, **172**, 117–145.

Vail, P.R., Mitchum, R.M. and Thompson, S. (1977) Seismic stratigraphy and global changes of sea level, Part 4: Global cycles of relative changes of sea level. In: *Seismic Stratigraphy – Applications to Hydrocarbon Exploration* (Ed. C.E. Payton), pp. 83–98. Memoir 26, American Association of Petroleum Geologists, Tulsa, OK.

Van Wagoner, J.C., Posamentier, H.W., Mitchum, R.M., *et al.* (1988) An overview of the fundamentals of sequence stratigraphy and key definitions. In: *Sea-level Changes: an Integrated Approach* (Eds C.K. Wilgus, B.S. Hastings, C.A. Ross, *et al.*), pp. 39–45. Special Publication 42, Society of Economic Paleontologists and Mineralogists, Tulsa, OK.

Varnes, D.J. (1958) Landslide types and processes, In: *Landslides and Engineering Practice* (Ed. E.D. Eckel), pp. 20–47. Special Report 29, Highway Research Board, Washington, DC.

Walling, D.E. (1999) Linking land use, erosion and sediment yields in river basins. *Hydrobiologia*, **410**, 223–240.

Walsh, J.P. and Nittrouer, C.A. (1999) Observations of sediment flux to the Eel continental slope, northern California. *Mar. Geol.*, **154**, 55–68.

Walsh, J.P., Nittrouer, C.A., Palinkas, C.M., *et al.* (2004) Clinoform mechanics in the Gulf of Papua. *Cont. Shelf Res.*, **24**, 2487–2510.

Washburn, L., Swenson, M.S., Largier, J.L., Kosro, P.M. and Ramp, S.R. (1993) Cross-shelf sediment transport by an anticyclonic eddy off northern California. *Science*, **261**, 1560–1564.

Watts, A.B. and Ryan, W.B.F. (1976) Flexure of the lithosphere and continental margin basins. *Tectonophysics*, **36**, 25–44.

Wheatcroft, R.A. (1990) Preservation potential of sedimentary event layers. *Geology*, **18**, 843–845.

Wheatcroft, R.A. (2002) *In situ* measurements of near-surface porosity in shallow-marine sands. *J. Ocean. Eng.*, **27**, 561–570.

Wheatcroft, R.A. (2006) Time-series measurements of macrobenthos abundance and sediment bioturbation intensity on a flood-dominated shelf. *Progr. Ocean*, **71**, 88–122.

Wheatcroft, R.A. and Borgeld, J.C. (2000) Oceanic flood deposits on the northern California shelf: large-scale distribution and small-scale physical properties. *Cont. Shelf Res.*, **20**, 2163–2190.

Wheatcroft, R.A. and Drake, D.E. (2003) Post-depositional alteration and preservation of sedimentary event layers on continental margins, I. Role of episodic sedimentation. *Mar. Geol.*, **199**, 123–137.

Wheatcroft, R.A. and Martin, W.R. (1996) Spatial variation in short-term (^{234}Th) sediment bioturbation intensity along an organic-carbon gradient. *J. Mar. Res.*, **54**, 763–792.

Wheatcroft, R.A., Sommerfield, C.K., Drake, D.E., Borgeld, J.C. and Nittrouer, C.A. (1997) Rapid and widespread dispersal of flood sediment on the northern California margin. *Geology*, **25**, 163–166.

Wiberg, P.L. (2000) A perfect storm: formation and potential for preservation of storm beds on the continental shelf. *Oceanography*, **13**, 93–99.

Wiberg, P.L., Drake, D.E. and Cacchione, D.A. (1994) Sediment resuspension and bed armoring during high bottom stress events on the northern California inner continental shelf: measurements and predictions. *Cont. Shelf Res.*, **14**, 1191–1219.

Wiberg, P.L., Drake, D.E., Harris, C.K. and Noble, M. (2002) Sediment transport on the Palos Verdes shelf over seasonal to decadal time scales. *Cont. Shelf Res.*, **22**, 987–1004.

Wright, L.D. (1977) Sediment transport and deposition at river mouths: a synthesis. *Geol. Soc. Am. Bull.*, **88**, 857–868.

Wright, L.D., Kim, S.-C. and Friedrichs, C.T. (1999) Across-shelf variations in bed roughness, bed stress and sediment suspension on the northern California continental shelf. *Mar. Geol.*, **154**, 99–115.

Wright, L.D., Friedrichs, C.T., Kim, S.C. and Scully, M.E. (2001) Effects of ambient currents and waves on gravity-driven sediment transport on continental shelves. *Mar. Geol.*, **175**, 25–45.

Wynn, R.B., Weaver, P.P.E., Ercilla, G., Stow, D.A.V. and Masson, D.G. (2000) Sedimentary processes in the Selvage sediment-wave field, NE Atlantic; new insights into the formation of sediment waves by turbidity currents. *Sedimentology*, **47**, 1181–1197.

Xu, J.P., Noble, M.A. and Rosenfeld, L.K. (2004) In-situ measurements of velocity structure within turbidity currents. *Geophys. Res. Lett.*, **31**, L09311, doi:10.1029/2004GLO19718.

Yun, J.W., Orange, D.L. and Field, M.E. (1999) Subsurface gas offshore of northern California and its link to submarine geomorphology. *Mar. Geol.*, **154**, 357–368.

Zhang, Y., Swift, D.J.P., Fan, S., Niederoda, A.W. and Reed, C.W. (1999) Two-dimensional numerical modeling of storm deposition on the northern California shelf. *Mar. Geol.*, **154**, 155–167.